BEATRYZ CARDOSO MENDES

DEVELOPMENT OF GEOPOLYMERIC MORTARS PRODUCED FROM INDUSTRIAL WASTES IN BOTH PRECURSOR AND ACTIVATOR PHASES

Thesis submitted to the Civil Engineering Graduate Program of the Universidade Federal de Viçosa in partial fulfillment of the requirements for the degree of *Doctor Scientiae*.

Adviser: Leonardo Gonçalves Pedroti

Co-advisers: Carlos Maurício F. Vieira
José Maria F. de Carvalho

VIÇOSA - MINAS GERAIS
2022

Ficha catalográfica elaborada pela Biblioteca Central da Universidade Federal de Viçosa - Campus Viçosa

T
M538d
2022

Mendes, Beatryz Cardoso, 1995-
Development of geopolymeric mortars produced from industrial wastes in both precursor and activator phases / Beatryz Cardoso Mendes. – Viçosa, MG, 2022.
1 tese eletrônica (120 f.): il. (algumas color.).

Texto em inglês.
Orientador: Leonardo Gonçalves Pedroti.
Tese (doutorado) - Universidade Federal de Viçosa, Departamento de Engenharia Civil, 2022.
Inclui bibliografia.
DOI: https://doi.org/10.47328/ufvbbt.2022.011
Modo de acesso: World Wide Web.

1. Polímeros inorgânicos. 2. Resíduos de vidro - Reaproveitamento. 3. Resíduos como material de construção. 4. Sustentabilidade. I. Pedroti, Leonardo Gonçalves, 1978-. II. Universidade Federal de Viçosa. Departamento de Engenharia Civil. Programa de Pós-Graduação em Engenharia Civil. III. Título.

CDD 22. ed. 624.1892

Bibliotecário(a) responsável: Alice Regina Pinto CRB6 2523

BEATRYZ CARDOSO MENDES

DEVELOPMENT OF GEOPOLYMERIC MORTARS PRODUCED FROM INDUSTRIAL WASTES IN BOTH PRECURSOR AND ACTIVATOR PHASES

Thesis submitted to the Civil Engineering Graduate Program of the Universidade Federal de Viçosa in partial fulfillment of the requirements for the degree of *Doctor Scientiae*.

APPROVED: January 5, 2022.

Assent:

Beatryz Cardoso Mendes

Beatryz Cardoso Mendes
Author

Leonardo Gonçalves Pedroti
Adviser

To my parents
Ilton and Maria Adenice,
to my brother Eduardo and
to Prof[a] Rita de Cássia S. S.
Alvarenga (in memorian)

ACKNOWLEDGEMENTS

Firstly, I thank God, who for His infinite Grace and Mercy brought me here, and the Virgin Mary, for the constant intercession along this journey.

To Federal University of Viçosa and to Civil Engineering Graduate Program, for the possibility of achieving another academic degree and the excellent teaching since graduation.

To the Coordenação de Aperfeiçoamento de Pessoal de Nível Superior – Brasil (CAPES) – Finance Code 001, which financed in part this study, and Fundação de Amparo à Pesquisa do Estado de Minas Gerais (FAPEMIG) for all the investment undertaken in carrying out this research.

To my adviser, Professor Dr. Leonardo Gonçalves Pedroti, who faced this mission with me and was always available give me all the necessary support. I thank him for all your attention, companionship, partnership, trust and patience. In addition to mentoring, he became a great friend (almost a father) over the years.

To my co-advisers, Professors Dr. Carlos Maurício Fontes Vieira and Dr. José Maria Franco de Carvalho, for the valuable considerations, directions and corrections, and for all the assistance provided during the research.

To professors Dr. José Carlos Lopes Ribeiro, Dr. Guilherme Jorge Brigolini and Dr. Jonas Alexandre, for the availability to participate in this process, and for the valuable contributions to the work.

To all professors of the Department of Civil Engineering of UFV, for all the knowledge transmitted and for having contributed to my professional and human qualification. I also thank, in general, the technicians and office assistants, always available to solve any problem.

To the Laboratory of Construction Materials, where I consider my second home since 2015 (DEC / UFV), and technicians Nathália, Wellington and José Carlos, for being always helpful and willing to help, besides being my company in many mornings and afternoons in the laboratory. I also thank them for the friendship, conversations and jokes that have made this process much more enjoyable.

To the Microscopy and Microanalysis Center (UFV), the Soil Mineralogy and Geochemistry Laboratories (DPS/UFV), the Construction Materials Laboratory (DECIV/UFOP), the Advanced Materials Laboratory (LAMAV/UENF), the Civil Engineering Laboratory (LECIV/UENF), and the X-Ray Diffraction And Scanning Electron Microscopy Laboratories (DPF/UFV), which assisted me in carrying out essential tests for conducting this research.

To the Research Group SICon, the PhD student Gustavo Lima, the master's student Igor Klaus and the interns Pedro, Carolina, Beatriz, Victor and Cássia, for all the help provided during the research.

To my colleagues and friends (from the lab and the others too) for making this journey much lighter, for the companionship, friendship and help, whether physical or spiritual. In particular, I thank Géssica, Cynthia, Luana, Márcia, Verônica, Rodrigo and the "Cenáculo do Senhor" Prayer Group for giving me daily support, for all the affection shown and for all the prayers.

Finally, I thank my parents Maria Adenice and Ilton for being my solid foundation and my refuge, and for having led me to what I am today. To my brother Eduardo, my faithful companion, for affection, laughter and complicity. To my boyfriend Michel, for all the care, patience and for always being by my side, celebrating with me this achievement. To all my family members, especially cousins, and other friends for being always close, praying and cheering for me.

“The Lord has done great things for us; oh, how happy we were!”

(PSalms 125: 3)

ABSTRACT

MENDES, Beatryz Cardoso, D.Sc., Universidade Federal de Viçosa, January, 2022. **Development of geopolymeric mortars produced from industrial wastes in both precursor and activator phases**. Adviser: Leonardo Gonçalves Pedroti. Co-advisers: Carlos Maurício Fontes Vieira and José Maria Franco de Carvalho.

Geopolymers are binder materials that can be an alternative to replace Portland cement. They are considered less aggressive to the environment because of the lower emission of CO_2 and use of energy in their production chain. However, in order to obtain this advantage, it is essential to use activators that were produced cleanly and sustainably, which is not the case of commercial products such as sodium silicate. This work aimed to manufacture a more eco-efficient product using industrial wastes. Geopolymeric pastes and mortars were produced from chamotte as precursor and waste glass as a component of an alternative activator. In the first experimental phase, it was evaluated the effect of molar concentration and waste glass content in the alkaline solutions. A factorial design of experiments with two factors – molar concentration and waste glass content – and three and four levels, respectively, was applied to analyze the effects. Physical and mechanical tests were performed, as well as the microstructural analyses. The environmental impacts of replacing the traditional activator by the WG-based one were also assessed. The best solutions were selected to develop the mortars, keeping chamotte as precursor and using river sand as fine aggregate. These mortars were produced and characterized for physical and mechanical properties. The results obtained showed that the WG content strongly affects the mechanical strength of geopolymers and the quality of the matrices, promoting a greater formation of geopolymerization products. Using an alternative alkaline solution can reduce 69.8% of the embodied energy and 78.0% of CO_2 footprint compared to the traditional waterglass-based activators. Therefore, this research contributes to technical literature on the application of industrial wastes in geopolymer and the understanding of geopolymerization process.

Keywords: Geopolymer. Waste glass. Chamotte. Sustainability.

RESUMO

MENDES, Beatryz Cardoso, D.Sc., Universidade Federal de Viçosa, janeiro de 2022. **Desenvolvimento de argamassas geopoliméricas produzidas com resíduos industriais nas fases precursora e ativadora**. Orientador: Leonardo Gonçalves Pedroti. Coorientadores: Carlos Maurício Fontes Vieira e José Maria Franco de Carvalho.

Geopolímeros são aglomerantes que podem ser uma alternativa para substituir o cimento Portland. Eles são considerados menos agressivos ao meio ambiente devido à menor emissão de CO_2 e menor consumo energético em sua cadeia produtiva. Entretanto, para que essa vantagem seja garantida, é essencial a aplicação de ativadores produzidos de forma limpa e sustentável, o que não é o caso dos ativadores comerciais, como o silicato de sódio. O objetivo do presente trabalho foi a fabricação de um produto eco-eficiente, empregando resíduos industriais como matérias-primas. Pastas e argamassas geopoliméricas foram produzidas utilizando chamote como precursor e resíduo de vidro como componente de um ativador alternativo. Na primeira fase experimental, avaliou-se o efeito da concentração molar e do teor de resíduo de vidro na solução alcalina, aplicando-se um planejamento experimental em fatorial com três e quatro níveis, respectivamente, para a análise dos efeitos. Ensaios físicos e mecânicos em pastas foram realizados, bem como análises microestruturais. Os impactos ambientais quando da substituição do ativador tradicional pelo ativador à base de resíduo de vidro também foram verificados. As melhores soluções foram selecionadas para a produção de argamassas, mantendo o chamote como precursor e utilizando areia de rio como agregado miúdo. As argamassas foram produzidas e caracterizadas fisicamente e mecanicamente. Os resultados obtidos demonstraram que a adição de resíduo de vidro afeta fortemente a resistência mecânica de geopolímeros e a qualidade das matrizes, promovendo uma maior formação dos produtos geopoliméricos. O uso de uma solução alcalina alternativa pode reduzir em 69,8 % a energia consumida e 78,0 % a emissão de CO_2, em comparação aos ativadores à base de silicato de sódio tradicionais. Portanto, a presente pesquisa contribui para a literatura técnica relacionada à aplicação de resíduos industriais em geopolímeros e o entendimento do processo de geopolimerização.

Palavras-chave: Geopolímero. Resíduo de vidro. Chamote. Sustentabilidade.

LIST OF ILLUSTRATIONS

ARTICLE 1

ARTICLE 2

ARTICLE 3

LIST OF TABLES

ARTICLE 1

ARTICLE 2

ARTICLE 3

SUMMARY

GENERAL INTRODUCTION

1 INITIAL CONSIDERATIONS

Alkali-activated binders are materials that have been widely studied around the world, especially in recent decades (LIU *et al.*, 2019; PROVIS, John L., 2014; SHI; JIMÉNEZ; PALOMO, 2011). These materials were developed as an alternative to replace Portland cement, used in the production of concrete, mortars and pastes. Alkali-activated materials are considered less aggressive from an environmental point of view, due to the lower CO_2 emission in relation to the Portland cement (KUA *et al.*, 2019; ZHUANG *et al.*, 2016). In addition, they have good mechanical and durability properties, such as high heat resistance, which has motivated several researchers to develop technological studies on this new type of material (GAVALI *et al.*, 2019; HEAH *et al.*, 2012).

According to Samarakoon *et al.* (2019), within the class of alkali-activated binders there is a subgroup, the group of geopolymers. These consist of three-dimensional aluminosilicates synthesized by a highly concentrated alkaline solution based on hydroxides and/or silicates. As precursors, materials rich in Si and Al are used, with low or no calcium content. Calcined clays (e.g. metakaolin) and fly ash are conventional powders applied as raw materials (PALOMO; GRUTZECK; BLANCO, 1999). The resulting product of the geopolymerization process are three-dimensional structures of silicoaluminates (N-A-S-H gel, N being alkaline metallic cation). Geopolymers are also designated, from a chemical point of view, as polysialates, and sialate is an abbreviation of silico-oxo-aluminate. Crystalline polysialates have structures similar to those of the zeolites, which are minerals formed from the alteration of pozzolanic rocks.

Provis *et al.* (2005) propose that the final "geopolymer" consists of the agglomeration of nanocrystals (zeolites) by the remaining aluminosilicate gel (amorphous), thus forming a high-performance mineral binder. The solid particles that have not reacted are connected inside this matrix by physical means. It is expected that the physical-chemical characteristics of the geopolymers are determined by the degree of crystalline ordering within the binder phase, which is conditioned by the choice of raw materials, the formulation of the mixture and the processing conditions.

Regarding the composition of raw materials, the parameters associated with the levels of SiO_2, Al_2O_3 and Na_2O are essential for the formation of the products of interest. Generally,

the increase in the SiO_2/Al_2O_3 ratio in the precursor contributes to increased compressive strength and reduced porosity. However, this trend of mechanical strength in relation to silica and alumina contents is not constant for all precursors, besides relying on other additional factors (LUUKKONEN *et al.*, 2018). It is emphasized that high amounts of silica reduce the reactivity of the system, making the reaction of materials difficult. This occurs because the Al – O – Si bonds are weaker than the Si – O – Si bonds; the tetrahedral coordination of Al^{3+} and Si^{4+} have rays equal to 0.39 and 0.26, respectively, indicating a stronger bond of Si – O (GARTNER; MACPHEE, 2011).

Another important point is the amount of alkalis in the system. This ratio is related to the degree of polymerization, since the alkali content should be sufficient to promote the solubilization of aluminosilicates; that is, the higher the concentration of alkaline ions, the higher the dissolution rate of the precursor's solid particles. Consequently, the compressive strength of the material increases (KHALE; CHAUDHARY, 2007; LUUKKONEN *et al.*, 2018). On the other hand, Novais *et al.* (2016) point out that very high concentrations can slow down the geopolymerization process as a result of limiting ion mobility in the solution.

In addition to the chemical composition, the particle size distribution of the precursor significantly influences the properties of geopolymeric materials, both in the fresh and hardened states (DIAZ; ALLOUCHE; EKLUND, 2010). Several studies regarding the application of fly ash confirm that the reduction of particles size contributes to a higher reactivity between the precursor and the alkaline solution, resulting in the increase of mechanical strength (ASSI; EDDIE DEAVER; ZIEHL, 2018; MARJANOVI *et al.*, 2015; PROVIS, John L.; DUXSON; VAN DEVENTER, 2010).

The conditions adopted in curing process also affect the synthesis and the type of product formed in the geopolymerization reactions. The increase of temperature during the curing period accelerates the dissolution reactions of silicates and aluminates. With the largest portion of Si dissolved in the system, more Si – O bonds are formed, increasing the content of more stable gel, rich in silica, and contributing to the gain of mechanical strength. In addition, the higher the curing temperature, the higher the water removal from the system, accelerating the growth of the gel phase. On the other hand, very high values can cause the substantial loss of water in fact necessary for the development of strength. Therefore, some authors indicate a temperature range between 30 °C and 90 °C (CHEN *et al.*, 2016; GRANIZO; PALOMO; FERNANDEZ-JIMÉNEZ, 2014).

In order to make geopolymer even more sustainable and solve the problem related to the incorrect disposal of solid waste, industrial by-products have been applied as precursors or

activators in geopolymeric materials. These raw materials must also present physical, chemical and mineralogical characteristics that justify their application in alkali-activated materials, providing good mechanical performance and durability. Some examples are wastes from the mining industry, rice husk ashes, chamotte, waste glass, biomass ashes, construction waste, among others (ALONSO *et al.*, 2019; ARULRAJAH *et al.*, 2016; CRISTELO *et al.*, 2018; MEJÍA; MEJÍA DE GUTIÉRREZ; PUERTAS, 2013; SASSONI *et al.*, 2016; VILLAQUIRÁN-CAICEDO, 2019; YE; ZHANG; SHI, 2017). In general, these materials have considerable levels of reactive silica and alumina, present pozzolanic activity, in addition to other characteristics such as particle size distribution and specific area similar to those of conventional raw materials, allowing the development of geopolymerization reactions (PROVIS; PALOMO; SHI, 2015; ROŻEK; KRÓL; MOZGAWA, 2019).

Chamotte, which consists of waste from red ceramic pieces, such as roof tiles and clay bricks, contains amorphous aluminosilicates. Therefore, it presents pozzolanic activity and potential use as a precursor. Although its reactivity is lower than that of metakaolin, for example, its value as a precursor can be optimized by controlling formulations and preparation conditions, being possible to achieve compressive strength values greater than 20 MPa (BERNAL *et al.*, 2016; GADO *et al.*, 2020; REIG *et al.*, 2013). Besides, chamotte is also attractive because it is a cheaper option and more suitable from the environmental point of view (KULOVANÁ *et al.*, 2016). Rakhimova and Rakhimov (RAKHIMOVA; RAKHIMOV, 2015) conducted a study to replace blast furnace slag by chamotte in alkali-activated pastes, and observed that substitutions between 15% and 40% promoted the increased of compressive strength at 28 days. According to Komnitsas *et al.* (2015), the mechanical strength can be increased by reducing the size of the particles of the chamotte. With the reduction of particle size, there is an increase in fineness and the specific area of the material, making the alkali-activation process more intense.

For the activation of geopolymers using chamotte as a precursor, Wong *et al.* (2018) suggest that the concentration of the activating solution should be in the range between 5 M and 8 M. Lower concentrations result in the decrease of mechanical strength, due to the insufficient amount of alkalis for balancing the loads in the geopolymeric system. Higher concentrations, in turn, can cause carbonation, which reduces NaOH reactivity. In addition, the supply of soluble silicates to the system – such as the addition of sodium silicate, or another source rich in silicates – promotes the improvement of mechanical strength, due to the greater formation of Si-O-Si bonds. On the other hand, Komnitsas *et al.* (2015) obtained satisfactory results for concentrations of up to 12 M. Also according to the same authors, the mechanical strength can

be increased by reducing the size of the particles of chamotte. With the reduction of particle size, there is an increase in fineness and the specific area of the material, making the alkali-activation process more intense. The authors have adopted the average particle diameter around 20 to 25 μm (FOŘT *et al.*, 2018; ROVNANÍK *et al.*, 2018; TUYAN; ANDIÇ-ÇAKIR; RAMYAR, 2018).

Waste glass is a waste produced in large quantities, being commonly disposed of in landfills. Although the waste can be recycled in several ways, this process inside the glass industry is complicated by logistical issues such as the variety of colors, chemical composition, amount of impurities and different toxic elements linked to the residue, making its reuse expensive and impractical (MENCHACA-BALLINAS; ESCALANTE-GARCIA, 2019; RASHID *et al.*, 2018).

Given this situation, it is essential to search for ways to reuse waste glass. It presents high levels of SiO_2 in its composition (> 60 %), being a large part in the amorphous condition. This makes the waste a viable alternative for the production of alkaline sodium silicate solutions, replacing commercial products. Studies have shown that the levels of mechanical strength and the phases formed in geopolymerization are similar to those observed with the use of conventional activators (PUERTAS; TORRES-CARRASCO; ALONSO, 2015; VINAI; SOUTSOS, 2019). Using fly ash of class F as precursor, Torres-Carrasco and Puertas (2015) produced geopolymeric pastes activated with NaOH 10 M solution plus varied amounts of urban waste glass (10, 15 and 25 g per 100 ml of solution). At 28 days, the compressive strength of the pastes produced with 15 g of waste glass was higher than 37 MPa, a value comparable to those obtained with commercial sodium silicate. However, the addition of more waste glass (25 g) promoted the decrease in mechanical strength, due to the decrease in pH and excessive increase of SiO_2/Na_2O ratio in the activator.

Tchakouté *et al.* (2016) and Vinai and Soutsos (2019) also used waste glass as an activator in geopolymers based on metakaolin and fly ash, respectively, and obtained compressive strength values about 40 MPa. After a cost analysis, Vinai and Soutsos (2019) observed that when the waste glass-based activator is used, it corresponds to only 14 % of the total cost of alkaline concrete. With the use of commercial activators, this percentage rises to 41 %.

In view of the above, the objectives of this research are: to evaluate the physical and mechanical behavior of geopolymeric pastes and mortars, produced with industrial wastes – chamotte and waste glass – in both phases (precursor and activator). Microstructural analyses

were also performed, in order to better understand the effect of molar concentration and content of waste glass on the chemical characteristics and development of geopolymerization reactions.

2 OBJECTIVES

2.1 General objectives

The general objective of this research is the formulation and assessment of physical and mechanical performance of geopolymeric pastes and mortars, produced from industrial wastes in both phases – precursor and activator.

2.2 Specific objectives

To achieve the general objective of this research, the following specific objectives were defined.

i. Investigate the influence of waste glass, obtained from polishing process, as activator on the physical, chemical and mechanical properties of chamotte-based pastes.
ii. Determine the best mixtures, by means of a statistical analysis and aiming at maximizing the mechanical strength.
iii. Assess the reaction kinetics, mechanical and microstructural properties of the best pastes.
iv. Evaluate the physical and mechanical properties of geopolymeric mortars, based on the best pastes obtained previously.

3 JUSTIFICATION

The cement industry is recognized by the significant impacts caused in social, economic and environmental areas. One ton of CO_2 is emitted into the atmosphere, approximately, for each ton of cement produced. The total emission complains the CO_2 formed in the clinker production and the CO_2 resulting from burning the fuel used in the binder manufacturing process (ALI; SAIDUR; HOSSAIN, 2011; EL-GAMAL; SELIM, 2017). Damilola (2013) highlights that, in few years, the pollution generated by cement industry will represent 17% of the global emission of CO_2. In view of this scenario, the study and development of alkali-activated materials becomes attractive due to the need of greater environmental conscience and

sustainability in the civil construction sector (HASSAN; ARIF; SHARIQ, 2019). Besides the reduction of CO_2 emission, the production of geopolymer is capable of promoting an energy saving equal to 60% compared to Portland cement manufacturing (KANTARCI; TÜRKMEN; EKINCI, 2019). However, the production chain of geopolymer should be geared toward this purpose to ensure these advantages (PROVIS, 2018).

The industrial wastes considered in this research present potential to be applied as raw materials in geopolymer production. Chamotte present behavior and characteristics similar to metakaolin, which is a conventional precursor. As it is generated after firing process, normally around 800°C (AZEVEDO *et al.*, 2020), chamotte does not need additional thermal treatment to become amorphous and reactive. The only treatment that should be applied is grinding, in order to reduce the particle size and obtain a particle size distribution close to that of metakaolin. On the other hand, the waste glass is rich in SiO_2 and Na_2O, and can present small particles that facilitate the dissolution (POURABBAS BILONDI; TOUFIGH; TOUFIGH, 2018). Thus, this waste presents physical and chemical properties that justify its application in activator solutions, replacing the commercial sodium silicate.

The study on the replacement of conventional activators by an alternative one is also justified by economic issues – the costs associated to geopolymer production. Pacheco-Torgal et al. (PACHECO-TORGAL *et al.*, 2012) discuss the high costs of alkali-activated binders in relation to the Portland cement, which can discourage its use. McLellan *et al.* (2011) analyzed the costs of geopolymer production in an Australian industry. They concluded that the sodium silicate was the most expensive raw material compared to others (metakaolin, fly ash and sodium hydroxide), corresponding to US$ 400/ton of geopolymer, approximately. Therefore, the substitution of commercial sodium silicate by an industrial waste will make the product more competitive and more viable to be implemented in construction process, without loss of technical performance.

4 NOVELTY

The results of the experimental programming will contribute to the state of the art on geopolymer science, since the influence of two industrial wastes is being investigated, and few studies approach the application of wastes in both parts – precursor and activator.

The combination of chamotte as precursor and waste glass as additional activator was not explored yet, considering the published works in national and international journals. About the use of waste glass as an activator, there are researches in the literature, but with no

discussions about the interaction between the content of waste glass and the molar concentration of the NaOH-based solution. Besides, there are few studies comprising a deeply investigation about the reaction development of chamotte-based geopolymer by means of calorimetric technique.

5 WORK STRUCTURE

This work was structured in five sections, as follows:

- *General Introduction*: presents the initial considerations that explain the main concepts and contextualizes the work; the general and specific objectives; the justifications for the development of this work, highlighting its relevance in the field of civil engineering and materials science; the novelty of this research; and the work structure.
- *Article 1*: *Application of eco-friendly alternative activators in alkali-activated materials: a review* – presents a review about the use of conventional and alternative activators used in geopolymer production. The alternative activators consisted of silica fume and industrial wastes that present substantial contents of amorphous silica, such as the waste glass, one of the raw materials adopted in the present research.
- *Article 2*: *Evaluation of eco-efficient geopolymer using chamotte and waste glass-based alkaline solutions* – presents the study of geopolymeric pastes produced from chamotte as precursor and waste-glass based solutions. Twelve alkaline solutions with different NaOH molar concentrations and waste glass content were tested, using a factorial design of experiments. The pastes were characterized for bulk density, flexural and compressive strength. Microstructural analyses were performed, such as XRD, FT-IR and SEM/EDS techniques.
- *Article 3*: *Physical and mechanical characterization of mortars produced from chamote and waste glass geopolymer binder* – presents the production and characterization of mortars, produced from the best pastes obtained in Chapter 2. Properties such as consistency index, incorporated air and mechanical strength were evaluated.

- *General conclusions*: presents the final considerations of this research and suggestions for future works in this field.

REFERENCES

ALI, M. B.; SAIDUR, R.; HOSSAIN, M. S. A review on emission analysis in cement industries. **Renewable and Sustainable Energy Reviews**, v. 15, n. 5, p. 2252–2261, jun. 2011. Disponível em: <https://linkinghub.elsevier.com/retrieve/pii/S1364032111000566>.

ALONSO, M. M. et al. Olive biomass ash as an alternative activator in geopolymer formation: A study of strength, durability, radiology and leaching behaviour. **Cement and Concrete Composites**, v. 104, p. 103384, 2019. Disponível em: <https://doi.org/10.1016/j.cemconcomp.2019.103384>.

ARULRAJAH, A. et al. Strength and microstructure evaluation of recycled glass-fly ash geopolymer as low-carbon masonry units. **Construction and Building Materials**, v. 114, p. 400–406, 2016. Disponível em: <http://dx.doi.org/10.1016/j.conbuildmat.2016.03.123>.

ASSI, L. N.; EDDIE DEAVER, E.; ZIEHL, P. Effect of source and particle size distribution on the mechanical and microstructural properties of fly Ash-Based geopolymer concrete. **Construction and Building Materials**, v. 167, p. 372–380, 2018. Disponível em: <https://doi.org/10.1016/j.conbuildmat.2018.01.193>.

AZEVEDO, A. R. G. et al. Potential use of ceramic waste as precursor in the geopolymerization reaction for the production of ceramic roof tiles. **Journal of Building Engineering**, v. 29, p. 101156, maio 2020. Disponível em: <https://linkinghub.elsevier.com/retrieve/pii/S2352710219320200>.

BERNAL, S. A. et al. Management and valorisation of wastes through use in producing alkali-activated cement materials. **Journal of Chemical Technology and Biotechnology**, v. 91, n. 9, p. 2365–2388, 2016.

CHEN, L. et al. Preparation and properties of alkali activated metakaolin-based geopolymer. **Materials**, v. 9, n. 9, p. 1–12, 2016.

CRISTELO, N. et al. Stabilisation of construction and demolition waste with a high fines content using alkali activated fly ash. **Construction and Building Materials**, v. 170, p. 26–39, 2018. Disponível em: <https://doi.org/10.1016/j.conbuildmat.2018.03.057>.

DAMILOLA, O. M. Syntheses, Characterization and Binding Strength of Geopolymers: A Review. **International Journal of Materials Science and Applications**, v. 2, n. 6, p. 185, 2013. Disponível em: <http://www.sciencepublishinggroup.com/journal/paperinfo.aspx?journalid=123&doi=10.11648/j.ijmsa.20130206.14>.

DIAZ, E. I.; ALLOUCHE, E. N.; EKLUND, S. Factors affecting the suitability of fly ash as source material for geopolymers. **Fuel**, v. 89, n. 5, p. 992–996, 2010. Disponível em:

<http://dx.doi.org/10.1016/j.fuel.2009.09.012>.

EL-GAMAL, S. M. A.; SELIM, F. A. Utilization of some industrial wastes for eco-friendly cement production. **Sustainable Materials and Technologies**, v. 12, p. 9–17, jul. 2017. Disponível em: <https://linkinghub.elsevier.com/retrieve/pii/S2214993717300167>.

FOŘT, J. et al. Application of waste brick powder in alkali activated aluminosilicates: Functional and environmental aspects. **Journal of Cleaner Production**, v. 194, p. 714–725, 2018.

GADO, R. A. et al. Alkali Activation of Waste Clay Bricks: Influence of The Silica Modulus, SiO2/Na2O, H2O/Na2O Molar Ratio, and Liquid/Solid Ratio. **Materials**, v. 13, n. 2, p. 383, 14 jan. 2020. Disponível em: <https://www.mdpi.com/1996-1944/13/2/383>.

GARTNER, E. M.; MACPHEE, D. E. A physico-chemical basis for novel cementitious binders. **Cement and Concrete Research**, v. 41, n. 7, p. 736–749, jul. 2011. Disponível em: <https://linkinghub.elsevier.com/retrieve/pii/S0008884611000822>.

GAVALI, H. R. et al. Development of sustainable alkali-activated bricks using industrial wastes. **Construction and Building Materials**, v. 215, p. 180–191, 2019. Disponível em: <https://doi.org/10.1016/j.conbuildmat.2019.04.152>.

GRANIZO, N.; PALOMO, A.; FERNANDEZ-JIMÉNEZ, A. Effect of temperature and alkaline concentration on metakaolin leaching kinetics. **Ceramics International**, v. 40, n. 7, p. 8975–8985, ago. 2014. Disponível em: <https://linkinghub.elsevier.com/retrieve/pii/S0272884214002703>.

HASSAN, A.; ARIF, M.; SHARIQ, M. Use of geopolymer concrete for a cleaner and sustainable environment – A review of mechanical properties and microstructure. **Journal of Cleaner Production**, v. 223, p. 704–728, jun. 2019. Disponível em: <https://linkinghub.elsevier.com/retrieve/pii/S0959652619307401>.

HEAH, C. Y. et al. Study on solids-to-liquid and alkaline activator ratios on kaolin-based geopolymers. **Construction and Building Materials**, v. 35, p. 912–922, 2012. Disponível em: <http://dx.doi.org/10.1016/j.conbuildmat.2012.04.102>.

KANTARCI, F.; TÜRKMEN, İ.; EKINCI, E. Optimization of production parameters of geopolymer mortar and concrete: A comprehensive experimental study. **Construction and Building Materials**, v. 228, p. 116770, dez. 2019. Disponível em: <https://linkinghub.elsevier.com/retrieve/pii/S0950061819321889>.

KHALE, D.; CHAUDHARY, R. Mechanism of geopolymerization and factors influencing its development: A review. **Journal of Materials Science**, v. 42, n. 3, p. 729–746, 2007.

KOMNITSAS, K. et al. Effect of synthesis parameters on the quality of construction and demolition wastes (CDW) geopolymers. **Advanced Powder Technology**, v. 26, n. 2, p. 368–376, mar. 2015. Disponível em: <https://linkinghub.elsevier.com/retrieve/pii/S0921883114003057>.

KUA, T.-A. et al. Environmental and economic viability of Alkali Activated Material (AAM) comprising slag, fly ash and spent coffee ground. **International Journal of Sustainable Engineering**, v. 12, n. 4, p. 223–232, 4 jul. 2019. Disponível em: <https://www.tandfonline.com/doi/full/10.1080/19397038.2018.1492043>.

KULOVANÁ, T. et al. Mechanical, durability and hygrothermal properties of concrete produced using Portland cement-ceramic powder blends. **Structural Concrete**, v. 17, n. 1, p. 105–115, mar. 2016. Disponível em: <http://doi.wiley.com/10.1002/suco.201500029>.

LIU, Y. et al. An overview on the reuse of waste glasses in alkali-activated materials. **Resources, Conservation and Recycling**, v. 144, p. 297–309, maio 2019. Disponível em: <https://linkinghub.elsevier.com/retrieve/pii/S0921344919300631>.

LUUKKONEN, T. et al. One-part alkali-activated materials: A review. **Cement and Concrete Research**, v. 103, n. November 2017, p. 21–34, 2018.

MARJANOVI, N. et al. Comparison of two alkali-activated systems : mechanically activated fly ash and fly ash-blast furnace slag blends. v. 108, p. 231–238, 2015.

MCLELLAN, B. C. et al. Costs and carbon emissions for geopolymer pastes in comparison to ordinary portland cement. **Journal of Cleaner Production**, v. 19, n. 9–10, p. 1080–1090, jun. 2011. Disponível em: <https://linkinghub.elsevier.com/retrieve/pii/S0959652611000680>.

MEJÍA, J. M.; MEJÍA DE GUTIÉRREZ, R.; PUERTAS, F. Ceniza de cascarilla de arroz como fuente de sílice en sistemas cementicios de ceniza volante y escoria activados alcalinamente. **Materiales de Construccion**, v. 63, n. 311, p. 361–375, 2013.

MENCHACA-BALLINAS, L. E.; ESCALANTE-GARCIA, J. I. Low CO2 emission cements of waste glass activated by CaO and NaOH. **Journal of Cleaner Production**, v. 239, p. 117992, dez. 2019. Disponível em: <https://linkinghub.elsevier.com/retrieve/pii/S0959652619328628>.

NOVAIS, R. M. et al. Waste glass from end-of-life fluorescent lamps as raw material in geopolymers. **Waste Management**, v. 52, p. 245–255, 2016. Disponível em: <http://dx.doi.org/10.1016/j.wasman.2016.04.003>.

PACHECO-TORGAL, F. et al. Durability of alkali-activated binders: A clear advantage over Portland cement or an unproven issue? **Construction and Building Materials**, v. 30, p. 400–405, 2012. Disponível em: <http://dx.doi.org/10.1016/j.conbuildmat.2011.12.017>.

PALOMO, A.; GRUTZECK, M. W.; BLANCO, M. T. Alkali-activated fly ashes: A cement for the future. **Cement and Concrete Research**, v. 29, n. 8, p. 1323–1329, 1999.

POURABBAS BILONDI, M.; TOUFIGH, M. M.; TOUFIGH, V. Using calcium carbide residue as an alkaline activator for glass powder–clay geopolymer. **Construction and Building Materials**, v. 183, p. 417–428, 2018. Disponível em: <https://doi.org/10.1016/j.conbuildmat.2018.06.190>.

PROVIS, J. L. et al. The role of mathematical modelling and gel chemistry in advancing

geopolymer technology. **Chemical Engineering Research and Design**, v. 83, n. 7 A, p. 853–860, 2005.

PROVIS, John L. Alkali-activated materials. **Cement and Concrete Research**, v. 114, p. 40–48, 2018. Disponível em: <http://dx.doi.org/10.1016/j.cemconres.2017.02.009>.

_____. Geopolymers and other alkali activated materials: Why, how, and what? **Materials and Structures/Materiaux et Constructions**, v. 47, n. 1–2, p. 11–25, 2014.

PROVIS, J. L.; DUXSON, P.; VAN DEVENTER, J. S. J. The role of particle technology in developing sustainable construction materials. **Advanced Powder Technology**, v. 21, n. 1, p. 2–7, 2010. Disponível em: <http://dx.doi.org/10.1016/j.apt.2009.10.006>.

PROVIS, J. L.; PALOMO, A.; SHI, C. Advances in understanding alkali-activated materials. **Cement and Concrete Research**, v. 78, p. 110–125, 2015. Disponível em: <http://dx.doi.org/10.1016/j.cemconres.2015.04.013>.

PUERTAS, F.; TORRES-CARRASCO, M.; ALONSO, M. M. Reuse of urban and industrial waste glass as a novel activator for alkali-activated slag cement pastes: a case study. **Handb. Alkali-Activated Cem. Mortars Concr.** [S.l.]: Elsevier, 2015. p. 75–109. Disponível em: <https://linkinghub.elsevier.com/retrieve/pii/B9781782422761500046>.

RAKHIMOVA, N. R.; RAKHIMOV, R. Z. Alkali-activated cements and mortars based on blast furnace slag and red clay brick waste. **Materials & Design**, v. 85, p. 324–331, nov. 2015. Disponível em: <https://linkinghub.elsevier.com/retrieve/pii/S0264127515300241>.

RASHID, K. et al. Analytical framework for value added utilization of glass waste in concrete: Mechanical and environmental performance. **Waste Management**, v. 79, p. 312–323, set. 2018. Disponível em: <https://linkinghub.elsevier.com/retrieve/pii/S0956053X18304835>.

REIG, L. et al. Properties and microstructure of alkali-activated red clay brick waste. **Construction and Building Materials**, v. 43, p. 98–106, jun. 2013. Disponível em: <https://linkinghub.elsevier.com/retrieve/pii/S0950061813001013>.

ROVNANÍK, P. et al. Rheological properties and microstructure of binary waste red brick powder/metakaolin geopolymer. **Construction and Building Materials**, v. 188, p. 924–933, nov. 2018. Disponível em: <https://linkinghub.elsevier.com/retrieve/pii/S0950061818320907>.

ROŻEK, P.; KRÓL, M.; MOZGAWA, W. Geopolymer-zeolite composites: A review. **Journal of Cleaner Production**, v. 230, p. 557–579, set. 2019. Disponível em: <https://linkinghub.elsevier.com/retrieve/pii/S0959652619316786>.

SAMARAKOON, M. H. et al. Recent advances in alkaline cement binders: A review. **Journal of Cleaner Production**, v. 227, p. 70–87, 2019. Disponível em: <https://doi.org/10.1016/j.jclepro.2019.04.103>.

SASSONI, E. et al. Valorization of brick waste by alkali-activation: A study on the possible use for masonry repointing. **Ceramics International**, v. 42, n. 13, p. 14685–14694, out. 2016.

Disponível em: <https://linkinghub.elsevier.com/retrieve/pii/S0272884216309191>.

SHI, C.; JIMÉNEZ, A. F.; PALOMO, A. New cements for the 21st century: The pursuit of an alternative to Portland cement. **Cement and Concrete Research**, v. 41, n. 7, p. 750–763, 2011.

TCHAKOUTÉ, H. K. et al. Geopolymer binders from metakaolin using sodium waterglass from waste glass and rice husk ash as alternative activators: A comparative study. **Construction and Building Materials**, v. 114, p. 276–289, 2016.

TORRES-CARRASCO, M.; PUERTAS, F. Waste glass in the geopolymer preparation. Mechanical and microstructural characterisation. **Journal of Cleaner Production**, v. 90, p. 397–408, mar. 2015. Disponível em: <https://linkinghub.elsevier.com/retrieve/pii/S0959652614012815>.

TUYAN, M.; ANDIÇ-ÇAKIR, Ö.; RAMYAR, K. Effect of alkali activator concentration and curing condition on strength and microstructure of waste clay brick powder-based geopolymer. **Composites Part B: Engineering**, v. 135, n. September 2017, p. 242–252, 2018. Disponível em: <https://doi.org/10.1016/j.compositesb.2017.10.013>.

VILLAQUIRÁN-CAICEDO, M. A. Studying different silica sources for preparation of alternative waterglass used in preparation of binary geopolymer binders from metakaolin/boiler slag. **Construction and Building Materials**, v. 227, p. 1–13, 2019.

VINAI, R.; SOUTSOS, M. Production of sodium silicate powder from waste glass cullet for alkali activation of alternative binders. **Cement and Concrete Research**, v. 116, p. 45–56, fev. 2019. Disponível em: <https://linkinghub.elsevier.com/retrieve/pii/S0008884618307518>.

WONG, C. L. et al. Potential use of brick waste as alternate concrete-making materials: A review. **Journal of Cleaner Production**, v. 195, p. 226–239, set. 2018. Disponível em: <https://linkinghub.elsevier.com/retrieve/pii/S0959652618315397>.

YE, J.; ZHANG, W.; SHI, D. Properties of an aged geopolymer synthesized from calcined ore-dressing tailing of bauxite and slag. **Cement and Concrete Research**, v. 100, p. 23–31, out. 2017. Disponível em: <https://linkinghub.elsevier.com/retrieve/pii/S0008884616311218>.

ZHUANG, X. Y. et al. Fly ash-based geopolymer: Clean production, properties and applications. **Journal of Cleaner Production**, v. 125, p. 253–267, 2016. Disponível em: <http://dx.doi.org/10.1016/j.jclepro.2016.03.019>.

ARTICLE 1

APPLICATION OF ECO-FRIENDLY ALTERNATIVE ACTIVATORS IN ALKALI-ACTIVATED MATERIALS: A REVIEW [1]

Abstract:

Alkali-activated materials are a new class of compounds that have been studied by several authors worldwide. Alkali-activated binders can be competitive alternatives to traditional Portland cement, especially concerning CO_2 emissions into the environment. However, in order to obtain this advantage, it is essential to use activators that were produced cleanly and sustainably, which is not the case of commercial products such as NaOH or sodium silicate. This paper provides a brief discussion about the activators traditionally used, and a review of existing literature about alternative activators, produced from agricultural or industrial wastes. Factors such as molar ratios and preparation of the solution were highlighted. The mechanical behavior of the pastes and mortars was also assessed, showing that the performance of alternative activators can be similar or even better than the conventional ones. Finally, some topics for future research on new activators were identified, aiming to stimulate more studies in this field.

Keywords: alkali activated materials, activators, wastes, sustainability.

[1] Manuscript published by the Journal of Building Engineering. Accepted in 13 November 2020. Online available in 18 November 2020. First author: Beatryz Cardoso Mendes. https://doi.org/10.1016/j.jobe.2020.102010.

1 INTRODUCTION

Alkali-activated binders are relatively new materials and have been widely studied around the world [1–3]. These materials were developed as an alternative to replacing Portland cement, used in concretes, mortars and pastes. Alkali-activated binders are considered less aggressive from an environmental point of view, due to the lower emission of atmospheric CO_2 when compared to the Portland cement industry [4,5]. In addition, they have good mechanical and durability characteristics, such as high heat resistance, which has motivated several researchers to develop technological studies on this new type of material [6,7].

Alkali-activated binders, including those called “geopolymers”, can be defined as materials produced through a reaction of an aluminosilicate source - usually obtained in powder form, as an industrial residue or other low added value raw material - with an alkaline activator. This activator usually consists of an aqueous solution of hydroxides, silicates, carbonates, or alkaline sulfates [2].

According to Samarakoon et al. [8], within the class of alkali-activated binders is the geopolymers subgroup. These are differentiated by the series of reactions developed and the final products of these reactions, which vary according to the composition of the precursor and the concentration of the alkaline solution. In the case of alkali-activated materials, the precursor is essentially composed of Si, Al and high amounts of Ca. Some examples are blast furnace slag and steel slag. In addition, these materials require a low or medium activator concentration for their synthesis [9]. The products of the reaction between calcium-rich slags and alkaline hydroxides or silicates are generally hydrated sodium/potassium aluminum silicate gel (N(K)-A-S-H) and hydrated calcium aluminum silicate gel (C-A-S-H). The latter has a structure similar to the resulting gel from the hydration of Portland cement (C-S-H) but with lower Ca content and more aluminum substitutions in tetrahedral sets [8,10].

Geopolymers consist of three-dimensional aluminosilicates synthesized by a high concentration alkaline solution (hydroxide or silicate). As precursors, materials rich in Si and Al are used, with low or no calcium content. Calcined clays (e.g., metakaolin), fly ash and mining tailings with high percentages of silica and alumina can be applied as raw materials [9]. The resulting product from the geopolymerization process is three-dimensional structures of silico-aluminates (gel type N-A-S-H, N representing the alkaline cation). Geopolymers are also chemically referred to as poly(sialates), being sialate an abbreviation for silico-oxo aluminate. Crystalline poly(sialates) have structures similar to those of zeolites, minerals formed from the alteration of pozzolanic rocks [11,12].

Geopolymeric or alkali-activated materials can have a variety of properties and characteristics, which depend on the components used - including the type of activator - and the processing conditions. These properties include high mechanical strength, fire resistance, low shrinkage and low thermal conductivity. It is noteworthy that these attributes are not necessarily inherent to all types of formulations. In other words, the properties of the material can be modified or improved - according to the intended use of the product - through adjustments to mixtures or processing techniques [13,14].

This class of materials is very versatile due to the wide variety of raw materials and forms of production, in addition to being locally adaptable. Another major advantage that makes the use of alkali-activated binders attractive is the potential reduction in CO_2 emissions compared to the use of Portland cement-based products [15]. According to Turner and Collins [16], for each kilogram of processed cement, about 0.66 to 0.82 kg of CO_2 is released. The manufacture of concrete from geopolymers can result in a reduction in CO_2 emissions of 26 to 45% compared to the production of Portland cement. In addition, the raw materials used are generally industrial by-products, with little or no environmental impact attributed and low cost. However, it should be highlighted that this greater sustainability and reduction in CO_2 emissions is only possible if the production chain and the design of the mixtures are developed with these results in mind. If these issues are neglected throughout the process of choosing materials and materials preparation, alkali-activated products may have higher emissions than that of Portland cement-based concretes [2].

In most cases, alkaline activators are the main cause of environmental damage associated with alkali-activated binders, besides being the most expensive component. Sodium silicate, for example, has a high energy and environmental cost (≈0.30 kg CO_2 / kg) when produced traditionally [15,17]. Therefore, it is necessary to research and develop alkali-activated products with alternative and low-cost activators, produced preferably using residual materials and whose processing is not aggressive from an environmental point of view.

In the technical literature, much has been discussed about the incorporation of alternative raw materials as precursors in alkali-activated materials. However, studies on new activators have been less reported. In addition, there is still no consistent review about the types of non-conventional activators already developed and tested, nor their feasibility of application. Therefore, the focus of this work is the discussion - from environmental, technical and technological points of view – about conventional and alternative activators, highlighting their main effects in the alkali-activation process, final properties and potential applicability. Processing factors such as molar ratios, molar concentrations and preparations of the solutions

were mentioned, as well the mechanical behavior of pastes and mortars produced from non-conventional activators.

2 METHODOLOGY

In this work, articles published in journals relevant to the subject addressed were used as materials. The research sites used were ScienceDirect, Google Scholar and specific editorial sites. The focus of the research was on studies that address the effect caused by the activator on the alkali-activated materials produced, comparisons between two or more types of activators, and those that deal with alternative activators. After researching and reading the articles, the main information regarding the proposed theme was extracted, comparing the data found by the authors.

3 CONVENTIONAL ACTIVATORS

For alkali-activation reactions to occur, it is necessary to have an alkaline medium for the dissolution of aluminosilicates and/or calcium-based compounds present in the precursor. This medium consists of an alkaline solution with the presence of compounds called activators (

Figure 1.1). The type and dosage of the activator play an important role in controlling the rheology of the mixture in the fresh state and the structure and properties of the geopolymer in the hardened state [18].

Figure 1.1. Representation of synthesis of alkali-activated materials.

The activators commonly used are hydroxides (MOH) and silicates ($M_2O \cdot rSiO_2$), in which M corresponds to the alkaline element, usually sodium, potassium or calcium. These constituents can be applied individually or in a mixture. Soluble silicate provides additional SiO_2 to the system, while the hydroxide ensures the high alkalinity of the solution [19]. For the activation of calcium-rich precursors, such as slags, the use of compounds such as sodium carbonate and sulfate - Na_2CO_3 and Na_2SO_4, respectively - can also be effective [15,20,21].

The use of sodium carbonate as an activator can raise the pH of the solution present in the pores of alkali-activated slags, reaching values close to those observed in Portland cement-based concretes. In addition, this compound is less aggressive to the environment, cheaper and more available. However, it is considered a "weak" activator, since the reaction of the Ca^{2+} ions present in the precursor with the CO_3^{2-} ions of the activator, forming calcite, occurs before the pH reaches the value necessary for the dissolution of silica and the formation of C-A-S-H gel [20,22].

Most studies reported in the literature present sodium and potassium hydroxides and silicates as activators [23,24]. Table 1.1 shows the articles consulted, indicating the materials used as precursors and as activators for the production of alkali-activated binders, as well as other characteristics of the alkaline solution (such as concentration and hydroxide to silicate ratio).

Table 1.1. Alkali-activated materials produced from conventional activators.

Authors	Precursor	Activator	Product	Information on activating solution	Ref.
Ye et al.	Calcined ore-dressing tailing of bauxite and blast furnace slag	Sodium silicate and NaOH solution	Mortar	SiO_2/Na_2O = 1,80	[26]
Leong et al.	Fly ash (thermoelectric)	Sodium silicate, sodium hydroxide, potassium and calcium	Mortar	Series 1: NaOH 8M + Na_2SiO_3; Series 2: KOH 8M + Na_2SiO_3; Series 3: $Ca(OH)_2$ + Na_2SiO_3 - Silicate/base ratios: 0.5, 1, 1.5, 2, 2.5, 3	[27]
Dias and Silva	Metakaolin	Sodium and potassium hydroxide	Mortar	Two solutions with molar concentration of 10,0 mol/L (one with NaOH, and another with KOH)	[28]
Humad et al.	Granulated blast slag with high MgO content	Anhydrous sodium carbonate and sodium silicate	Concrete and paste	Sodium silicate solution + NaOH with SiO_2/Na_2O ratios of 1 e 1.5; Proportion of sodium carbonate powder: 3%, 5%, 10% e 14%	[20]
Clausi et al.	Fly ash, metakaolin and waste sandstone sludge	Sodium hydroxide solution	Paste	NaOH 8M e 12M solutions	[29]
Zaharaki, Galetakis and Komnitsas	Electric arc furnace slag + Red mud + RCD	NaOH + Sodium silicate	Paste	NaOH + sodium silicate solutions with molar ratio of 8M, 10M and 12M	[30]
Adesanya et al.	Ladle slag	Sodium silicate and potassium hydroxide	Paste	Varying quantities of sodium silicate and KOH	[31]

Table 1.1. Alkali-activated materials produced from conventional activators (continuation).

Authors	Precursor	Activator	Product	Information on activating solution	Ref.
Reig et al.	Chamotte (powder) + calcium aluminate cement	NaOH + Sodium silicate	Mortar	SiO_2/Na_2O = 1,60 (molar ratio)	[32]
Novais et al.	Waste glass (fluorescent lamps) and metakaolin	NaOH + Hydrated sodium silicate	Paste	Na_2SiO_3/NaOH = 1.43; NaOH solutions: 10M and 12M	[33]
Zhang et al.	Blast furnace slag, fly ash and waste glass (powder)	NaOH	Paste	NaOH 4M solution	[34]
Arulrajah et al.	Waste glass and fly ash	NaOH + Sodium silicate	Paste	NaOH + sodium silicate solution with the following proportions Na_2SiO_3: NaOH: 90:10, 70:30, 50:50. The concentration of NaOH was established at 8M	[35]
Ranjbar et al.	Palm oil fuel ash and fly ash	NaOH + Sodium silicate	Mortar	NaOH 16M + sodium silicate solution with Na_2SiO_3/NaOH ratio of 2.5	[36]
Gao et al.	Slag, municipal solid waste incineration (MSWI) bottom ash and waste granite powder	NaOH + Sodium silicate	Mortar	NaOH + sodium silicate solution with module (SiO_2/Na_2O) of 1.4	[23]
Robayo et al.	Chamotte	NaOH + Sodium silicate	Paste	NaOH + sodium silicate solution at varied concentrations of Na_2O (2-10%)	[24]
Rakhimova and Rakhimov	Blast furnace slag and chamotte	Sodium silicate and sodium carbonate	Paste and mortar	Sodium silicate solution and sodium carbonate with SiO_2/Na_2O modules of 1.5	[37]
Poinot et al.	Boiler ash, clay and hydrated lime	NaOH	Brick	NaOH solutions of 2M and 5M	[38]
Nazari and Sanjayan	Aluminum slag and iron slag	NaOH + Sodium silicate	Concrete	NaOH solutions of 8M, 12M e 16M + sodium silicate. The proportion of silicate in NaOH solution was 2.5:1	[39]
Abdalqader et al.	Fly ash and slag	Sodium carbonate	Paste	Na_2CO_3 contents in the solutions were 5% and 10% by weight of the powder mixtures	[21]
Zawrah et al.	Blast furnace slag and chamotte	NaOH + Sodium silicate	Paste	NaOH solution 8 mol / L + sodium silicate, with Na_2SiO_3 / NaOH ratio of 2.5 by volume	[40]
Tekin	Marble, travertine and volcanic tuff wastes	NaOH	Paste	1M, 5M and 10M NaOH solutions	[41]
Sun et al.	Waste ceramic	Sodium silicate, sodium and potassium hydroxide	Paste	Nine activating solutions with varying percentages of sodium silicate, and sodium and potassium hydroxides	[42]
Ahmari, Parameswaran and Zhang	Copper mine tailings and low-calcium flash-furnace copper smelter slag	NaOH	Paste	10M and 15M NaOH solutions	[43]
Ascensão et al.	Red mud and metakaolin	NaOH + Sodium silicate	Paste	10M NaOH solution + sodium silicate	[44]
Reig et al.	Chamotte	NaOH + Sodium silicate	Paste and mortar	Solutions prepared with NaOH and sodium silicate, varying the concentration of Na^+ ions (2.5, 5, 6, 7, 7.5, 8, 9 and 10) molar	[45]
Yliniemi et al.	Recovered fuel biofuel fly ash from fluidised-bed combustion+ metakaolin + slag	Sodium silicate	Paste	Sodium silicate solution with SiO_2 / Na_2O molar ratio of 2.5	[46]

Table 1.1. Alkali-activated materials produced from conventional activators (continuation).

Authors	Precursor	Activator	Product	Information on activating solution	Ref.
Nazari et al.	Fly ash and rice husk ash	NaOH + Sodium silicate	Paste	4M, 8M and 12M NaOH solution + sodium silicate, with Na_2SiO_3 / NaOH solutions ratio of 2.5 by weight	[47]
Novais et al.	Biomass fly ash and metakaolin	NaOH + Sodium silicate	Paste	12M NaOH solution + sodium silicate	[48]
Ozer and Uzun	Metakaolin	NaOH + Sodium silicate	Paste	8M NaOH solution; 8M NaOH solution + sodium silicate solution	[49]
Redden and Neithalath	Glass powder, fly ash, metakaolin and slag	NaOH	Mortar	4M, 6M and 8M NaOH solutions	[50]
Cristelo et al.	Construction and demolition waste and fly ash	NaOH + Sodium silicate	Paste	10M NaOH solution + sodium silicate; NaOH / sodium silicate ratio of 2 (by weight)	[51]
Fort et al.	Chamotte powder	NaOH + Sodium silicate	Paste	Mixture of NaOH and sodium silicate, with SiO_2 / Na_2O molar ratio of 1.6	[52]
Lu and Poon	Waste glass, fly ash and blast furnace slag	NaOH	Mortar	10M NaOH solution	[53]
Manjunath et al.	Blast furnace slag and fine quartz powder	NaOH + Sodium silicate	Mortar	NaOH + sodium silicate solutions with percentages of Na_2O: 5%, 6% and 7%	[54]
Tuyan, Çakir and Ramyar	Chamotte powder	NaOH + Sodium silicate	Mortar	NaOH + sodium silicate solution (SiO_2 / Na_2O module of 3.0 in the silicate)	[55]
Rovnaník et al.	Chamotte and metakaolin powder	NaOH + Sodium silicate	Paste	NaOH + sodium silicate solution with 1.4 module (SiO_2 / Na_2O)	[56]
Abdollahnejad et al.	Blast furnace slag and recycled ceramic aggregates	Sodium metasilicate	Mortar	Sodium metasilicate solution with 0.9 module (SiO_2 / Na_2O)	[57]
Robayo-Salazar et al.	Natural volcanic pozzolan and blast furnace slag	NaOH + Sodium silicate	Concrete	1.09 NaOH + sodium silicate solution with module (SiO_2 / Na_2O) of 1.09	[58]
Tho-In et al.	Waste glass powder and fly ash	NaOH + Sodium silicate	Paste	NaOH solution + sodium silicate 12M	[59]
Batista et al.	Metakaolin and silica fume	NaOH + Sodium silicate	Mortar	NaOH + sodium silicate solutions with varying proportions, guaranteeing SiO_2 / Al_2O_3 ratios of 3 and 3.8, and Na_2O / SiO_2 of 0.26	[60]
Rocha et al.	Metakaolin	NaOH, KOH, sodium silicate and potassium silicate	Mortar	Activating solutions with varying percentages of sodium and potassium silicates, and sodium and potassium hydroxides	[19]
Vargas et al.	Fly ash	NaOH	Mortar	NaOH solution, with variable NaOH content according to the desired Na_2O / SiO_2 molar ratios (0.2, 0.3 and 0.4)	[61]
Tanzer et al.	Blast furnace slag	Sodium and potassium hydroxide, sodium and potassium silicates	Paste	Solutions with variable SiO_2 / M_2O module, but constant alkali concentration equal to 2 mol/kg	[62]
Yang et al.	Blast furnace slag	Calcium hydroxide, sodium silicate and sodium carbonate	Mortar	Activators were added in solid and dry condition (With 7.5% Ca $(OH)_2$ in all formulations)	[63]
Wang et al.	Metakaolin	NaOH and sodium silicate	Paste	NaOH + sodium silicate solutions; NaOH:sodium silicate ratio equal to 4.15:1 (by weight). NaOH concentrations were 4, 6, 8, 10 and 12 mol / L	[64]
Phoo-ngernkham et al.	Fly ash and Blast furnace slag	NaOH and sodium silicate	Paste	NaOH solution (NH) 10 mol/L; sodium silicate solution (NS) and NaOH + sodium silicate (NHNS) with NH/NS ratio equal to 2.0	[65]

Table 1.1. Alkali-activated materials produced from conventional activators (continuation).

Authors	Precursor	Activator	Product	Information on activating solution	Ref.
Phoo-ngernkham et al.	Fly ash and Portland cement	NaOH and sodium silicate	Mortar	NaOH solution (NH) 10 mol/L; sodium silicate solution (NS) and NaOH + sodium silicate (NHNS) with NH/NS ratio equal to 2.0	[66]

Rocha et al. [19] evaluated the performance of Metakaolin-based geopolymers produced from four different alkaline solutions: NaOH + Na_2SiO_3; NaOH + K_2SiO_3; KOH + Na_2SiO_3; and KOH + K_2SiO_3. The authors observed that the mechanical, thermal and morphological behavior of geopolymers varies according to the activator used. In terms of mechanical strength, the best results correspond to samples prepared with sodium hydroxide. The pieces made with potassium silicate showed uniform morphology and a dense gel phase. The samples with the sodium silicate exhibited a microstructure with pores and micro-cracks.

Fernández-Jiménez and Palomo [25] studied the effect of three types of activators on the alkali-activation of class F fly ash: NaOH, NaOH + sodium silicate, and NaOH + sodium carbonate. The authors concluded that the addition of sodium silicate in the NaOH solution increased the degree of condensation and, consequently, the mechanical strength. The addition of carbonate ions was not satisfactory: the formation of sodium bicarbonate resulted in an increase in the acidity of the system and a reduction in reactivity between the components.

Humad et al. [20] produced concretes and pastes from granulated blast furnace slag with a high content of MgO, anhydrous sodium carbonate (powder) and sodium silicate solution. The authors observed that the concretes activated with sodium carbonate showed less abatement, in the fresh state, and shorter initial setting times in relation to the concretes produced with sodium silicate. The combination of 5% sodium silicate and 5% sodium carbonate (by weight) resulted in an increased slump and setting times without significant loss of mechanical strength.

Rakhimova and Rakhimov [37] investigated the alkali-activation of blast furnace slag and ceramic bricks waste (chamotte) using sodium silicate and sodium carbonate as activators. In general, regardless of the content of the chamotte incorporated as a precursor, the highest values of axial compressive strength were found in pastes and mortars produced with sodium silicate as an activator. The authors concluded that the factor that most influenced mechanical strength was the type of alkaline solution used.

Zhang et al. [67] point out that the use of activators with dissolved silicates is preferable to the use of only hydroxide and carbonate since the products formed tend to develop greater strength and denser microstructures. On the other hand, silicate-based activators are much more

complex from the chemical point of view, being able to reduce the crystalline formation that occurs when only hydroxide is used. The authors indicate that the addition of dissolved silicates must be such that it keeps the SiO_2/Na_2O ratio between 1 and 2. Other authors also confirm that the SiO_2/Na_2O ratio influences the degree of polymerization and the mechanical strength gain of alkaline fly ash. activated [60]. Vargas et al. [60] concluded that geopolymer mortars based on fly ash, subjected to curing at 80 °C, showed greater compressive strength (13.74 MPa at 28 days) for a molar ratio SiO_2/Na_2O equal to 2.5.

The researches of Phoo- ngernkham et al. [65,66] corroborate the finding of Zhang et al. [67]. The authors observed that higher values of compressive strength were found with the use of mixed solution of sodium silicate and sodium hidroxide, or only sodium silicate, in álcali-activated materials from fly ash and blast furnace slag. This increase was more expressive in the mixtures with higher contents of blast furnace slag, which is rich in calcium. For mortars produced from fly ash and Portland cement, the mechanical properties were more satisfactory with the use of mixed solution. In these cases, the silica dissolved in the solution reacts quickly with the calcium from precursors and leads to the improve of mechanical strenght. The sodium hydroxide is important to the solubilization of silica and alumina, but this solubilization and subsequent reactions are low at room temperatures mainly.

Heah et al. [6] produced geopolymers using kaolin as a precursor, and sodium hydroxide and silicate as activators. In the paper, the authors tested several $Na_2SiO_3/NaOH$ ratios and solid to liquid (S/L) ratios. Based on the results of mechanical strength, the authors concluded that the most satisfactory ratios were S/L = 1.0 and $Na_2SiO_3/NaOH = 0.32$. In terms of molar ratios between oxides, the optimal relationships correspond to $Al_2O_3/Na_2O = 1.09$ and $SiO_2/Na_2O = 3.58$. This last value is above those reported in previous works.

Regarding the alkali metal (Na or K), research shows that potassium hydroxide favors the formation of geopolymers, based on Metakaolin, with higher values of compressive strength [68]. The difference between the two compounds is in the size of the cation. K^+ is larger than Na^+; therefore, the K^+ ion is more basic, allowing a higher rate of solubilization and dissolution of polymeric ionization. This results in a dense polycondensation reaction, which promotes a greater formation of the geopolymer network and a consequent increase in the matrix compressive strength. Na^+ has strong pair formation with the smaller silicate oligomers; these pairs, however, do not readily connect with other silicate anions, which makes it difficult to form larger oligomers. K^+, in turn, favors the formation of larger oligomers, with which $Al(OH)^{4-}$ ions bind more easily. In summary, the larger size of the cation K^+ can contribute to a higher degree of polycondensation [69,70].

Tanzer et al. [62] produced alkali-activated binders based on blast furnace slag and investigated the use of alkaline solutions with potassium hydroxide and sodium hydroxide, with and without the addition of sodium and potassium silicate solutions. The authors observed that the highest values of axial compressive strength were obtained for binders activated with potassium-based compounds, reaching values around 85 MPa at 28 days. The binders produced with sodium hydroxide and silicate reached about 70 MPa at the same age.

Another great advantage of potassium-based compounds is the lesser development of efflorescence when exposed to the atmosphere. In addition, the potassium ion makes the material more refractory in relation to the use of sodium-based compounds, being more suitable for the production of binders that will be exposed to high temperatures [71].

Even so, sodium-based compounds are used more than potassium, due to the cost and availability of these products compared to potassium hydroxide and silicate. However, the use of these commercial products increases the energy incorporated and the CO_2 emissions associated with alkali-activated binders because of the manufacturing process. Sodium hydroxide is produced through the chlorine-alkaline process, which consists of processing saltwater by electrolysis. After an emission analysis carried out in an Australian industry, it was found that 1.915 kg of CO_2 is emitted in the production of 1 kg of commercial NaOH. The manufacture of sodium silicate, in turn, involves the calcination of silica sand and sodium carbonate at a temperature around 1400 and 1500 °C. It is estimated that the total CO_2 emission per kg of sodium silicate, traditionally produced, is around 1.514 kg [16,72].

The use of calcium hydroxide as an activator is common in alkali-activation of blast furnace slag or other precursors rich in calcium, but it can also be applied to materials such as metakaolin. An advantage of this activator is the low cost compared to compounds based on sodium and potassium. On the global market, the cost of calcium hydroxide is at least 5 to 6 times lower than the cost of sodium hydroxide [73]. According to Akturk et al. [74], $Ca(OH)_2$ can accelerate the activation reactions in blast furnace slag and, consequently, promote the gain of mechanical strength. This is due to the ability of the compound to remove carbonate ions if they occur in raw materials, which promotes an increase in pH. Besides, $Ca(OH)_2$ favors the formation of the C-A-S-H phase, which guarantees mechanical strength to the product and makes the structure denser [75].

Yang et al. [63] studied the hydration products and mechanical strength development of alkali-activated slag with sodium hydroxide and other auxiliary activators - sodium silicate and sodium carbonate. The authors observed that mortars produced with $Ca(OH)_2$ and Na_2SiO_3 showed greater compressive strength compared to mortars based on $Ca(OH)_2$ and Na_2CO_3, at

28 days. The use of supplementary activators in conjunction with calcium hydroxide promoted the reduction of unreacted phases, and increased density and growth of hydration products.

In addition to the type of compound - hydroxide, silicate or carbonate - and the type of cation, the molar concentration of the alkaline solution also interferes in the development of precursor activation reactions. According to Barbosa et al. [76], the optimum concentration of the activator depends on the precursor used and should be sufficient to balance the Si and Al tetrahedral charges without an excess of the base (NaOH, for example), which can result in the formation of carbonate salts. Reig et al. [45] evaluated the compressive strength of geopolymers based on ceramic brick waste and observed that, at 7 days, the highest strength (approx. 15 MPa) was found in mortars with a molar concentration of NaOH equals to 5.0 mol/L. For concentrations of 7.5 and 10.0 mol/L, a progressive drop in mechanical strength was observed (11 MPa and 7 MPa, respectively).

Wang et al. [64] investigated the geopolymerization of metakaolin with NaOH. They also found that the concentration of the alkaline solution strongly influences the physical and mechanical properties of the products. Flexural strength, axial compressive strength and apparent density of geopolymer pastes increased according to the increase in the NaOH concentration of the solution, which varied between 4-12 mol/L. This behavior can be explained by the more intense dissolution of the metakaolin particles and by the higher condensation speed of the monomers in the presence of a high concentration of NaOH.

4 ALTERNATIVE ACTIVATORS

Although the alkali-activated binders present lower CO_2 footprint than the Portland cement and epoxy resin-based binders [77], the use of industrial silicates - such as sodium silicate - contributes to the increase in the emission of CO_2 and energy associated with the production of alkali-activated binders. It occurs due to the manufacturing process of these compounds [72]. Also, these materials are, in the vast majority, dangerous due to high pH and toxicity, and are expensive [73]. This situation has led to the development of new activators from waste (industrial or agricultural) or low-cost materials, rich in silica and/or alkaline cations (sodium and potassium). A fundamental characteristic is that these materials are soluble, enabling the release of the ions necessary for the development of alkaline activation. Besides, it is necessary to ensure that the activating solution has a pH high enough to promote the dissolution of aluminate and silicate ions and to hydrolyze the surface of the raw material particles [78].

The following is an approach to the research already developed focused on replacing conventional activators with alternative materials. The topics were divided according to the most frequent materials in the consulted technical literature. Table 1.3 presents an overview of the articles consulted, with the main information related to the processing and characterization of the resulting alkali-activated materials.

4.1 Rice husk ash

Rice husk is an agricultural by-product of rice mills, available in several regions of the world, especially in underdeveloped countries. Given the need to dispose of this waste properly, and to produce energy from renewable sources, a solution adopted was the burning of rice husks for electricity generation, as a kind of sustainable biomass [102]. After burning, about 25% of the initial mass is transformed into ashes, generating another residue called rice husk ash (RHA) [103]. The ashes are produced at temperatures up to 800 °C, much lower than those applied in the production of Portland cement clinker and sodium silicate, for example [104].

Ashes are highly porous particles with low specific weight and a large surface area. When obtained from controlled combustion, the specific surface can reach 50,000 m² / kg, while the particle size is around 10–75 μm, high values compared to silica fume, for example [105]. Depending on the burning conditions of the rice husks, the silica content in the RHA varies between 90 and 95 wt. %, and this silica occurs, predominantly, in an amorphous phase. There may also be crystalline phases and elements such as potassium and calcium. The predominance of amorphous silica makes the ash reactive and suitable to be used as a pozzolan [106,107]. The compositions of rice husk ash applied in the consulted studies are shown in Table 1.2.

Table 1.2. Chemical composition of RHA used by the studied authors (%).

Author	SiO_2	Al_2O_3	Fe_2O_3	CaO	MgO	K_2O	Na_2O	TiO_2	LOI
Bouzón et al.	85.58	0.25	0.21	1.83	0.50	3.39	-	-	6.99
Bernal et al.	*	*	*	*	*	*	*	*	*
Tong et al.	90.5	0.3	0.2	0.9	0.4	2.0	0.1	-	3.8
Mejía et al.	94.4	0.2	0.2	-	-	-	-	-	2.8
Geraldo et al.	89.51	0.13	0.05	-	0.30	1.68	-	-	6.95

* No composition provided

It is observed that the chemical compositions obtained by the authors were similar, even though the RHA came from different sources. The high silica content, in the range of 85-95%, stands out. However, not all this content can be considered as amorphous and reactive silica, as verified by Mejía et al. [81]. Regarding loss on ignition, Bouzón et al. [79] and Geraldo et al.

[83] found values around 7%, approximately double that verified by Tong et al. [82] and Mejía et al. [81].

Table 1.3. Overview of the consulted articles on alternative activators.

Authors	Alternative activator	Precursor	Preparation of the solution	Ratios	Characterization tests	Ref
Bouzón et al.	Rice husk ash	Fluid catalytic cracking catalyst	The NaOH and RHA were suspended in deionized water, refluxed and cooled before use	NaOH/RHA = 1.03 (by weight)	Flexural and compressive strength, TGA analysis, microscopic studies by SEM	[79]
Bernal et al.	Rice husk ash and sílica fume	Residue	The SF or RHA and NaOH were mixed for 10 min, and sealed in plastic containers immersed in a water bath at room temperature (25ºC) for 24 h before use	Na_2O/SiO_2 molar ratio = 0.25 (activator and solid precursor)	Compressive strength, TGA and FTIR analysis	[80]
Mejía et al.	Rice husk ash	Blast furnace slag and metakaolin	Mix of RHA and NaOH. Preparation details were not described	Module solution SiO_2/Na_2O = 1.20, 0.49 and 0.19 for slag, fly ash and slag/fly ash blend, respectively	Compressive strength, microstructural analysis (XRD, NMR and SEM)	[81]
Tong et al.	Rice husk ash	Fly ash and blast furnace slag	Sodium silicate solution was produced by a hydrothermal method, dissolving RHA powder into NaOH solution heated and kept under magnetic stirring	SiO_2/Na_2O mass ratio of 1.0; Na_2O/binder mass percentage of 7.5%	Compressive strength, initial and final setting times, heat of hydration (calorimetry) and microstructural characterization (XRD, TGA and FTIR)	[82]
Geraldo et al.	Rice husk ash	Fly ash	RHA was added to a NaOH solution and mixed with a magnetic stirrer with heating (90 °C ± 5 °C) for 30 min. After, it was stored and cooled at room temperature	Na_2O/SiO_2 molar ratio = 1.1 in the geopolymer matrix	Setting times, heat of hydration (calorimetry), consistency, flexural and compressive strength, air permeability, total water absorption and voids, capillary water absorption and SEM observations	[83]
Torres-Carrasco and Puertas	Glass waste	Metakaolin and water treatment sludge	The glass waste was mixed with the NaOH 10M and magnetically stirred at 80ºC for 6 hours. The solution was filtered, and the liquid used as the activator	SiO_2/Na_2O percentage ratios of 0.10, 0.11 and 0.16	Bending and compressive strength, porosity (Hg intrusion) and microstructural (XRD, FTIR, NMR and BSEM/EDX)	[84]
Vinai and Soutsos	Glass waste	Fly ash	The authors developed an activator powder by mixing NaOH and glass waste and putting it in an oven at 330°C for 2 hours	SiO_2:Na_2O molar ratios of 4:1, 2:1 and 1:1	Compressive strength	[85]
Tchakouté et al.	Glass waste	Fly ash and blast furnace slag	The NaOH and glass waste were mixed with a 200 mL of distilled water for 2 h at 100°C using a magnetic stirred. The solutions were subsequently filtered and the liquid was used as the activator.	SiO_2/Na_2O and H_2O/Na_2O molar ratios of 1.5 and 10, respectively	Compressive strength and microstructural analysis (XRD, IR absorption, TGA, ESEM and MIP)	[72]
Zivica	Silica fume	Metakaolin	No details about the activating solution were provided	No information provided	Compressive strength, TGA/DTA analysis, porosity (Hg intrusion) and specific surface area	[86]

Table 1.3. Overview of the consulted articles on alternative activators (continuation).

Authors	Alternative activator	Precursor	Preparation of the solution	Ratios	Characterization tests	Ref
Villaquirán-Caicedo	Silica fume	Portland cement and blast furnace slag	The alternative waterglass was obtained by adding of SF with potassium hydroxide pellets with tap water to achieve a concentration of 9.3 M and a pH = 13. This solution is allowed to stand for 20 h at room temperature	No information provided	Compressive strength, initial and final setting times and microstructural analysis (SEM, FTIR and TGA/DTG)	[87]
Rodriguez et al.	Nanossilica	Metakaolin	Alkali-activators were prepared by the dissolution of NaOH or KOH pellets with the nanossilica	Molar oxide ratio SiO_2/M_2O = 1.16	Compressive strength, porosity (Hg intrusion) and microstructure analysis (XRD, TGA and SEM)	[88]
Moraes et al.	Sugar cane straw ash	Fly ash	The SCSA was dry mixed with NaOH in the thermal bottle, followed by the addition of water over the solids and the stirring of the solution for one minute. The thermal bottle was then sealed with a cap and the suspension was left in the thermal bottle until it returned to room temperature	The water/NaOH/SCSA mass ratio in g was 202.5/32.4/x, where x = 29.5, 44.3, 59.0 and 73.8 for SiO_2/Na_2O molar ratios of 0.73, 1.09, 1.46 and 1.82 respectively	Compressive strength and microstructural analysis (XRD, FTIR, TGA and FESEM)	[89]
Alonso et al.	Olive biomass ash	Blast furnace slag	The activator and precursor were mixed at solid states	No information provided	Flexural and compressive strength, reactivity (calorimetry), radionuclide activity and leaching	[90]
Pinheiro et al.	Olive biomass ash	Blast furnace slag and coal ash	The activator and precursor were mixed at solid states	No information provided	Flexural and compressive strength, porosity (Hg intrusion) and microstructure analysis (XRD, TG/DTG and SEM)	[91]
Font et al.	Olive biomass ash	Blast furnace slag	Mixture of olive biomass ash and water	OBA/water ratio of 0.47 (18.8% of OBA in relation to BFS)	Compressive strength and thermogravimetric analysis	[92]
Soriano et al.	Almond-shell biomass ash	Blast furnace slag	The milled ash was first dry-mixed with BFS and then mixed with still water	20% replacement of BFS and 20% addition (ABA in powder)	Compressive strength and thermogravimetric analysis	[93]
Ban et al.	High calcium wood ash	Fly ash	No information provided	50%-100% replacement of binder (FA) by weight	Compressive and flexural strength, ultrasonic pulse velocity, dynamic modulus, water absorption, total porosity and capillary absorption tests	[94]
Peys et al.	Maize cob ashes	Metakaolin	The activator and precursor were mixed at solid states	Mass ratio of ash to metakaolin of 0.3, 0.6 and 0.9	Compressive strength and microstructural analyses (XRD, FTIR, SEM, EPMA and calorimetry)	[95]
Bilondi et al.	Calcium carbide residue	Blast furnace slag	Mixture of CCR and water	No information provided	Compressive strength and SEM-EDX analysis	[96]
Phetchuay et al.	Calcium carbide residue	Glass powder	The activator and precursor were mixed at solid states	It was added 7% of CCR by mass	Compressive strength and SEM analysis	[97]

Table 1.3. Overview of the consulted articles on alternative activators (continuation).

Authors	Alternative activator	Precursor	Preparation of the solution	Ratios	Characterization tests	Ref
Fernández-Jiménez et al.	Cleaning solution from aluminum industry	Fly ash	No preparation required	Alkali concentration of approximately 5M	Flexural and compressive strength, heat evolution (calorimetry) and microstructural analyses (XRD, NMR, SEM and EDX)	[98]
Van Riessen et al.	Bayer liquor	Fly ash	No preparation required	No information provided	Compressive strength and SEM analysis	[99]
Choo et al.	Red mud	Fly ash	Fly ash samples were mixed with the red mud in the dry state	Mass of red mud/total mass ranging from 0% to 60%	Compressive strength, pH measurements and microstructural analyses (SEM and XRD)	[100]
Font et al.	Diatomaceous earth	Fluid cracking catalyst residue	The water, NaOH and solid silica source were mixed into a thermal bottle for 24 h.	No information provided	Compressive strength and thermogravimetric analysis	[101]

This residue has already been applied in conventional Portland cement-based products, such as concrete and mortar, to reduce permeability and increase resistance to acids and sulfates [108]. Recent studies have investigated the use of RHA in alkali-activated materials, in partial replacement of fly ash [109], or in the production of alkaline sodium silicate solutions for "two-part" geopolymers [106].

Bouzón et al. [79] produced alkaline solutions for alkali-activation from sodium hydroxide and rice husk ash - in the natural state (average diameter of 62.3 μm) and ground (average diameter of 20.3 μm). Two series of mortars were produced, using fluid catalytic cracking catalyst residue as a precursor: the first, with the alkaline solution made with RHA; the second, with the solution made from sodium hydroxide and sodium silicate, considered as the control or reference mortar. The specimens were cured at 65 ° C and relative humidity between 95-100%. Flexural and axial compressive strength tests were performed after one day of curing. The strengths obtained for the reference mortar were 8.45 MPa and 40.9 MPa, respectively. The mortar produced with ground RHA exceeded these values, reaching about 43 MPa for compressive strength. In general, mortars based on RHA/NaOH showed values of compressive strength in the range of 31-43 MPa, similar to the value obtained for the control mortar, produced with industrial sodium silicate.

Bernal et al. [80] developed activators based on RHA and aqueous NaOH for the activation of mixtures of Metakaolin and blast furnace slag. The rice husk ash used contained 68% amorphous silica, and less than 2% of unburned carbon. The performance of the RHA-based activator was compared to that of commercial sodium silicate. Alkali activated pastes were produced with metakaolin and the following percentages of blast furnace slag: 0, 20%, 40%, 60% and 80%. The dosage of the RHA content in the activator solution was based on the desired SiO_2 / Al_2O_3 ratio (equal to 3). The molded specimens were kept in room temperature for the first 24 hours and subsequently subjected to thermal curing at 60 °C for 24 hours. After this period, the specimens remained at room temperature for 7 days, until the compressive strength test. In the addition of 20% and 40% blast furnace slag, the mechanical strength of the specimens activated with RHA was higher than that of the reference specimens, produced with sodium silicate solution; the values obtained were around 35 and 45 MPa, respectively.

Mejía et al. [81] used two different types of RHA for the alkali-activation of fly ash, blast furnace slag and a mixture between the two materials (1:1). The alkaline solution contained, in addition to RHA, sodium hydroxide. For comparison, solutions were also prepared with NaOH and commercial sodium silicate. Pastes were produced and evaluated for compressive strength, mineralogy and microstructure. For this, prismatic specimens (1x1x6)

cm³ were produced. Pastes made only with fly ash were cured at 80 °C for 24 h; the rest were cured at room temperature and 95% relative humidity. An interesting point, noted by the authors is that both amorphous and crystalline silica can be dissolved in NaOH due to their high alkalinity, only under different conditions. Amorphous silica can dissolve at low temperatures, whereas the crystalline has solubility for high temperatures or longer reaction times. The results showed that the agro-industrial by-product can be used to obtain alkali-activated materials with compressive strength in the order of 42 MPa at 7 days. The values found were lower than those obtained for the commercial activator, but they are still satisfactory.

Tong et al. [82] proposed a study to optimize the production of alkaline solutions based on RHA and NaOH, and the alkaline activation of a mixture with 60% fly ash of class F and 40% of blast furnace slag. For the verification of mechanical strength and microstructural analysis, mortars and pastes were produced, respectively. The rice husk ash was ground to an average diameter between 5 and 10 μm. A commercial sodium silicate solution was also used to manufacture reference specimens. Cubic specimens were produced, with dimensions (50 x 50 x 50) mm³, cured at room temperature (20 ± 2 °C) and controlled relative humidity (50 ± 5%). The characteristics determined were: the initial and final setting times; compressive strength at 1, 7 and 28 days; and the microstructure aspects of alkali-activated pastes. The initial and final setting times were shorter for the mortar produced with an RHA-based activator, suggesting that the silicates in the RHA-derived solution are more readily available for the reaction. The mechanical performances at 1 and 7 days were similar to those obtained with the commercial sodium silicate solution; at 28 days, the compressive strength was even higher, reaching approximately 60 MPa. From XRD and FTIR analyzes, it was observed that there were no significant differences between the samples activated with RHA and commercial sodium silicate. These results confirm the equivalence of the alternative to the conventional activator, and its potential for an application, not only in terms of the environmental aspects, but also from an economic point of view. The authors concluded that the use of RHA-based solutions reduces the cost of alkali-activation by up to 55%.

Geraldo et al. [83] used RHA-based alkaline solutions for the geopolymerization of mixtures of metakaolin with water treatment sludge (WTS). Mortars were produced with a precursor to sand ratio of 1 : 3, and percentages of 0%, 15%, 30% and 60% WTS. Prismatic specimens measuring (40 x 40 x 160) mm³ were used, and the cure was carried out at room temperature (25 ± 2 °C; 60% RH). After carrying out the compressive strength test, at 28 days, it was observed that the values varied between 9.1 and 29.2 MPa, with the highest value corresponding to the mortar containing no WTS (0%). At 90 days, the reference mortar reached

about 40 MPa, suggesting the continuity of reactions at older ages. Again, the authors indicated that the use of RHA for the production of an alternative sodium silicate is an effective and viable alternative in environmental and economic terms. According to Mellado et al. [110], the use of RHA reduces CO_2 emissions in geopolymers by 50%.

4.2 Glass waste

Glass is an inorganic substance, amorphous and physically homogeneous, resulting from the cooling of a paste formed by the fusion of oxides or their derivatives, with silicon oxide (SiO_2) as its primary component. The paste hardens as its viscosity increases, without any crystallization or structural organization. In general, the glass is transparent, but it can also be opaque or translucent [111].

One of the types of existing glass is soda-lime glass, used in packaging, civil construction and the automotive industry. Because of this vast application, the waste generated has become an important solid industrial and urban waste, causing environmental and economic problems concerning the high volume that must be managed. In Hong Kong, for example, around 300 tons of glass waste is disposed of in landfills every day [112]. Although the waste can be recycled in different ways, this process in the glass industry is complicated by logistical issues such as the variety of colors and chemical composition, making its reuse expensive and impractical [113].

Given this situation, it is essential to look for ways to reuse glass waste and effectively reduce the amount of material that requires disposal in landfills [112]. Civil construction is a sector capable of absorbing large quantities of residual materials in the production of cement, concrete, ceramics, among others. Due to the chemical composition of the residue, rich in silica, and its high amorphous phase content (Figure 1.2), it may be suitable for the production of alkali-activated materials as a source of silica in the system.

Using class F fly ash as a precursor, Torres-Carrasco and Puertas [84] produced geopolymeric pastes activated with three types of activators: an 8 M NaOH solution; 10 M NaOH solution + 15% commercial sodium silicate; and 10 M NaOH solution + varying amounts of urban glass waste (10, 15 and 25 g per 100 mL of solution). The prismatic specimens, with dimensions (1 x 1 x 6) cm^3, were cured, initially, in an oven at 85 °C, for 20 hours; then, they were placed in a humid chamber with 99% relative humidity and temperature of 20 ± 2 °C until the date of the mechanical tests. At 28 days, the compressive strength of pastes produced with 15 g of glass waste and 100 mL of 10 M NaOH was higher than 37 MPa,

a value verified for pastes produced with industrial sodium silicate. However, the addition of more waste (25 g) promoted a drop in mechanical performance, due to the decrease in pH and an increase in the SiO_2/Na_2O ratio in the activator. The variation in this relationship can promote changes in the degree of polymerization of the dissolved species. The XRD patterns of the waterglass-activated pastes and the glass waste (15 g) were very similar, with zeolitic-like phases being found as chabazite-Na. This indicates the feasibility of replacing commercial sodium silicate with an alkaline solution produced with NaOH and glass waste.

Figure 1.2. XRD patterns: (a) of raw glass powder [85]; (b) waste glass [72].

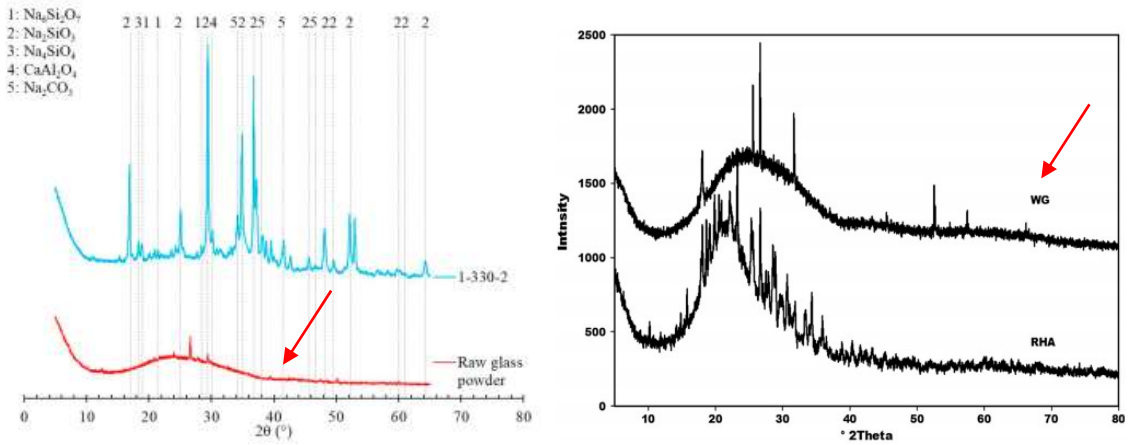

Vinai and Soutsos [85] produced alkali-activated mortars with alkaline NaOH solution and ground glass waste, and blast furnace slag and fly ash as precursors. The proportions between the precursors were defined according to the desired SiO_2/Al_2O_3 ratios from 4 : 1 to 1 : 1. The specimens produced with the fly ash/GGBS mixture were cured at room temperature, in the air. The specimens containing only fly ash were cured in an oven at 70 °C until the date of the mechanical strength test. The authors carried out several series of mortars, varying other parameters involving the dosage of activators. In general, the compressive strength values of mortars produced with glass waste solutions were very close to the values obtained using commercial sodium silicate, and higher when compared to mortars produced using only NaOH. At 28 days, compressive strengths between 40 and 50 MPa were found. The cost analysis showed that the glass-based activator represented 14% of the cost of its correspondent alkali-activated concretes, while the commercial activators represented about 41%. In addition, alkali-activated concretes with the alternative activator have a lower cost than Portland cement-based concretes - normal or high strength (disregarding the costs of transporting waste).

Tchakouté et al. [72] synthesized an alkaline solution from discarded glass bottles and collected in garbage cans. These bottles were broken, and then the pieces were ground in a ball mill. The alternative activator was produced by adding the powdered glass waste, commercial NaOH and water. Then, metakaolin-based pastes were produced, keeping the ratio activator solution to metakaolin in 0.83 by mass. Cylindrical specimens were molded, with dimensions (20 x 40) mm (diameter x height), and the compressive strength tests were performed at 7, 14, 21, 28 and 56 days. The compressive strength values ranged from 22.9 MPa (7 days) to 39.7 MPa (56 days). The authors also produced an alternative solution based on rice husk ash, and observed that the mechanical strength was higher in the specimens produced with a solution based on glass waste. This indicates that the glass waste solution generated higher amounts of soluble Si ions which was confirmed by FTIR analysis (absence of the 1085 cm^{-1} peak). In other words, the difference in mechanical strength is linked to the fact that the solutions present different rates of silicate release in the early stages of geopolymerization.

4.3 Silica fume

Silica fume is an additional cementitious material that promotes pozzolanic reactions. Silica fume can be defined as a very fine amorphous silica powder, produced in electric arc furnaces as a by-product resulting from the manufacture of silicon alloys or elemental silicon [114]. This material has high amounts of SiO_2 (in its vitreous phase) and very small spherical particles, inferior to those of Portland cement, and these are the reasons for its high pozzolanic activity [115]. The particle sizes reported in the studies are listed in Table 1.4. In concrete, the addition of silica fume promotes several improvements, such as the increase in mechanical strength, due to pozzolanic reactions with free lime; increasing the packing of the particles and reducing the permeability, since the small particles fill the voids of the matrix between the cement grains; and finally, improving connections at the paste-aggregates interface [114,116].

Table 1.4. Particle sizes and specific surface area of silica fume used by the related authors (%).

Author	Particle size	Specific area (m^2/kg)
Zivica	*	15898
Bernal et al.	Range = 1-500 μm d_{50} = 64.1 μm	*
Villaquirán-Caicedo	d_{50} = 21.50 μm d_{10} = 3.62 μm d_{90} = 42.30 μm	*

*No information provided

Due to its very small particle size and amorphous character, silica fume is highly reactive and can be used in the production of alkali-activated materials as a source of silicates, either in mixture with the precursor, or in the production of the activating solution since it can replace the conventionally used sodium or potassium silicates.

In geopolymers produced from fly ash with high calcium content, the silica fume increased the setting time and the compressive strength up to certain levels (10%), besides accelerate the geopolymerization reactions [117]. Sukontasukkul et al. [117] also observed that the use of silica fume in addition to the precursor tends to reduce the workability of the mixture and increase the water requirement due to its finess. Thus, the incorporation of silica fume in the alkaline solution can be more effective.

Zivica [86] studied the alkali-activation of mortars produced with mixtures of Portland cement and blast furnace slag, and alkaline solution using silica fume as a source of soluble silicates. Cubic specimens, with 20 mm edges, were molded and cured at room temperature (20 °C) until the test date. Compressive strength was obtained at 1, 7 and 28 days. At 28 days, the compressive strength obtained for the mortar with 10% Portland cement and 90% slag was approximately 47 MPa, higher than the value obtained for the mortar made only with Portland cement as a binder. At 90 days, the mortar with 30% Portland cement and 70% slag exceeded 50 MPa. It was observed that the silica fume activator causes positive effects in the mortar, promoting the intensification of the formation of hydrated calcium silicates and the densification of the porous structure formed.

Villaquirán-Caicedo [87] produced an alternative activator using potassium hydroxide and silica fume, with a concentration of 9.3 M and pH equal to 13. This activator was used in the production of pastes with metakaolin as a source of aluminosilicates. As a reference, one of the pastes was prepared with only commercial potassium silicate. Cubic specimens, with 20 mm edges, were molded and cured at 70 °C for 20 h; then, they were demolded and placed in a chamber with 90% relative humidity and a temperature of 25 °C, until the date of the mechanical tests. The tests of axial compressive strength were performed at 7, 28, 180 and 360 days. The replacement of 50% of the commercial activator by the alternative activator promoted an increase in mechanical strength at all ages evaluated, with values higher than 60 MPa being reached at 7 days. The total replacement of the commercial activator for the alternative caused the decrease of strength compared to the partial replacement; however, the values obtained were still higher than those found in the paste produced with 100% commercial activator. Microstructural analysis of pastes after rupture indicated a predominant amorphism, and the

only mineral phase detected was anatase. SEM images revealed the presence of micropores and cracks, and a heterogeneous appearance.

The author reported previously also points out that, given the results obtained in her work, the use of silica fume in the activating solution causes the highest availability of Si ions in the system in the initial stages, since the silica fume dissolves more intensely compared to other sources of soluble silica, such as rice husk ash. Thus, the hardening of pastes with silica fume is faster in the early ages; then, the availability of ions decreases and polycondensation occurs at slower rates.

In addition to developing an RHA-based activator, Bernal et al. [80] also produced alkaline solutions with silica fume. The mechanical performance of the pastes produced with the two activators was experimentally similar. On the other hand, the authors observed that the pastes produced with silica fume showed greater variability in the results of compressive strength. One possible explanation is the increase in the brittleness of the pastes due to the inclusion of silica.

4.4 Other activators

In addition to the aforementioned raw materials, others have been used in the production of alternative activators, but with less frequent mentions in the literature. Rodriguez et al. [88] investigated the alkali-activation of fly ash with low calcium content, activated by chemically modified nanosilica in solution with sodium or potassium hydroxide. The produced binders presented mechanical strength similar to those obtained from commercial silicates, and lower porosity and water demand. This is attributed to the slightly “late” release of the silica present in the nanosilica particles, which remains in suspension in the initial stages.

Moraes et al. [118] produced activating solutions from sugarcane straw ashes (SCSA), obtained by the straw self-combustion process, and sodium hydroxide. The ashes are basically composed of SiO_2 (58.6%), Al_2O_3 (9.0%) and Fe_2O_3 (8.4%). The best results were obtained for the suspension kept in a thermos for 24 hours, and molar ratio SiO_2 / Na_2O in the solution equal to 1.46. Mortars were prepared using blast furnace slag as a precursor. The compressive strength obtained at 28 days was lower than that found in mortars produced with commercial sodium silicate; even so, it was over 50 MPa.

Alonso et al. [90] also used an agricultural by-product, olive biomass ash (OBA) (both fly and bottom ash), as an activator in the alkali-activation of blast furnace slag and coal ash. Unlike the previous cases, only the ash and water constituted the evaluated activating solution.

The chemical composition of the ashes is shown in Table 1.5. The results obtained in the slurry pastes were satisfactory, and the mechanical performance was close to the reference pastes produced with commercial KOH. Alkali-activation of coal ash proved to be impracticable, since the reached pH was not sufficient to promote the dissolution of the precursor. Pinheiro et al. [91] and Font et al. [92] developed a similar study, also using olive biomass ashes as an activator and blast furnace slag as a precursor. Again, the mechanical performances showed the high efficiency of the activator. In the first study, values of 38.38 MPa and 7.01 MPa in the compressive and flexural strength tests, respectively, were reached. In the second one, the mechanical behavior of OBA-based mortars was better compared to mortars activated with KOH, suggesting a synergic process in terms of both the filler and chemical effects.

Table 1.5. Chemical composition (%) of olive biomass ashes used by Alonso et al. [90].

Sample	SiO_2	Al_2O_3	Fe_2O_3	CaO	MgO	K_2O	Na_2O	TiO_2	P_2O_5
OBFA	12.60	2.97	2.30	20.21	4.85	26.34	1.12	0.24	3.84
OBBA	23.61	5.41	6.12	20.61	6.02	17.31	1.29	0.83	4.04

Other ashes from agricultural wastes were already applied as alternative activators, such as high calcium wood ash (HCWA) and almond-shell biomass ash (ABA). According to Ban et al. [94], the high calcium wood ash, a by-product from timber manufacturing industry, is suitable to be used as activator and source of potassium ions. Mortars produced by HCWA and fly ash presented flexural strength about 2 MPa at 28 days. The strength development and harderning of the samples were mainly governed by geopolymeric reactions, from the dissolution of fly ash, and hydraulic reactions of HCWA, occurring the formation of K-A-S-H and secondary C-S-H gels. Soriano et al. [93] studied the addition of almond-shell biomass ash as activator in mortars with blast furnace slag. The authors proved that the compressive strength of ABA-based mortars (20% addition) was 71.7% higher than the mortars activated with KOH 8M solution, at 7 days. Besides, the almond-shell biomass ash also promotes the formation of C-S-H/C(K)-A-S-H gels, responsible for the strength development.

Peys et al. [95] proved that maize cob ashes (MCA) are reactives and suitable to be used as activator in metakaolin-based geopolymers. The ratio of 0.9 ash to metakaolin lead to the highest geopolymerization extent. Applying a pre-cure at 20º for 24h and subsequently open curing for 48h at 80º, the compressive strength of 40 MPa was reached at 7 days.

Bilondi et al. [96], Phetchuay et al. [97] and Phummiphan et al. [119] studied the application of calcium carbide residue as an activator in the geopolymerization of soils and fly ash, in order to promote their stabilization. The calcium carbide residue is an industrial by-

product resulting from the production process of acetylene gas (C_2H_2). Its use as an activator is justified by the significant presence of $Ca(OH)_2$ in its composition, and the high pH. Besides, the incorporation of CCR in buildings materials has both economic and environmental perspectives. In countries such as Thailand, this waste is disposed in landfills, which causes a huge environmental problem due to its high alkalinity [120]. The mentioned studies showed that this compound can be used as an effective activator, improving the mechanical behavior of the studied soils.

According to Hanjitsuwan et al. [121], the incorporation of CCR in alkali-activated materials has similar effect compared to the addition of Portland cement. The CCR is also very effective in the alkali-activation of others wastes, such as water treatment sludge and high calcium fly ash, and it can be applied in the production of repair binders and nonbearing masonry units [122,123]. The $Ca(OH)_2$ from CCR reacts with the soluble silica, producing more C-S-H and contributing to the increase of strength. With the incorporation of suitable contents, CCR-based pastes showed improved microstructure in comparison with the pastes without CCR replacement [123].

Other by-products that have the potential for use as activators in alkali-activated materials are the alkaline solutions generated in the aluminum industry. These solutions have a high pH, in addition to having significant amounts of soluble aluminum. Fernández-Jiménez et al. [98] used a solution resulting from washing the sand extrusion molds and other tools - alkaline cleaning solution (ACS), from an aluminum smelting industry. Van Riessen et al. [99], in turn, used “Bayer liquor”, resulting from the Bayer process applied in the production of alumina from bauxite ore. This liquor is rich in sodium aluminate but contains associated impurities. In both works, fly ash was used as a precursor, and the results of mechanical strength proved that the use of these solutions as activators is feasible from a technical and environmental point of view. In addition to promoting the dissolution of the precursor, they are also a low-cost source of alumina, being effective mainly in the alkali-activation of materials with a low reactive alumina content.

Choo et al. [100] produced one-part geopolymers using five types of fly ashes and red mud as NaOH supplier. Red mud is the solid waste resulting from the Bayer process, and presents high alkalinity (pH around 11). The best results of compressive strength corresponded to the pastes with the higher percentage of red mud: 60%. The higher the content of red mud, the higher the dissolution rate of the aluminossilicate precursor. The inorganic polymers activated by commercial NaOH (NaOH content at 3-5%) showed mechanical behavior similar to those of geopolymers produced with red mud. Although the compressive strength was low,

the developed geopolymers can possible be used in construction sites with low strength required.

Font et al. [101] investigated the use of residual diatomaceous earth (diatomite) as silica source in alkaline solutions. Diatomaceous earth is a sedimentary rock with a high reactive silica percentage formed by fossilized diatom residuals. The compressive strength of mortars activated with diatomite was lower than of those produced from sodium silicate and rice husk ash (RHA). However, values about 25 and 40 MPa at 28 days were found, indicating that these mortars can be used for structural purposes. Depending on the type of diatomite, the loss of ignition and organic matter content can be high. The authors concluded that the previous calcination of this material improves the mechanical properties of the mortars.

Figure 1.3 shows the main results of compressive strength, obtained by the authors studied, with the indication of the activator used. It is noted that, in general, the compressive strength values are in the range of 30 - 50 MPa. The mortar produced by Tong et al. [82], with RHA, was the one with the highest strength. Geraldo et al. [83], in turn, used this same material and obtained only 29.2 MPa of compressive strength. This may be related to the precursors adopted: the first used a mixture of fly ash and blast furnace slag; the second, metakaolin. The use of the slag provided the formation of the C-S-H gel, resulting in the gain of mechanical strength.

Others inconsistent results were 16 MPa obtained by Fernández-Jiménez et al. [98], 7.5 MPa obtained by Ban et al. [94] and 1.7 MPa found by Choo et al. [100]. In these studies, the precursor used was fly ash. The values found were low compared to other studies, but they were still similar to those obtained using only NaOH as an activator. This indicates that low mechanical strength is not associated with poor performance of the alternative activator (ACS), but it can be related to the production process or properties of the precursor.

5 FUTURE PERSPECTIVES

The current trend is the development of research on the use of sustainable raw materials (precursors or activators), in order to reduce the environmental impacts caused by the construction industry. Besides, researchers have sought to better understand the occurrence of alkali-activation reactions, the kinetics of the reactions, what are the factors that are relevant to their development, among other questions.

Figure 1.3. Compressive strength of (a) mortars and (b) pastes with alternative activators.

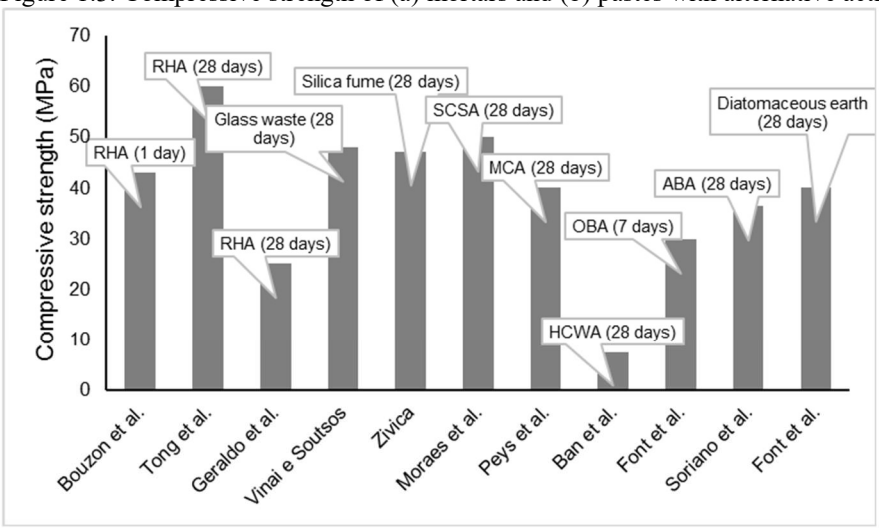

(a)

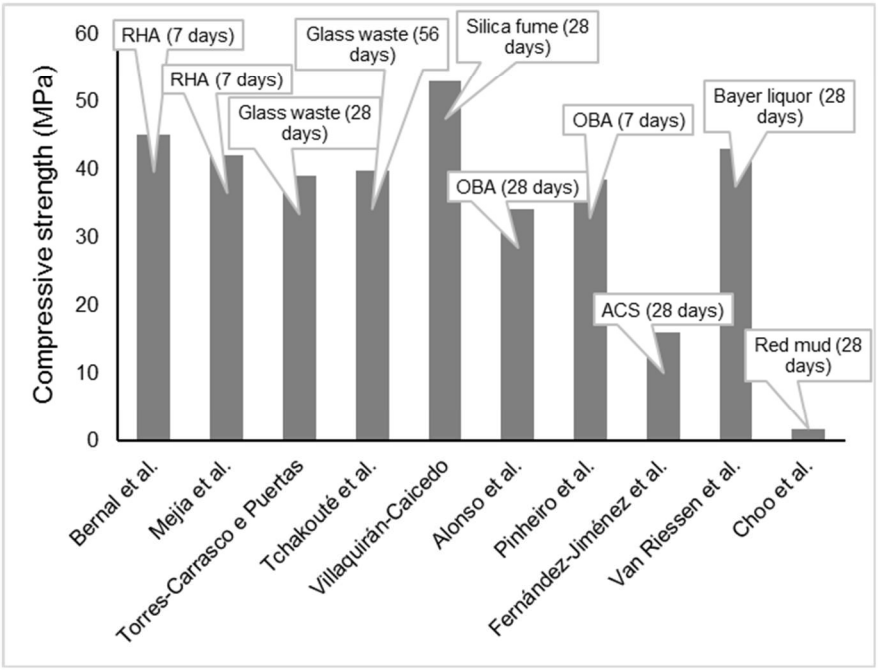

(b)

As seen previously, products with good mechanical strength have been produced, even using the alternative activators discussed here. The compressive strength values obtained are comparable to those of concretes, mortars and cementitious pastes, based on Portland cement. This makes the use of alkali-activated materials attractive for also structural functions. However, another point that deserves to be highlighted is durability.

Several authors have already demonstrated that alkali-activated materials produced with conventional activators have good durability characteristics, even superior to traditional

cementitious materials. In the case of geopolymers, for example, semi-crystalline species are similar to zeolites found in natural rocks and are very resistant to weathering.

What is still unclear is whether the products resulting from the use of alternative activators - such as rice husk ash, sugar cane bagasse ash and olive biomass - have the same durability conditions as conventional ones. On this topic, there is a need for further research and investigation on the performance of mortars, concrete or alkali-activated pastes when exposed to ultraviolet radiation, wetting and drying cycles, ice and thaw, carbonation, chloride attack, among others. The durability aspect is important since it is necessary to know if the material will present loss of strength if subjected to specific conditions, such as those mentioned above.

Another research priority would be the environmental characterization of mortar and alkali-activated concrete produced from industrial or agricultural wastes. Few studies have investigated the potential for leaching and solubilization of elements that can be dangerous to the environment or to the building user. This verification is important considering, above all, industrial residues, such as those from mining (i.e., Bayer liquor). These materials contain more impurities due to the various substances used in the exploration and processing of the ore.

The control of rheology is also little applied, especially in studies related to alternative activators. It is necessary to understand whether these activators cause significant changes in pastes, mortars or concretes in the fresh state, including in relation to consistency and workability.

6 ACKNOWLEDGMENTS

This study was financed in part by the Coordenação de Aperfeiçoamento Pessoal de Nível Superior – Brasil (CAPES) – Finance Code 001.The authors also want to thank the FAPEMIG and FAPERJ agencies for the financial support provided and SICON research group for the technical assistance.

REFERENCES

[1] Liu Y, Shi C, Zhang Z, Li N. An overview on the reuse of waste glasses in alkali-activated materials. Resour Conserv Recycl 2019;144:297–309. https://doi.org/10.1016/j.resconrec.2019.02.007.

[2] Provis JL. Geopolymers and other alkali activated materials: Why, how, and what? Mater

Struct Constr 2014;47:11–25. https://doi.org/10.1617/s11527-013-0211-5.

[3] Shi C, Jiménez AF, Palomo A. New cements for the 21st century: The pursuit of an alternative to Portland cement. Cem Concr Res 2011;41:750–63. https://doi.org/10.1016/j.cemconres.2011.03.016.

[4] Kua T-A, Imteaz MA, Arulrajah A, Horpibulsuk S. Environmental and economic viability of Alkali Activated Material (AAM) comprising slag, fly ash and spent coffee ground. Int J Sustain Eng 2019;12:223–32. https://doi.org/10.1080/19397038.2018.1492043.

[5] Zhuang XY, Chen L, Komarneni S, Zhou CH, Tong DS, Yang HM, et al. Fly ash-based geopolymer: Clean production, properties and applications. J Clean Prod 2016;125:253–67. https://doi.org/10.1016/j.jclepro.2016.03.019.

[6] Heah CY, Kamarudin H, Mustafa Al Bakri AM, Bnhussain M, Luqman M, Khairul Nizar I, et al. Study on solids-to-liquid and alkaline activator ratios on kaolin-based geopolymers. Constr Build Mater 2012;35:912–22. https://doi.org/10.1016/j.conbuildmat.2012.04.102.

[7] Gavali HR, Bras A, Faria P, Ralegaonkar R V. Development of sustainable alkali-activated bricks using industrial wastes. Constr Build Mater 2019;215:180–91. https://doi.org/10.1016/j.conbuildmat.2019.04.152.

[8] Samarakoon MH, Ranjith PG, Rathnaweera TD, Perera MSA. Recent advances in alkaline cement binders: A review. J Clean Prod 2019;227:70–87. https://doi.org/10.1016/j.jclepro.2019.04.103.

[9] Palomo A, Grutzeck MW, Blanco MT. Alkali-activated fly ashes: A cement for the future. Cem Concr Res 1999;29:1323–9. https://doi.org/10.1016/S0008-8846(98)00243-9.

[10] Provis JL, Bernal SA. Geopolymers and Related Alkali-Activated Materials. Annu Rev Mater Res 2014;44:299–327. https://doi.org/10.1146/annurev-matsci-070813-113515.

[11] Davidovits J. Geopolymers - Inorganic polymeric new materials. J Therm Anal 1991;37:1633–56. https://doi.org/10.1007/BF01912193.

[12] Davidovits J. Geopolymeric Reactions in Archaeological Cements and in Modern Blended Cements. Concr Int 1987;9:23–9.

[13] Duxson P, Fernández-Jiménez A, Provis JL, Lukey GC, Palomo A, Van Deventer JSJ. Geopolymer technology: The current state of the art. J Mater Sci 2007;42:2917–33. https://doi.org/10.1007/s10853-006-0637-z.

[14] Ma CK, Awang AZ, Omar W. Structural and material performance of geopolymer concrete: A review. Constr Build Mater 2018;186:90–102. https://doi.org/10.1016/j.conbuildmat.2018.07.111.

[15] Provis JL. Alkali-activated materials. Cem Concr Res 2018;114:40–8. https://doi.org/10.1016/j.cemconres.2017.02.009.

[16] Turner LK, Collins FG. Carbon dioxide equivalent (CO2-e) emissions: A comparison between geopolymer and OPC cement concrete. Constr Build Mater 2013;43:125–30. https://doi.org/10.1016/j.conbuildmat.2013.01.023.

[17] Heath A, Paine K, McManus M. Minimising the global warming potential of clay based geopolymers. J Clean Prod 2014;78:75–83. https://doi.org/10.1016/j.jclepro.2014.04.046.

[18] Zhang ZH, Zhu HJ, Zhou CH, Wang H. Geopolymer from kaolin in China: An overview. Appl Clay Sci 2016;119:31–41. https://doi.org/10.1016/j.clay.2015.04.023.

[19] Rocha T da S, Dias DP, França FCC, Guerra RR de S, Marques LR da C de O. Metakaolin-based geopolymer mortars with different alkaline activators (Na+and K+). Constr Build Mater 2018;178:453–61. https://doi.org/10.1016/j.conbuildmat.2018.05.172.

[20] Humad AM, Provis JL, Cwirzen A. Alkali activation of a high MgO GGBS – fresh and hardened properties. Mag Concr Res 2018;70:1256–64. https://doi.org/10.1680/jmacr.17.00436.

[21] Abdalqader AF, Jin F, Al-Tabbaa A. Development of greener alkali-activated cement: Utilisation of sodium carbonate for activating slag and fly ash mixtures. J Clean Prod 2016;113:66–75. https://doi.org/10.1016/j.jclepro.2015.12.010.

[22] Bernal SA, Provis JL, Myers RJ, San Nicolas R, van Deventer JSJ. Role of carbonates in the chemical evolution of sodium carbonate-activated slag binders. Mater Struct 2015;48:517–29. https://doi.org/10.1617/s11527-014-0412-6.

[23] Gao X, Yuan B, Yu QL, Brouwers HJH. Characterization and application of municipal solid waste incineration (MSWI) bottom ash and waste granite powder in alkali activated slag. J Clean Prod 2017;164:410–9. https://doi.org/10.1016/j.jclepro.2017.06.218.

[24] Robayo RA, Mulford A, Munera J, Mejía de Gutiérrez R. Alternative cements based on alkali-activated red clay brick waste. Constr Build Mater 2016;128:163–9. https://doi.org/10.1016/j.conbuildmat.2016.10.023.

[25] Fernández-Jiménez A, Palomo A. Composition and microstructure of alkali activated fly ash binder: Effect of the activator. Cem Concr Res 2005;35:1984–92. https://doi.org/10.1016/j.cemconres.2005.03.003.

[26] Ye J, Zhang W, Shi D. Properties of an aged geopolymer synthesized from calcined ore-dressing tailing of bauxite and slag. Cem Concr Res 2017;100:23–31. https://doi.org/10.1016/j.cemconres.2017.05.017.

[27] Leong HY, Ong DEL, Sanjayan JG, Nazari A. The effect of different Na2O and K2O ratios of alkali activator on compressive strength of fly ash based-geopolymer. Constr

Build Mater 2016;106:500–11. https://doi.org/10.1016/j.conbuildmat.2015.12.141.

[28] Dias DP, de Andrade Silva F. Effect of Na 2 O/SiO 2 and K 2 O/SiO 2 mass ratios on the compressive strength of non-silicate metakaolin geopolymeric mortars. Mater Res Express 2019;6:075514. https://doi.org/10.1088/2053-1591/ab179d.

[29] Clausi M, Fernández-Jiménez AM, Palomo A, Tarantino SC, Zema M. Reuse of waste sandstone sludge via alkali activation in matrices of fly ash and metakaolin. Constr Build Mater 2018;172:212–23. https://doi.org/10.1016/j.conbuildmat.2018.03.221.

[30] Zaharaki D, Galetakis M, Komnitsas K. Valorization of construction and demolition (C&D) and industrial wastes through alkali activation. Constr Build Mater 2016;121:686–93. https://doi.org/10.1016/j.conbuildmat.2016.06.051.

[31] Adesanya E, Ohenoja K, Kinnunen P, Illikainen M. Alkali Activation of Ladle Slag from Steel-Making Process. J Sustain Metall 2017;3:300–10. https://doi.org/10.1007/s40831-016-0089-x.

[32] Reig L, Soriano L, Borrachero M V., Monzó J, Payá J. Influence of calcium aluminate cement (CAC) on alkaline activation of red clay brick waste (RCBW). Cem Concr Compos 2016;65:177–85. https://doi.org/10.1016/j.cemconcomp.2015.10.021.

[33] Novais RM, Ascensão G, Seabra MP, Labrincha JA. Waste glass from end-of-life fluorescent lamps as raw material in geopolymers. Waste Manag 2016;52:245–55. https://doi.org/10.1016/j.wasman.2016.04.003.

[34] Zhang S, Keulen A, Arbi K, Ye G. Waste glass as partial mineral precursor in alkali-activated slag/fly ash system. Cem Concr Res 2017;102:29–40. https://doi.org/10.1016/j.cemconres.2017.08.012.

[35] Arulrajah A, Kua TA, Horpibulsuk S, Phetchuay C, Suksiripattanapong C, Du YJ. Strength and microstructure evaluation of recycled glass-fly ash geopolymer as low-carbon masonry units. Constr Build Mater 2016;114:400–6. https://doi.org/10.1016/j.conbuildmat.2016.03.123.

[36] Ranjbar N, Mehrali M, Alengaram UJ, Metselaar HSC, Jumaat MZ. Compressive strength and microstructural analysis of fly ash/palm oil fuel ash based geopolymer mortar under elevated temperatures. Constr Build Mater 2014;65:114–21. https://doi.org/10.1016/j.conbuildmat.2014.04.064.

[37] Rakhimova NR, Rakhimov RZ. Alkali-activated cements and mortars based on blast furnace slag and red clay brick waste. Mater Des 2015;85:324–31. https://doi.org/10.1016/j.matdes.2015.06.182.

[38] Poinot T, Laracy ME, Aponte C, Jennings HM, Ochsendorf JA, Olivetti EA. Beneficial use of boiler ash in alkali-activated bricks. Resour Conserv Recycl 2018;128:1–10. https://doi.org/10.1016/j.resconrec.2017.09.013.

[39] Nazari A, Sanjayan JG. Synthesis of geopolymer from industrial wastes. J Clean Prod

2015;99:297–304. https://doi.org/10.1016/j.jclepro.2015.03.003.

[40] Zawrah MF, Gado RA, Feltin N, Ducourtieux S, Devoille L. Recycling and utilization assessment of waste fired clay bricks (Grog) with granulated blast-furnace slag for geopolymer production. Process Saf Environ Prot 2016;103:237–51. https://doi.org/10.1016/j.psep.2016.08.001.

[41] Tekin I. Properties of NaOH activated geopolymer with marble, travertine and volcanic tuff wastes. Constr Build Mater 2016;127:607–17. https://doi.org/10.1016/j.conbuildmat.2016.10.038.

[42] Sun Z, Cui H, An H, Tao D, Xu Y, Zhai J, et al. Synthesis and thermal behavior of geopolymer-type material from waste ceramic. Constr Build Mater 2013;49:281–7. https://doi.org/10.1016/j.conbuildmat.2013.08.063.

[43] Ahmari S, Zhang L. Production of eco-friendly bricks from copper mine tailings through geopolymerization. Constr Build Mater 2012;29:323–31. https://doi.org/10.1016/j.conbuildmat.2011.10.048.

[44] Ascensão G, Seabra MP, Aguiar JB, Labrincha JA. Red mud-based geopolymers with tailored alkali diffusion properties and pH buffering ability. J Clean Prod 2017;148:23–30. https://doi.org/10.1016/j.jclepro.2017.01.150.

[45] Reig L, Tashima MM, Borrachero MV, Monzó J, Cheeseman CR, Payá J. Properties and microstructure of alkali-activated red clay brick waste. Constr Build Mater 2013;43:98–106. https://doi.org/10.1016/j.conbuildmat.2013.01.031.

[46] Yliniemi J, Pesonen J, Tiainen M, Illikainen M. Alkali activation of recovered fuel-biofuel fly ash from fluidised-bed combustion: Stabilisation/solidification of heavy metals. Waste Manag 2015;43:273–82. https://doi.org/10.1016/j.wasman.2015.05.019.

[47] Nazari A, Bagheri A, Riahi S. Properties of geopolymer with seeded fly ash and rice husk bark ash. Mater Sci Eng A 2011;528:7395–401. https://doi.org/10.1016/j.msea.2011.06.027.

[48] Novais RM, Buruberri LH, Ascensão G, Seabra MP, Labrincha JA. Porous biomass fly ash-based geopolymers with tailored thermal conductivity. J Clean Prod 2016;119:99–107. https://doi.org/10.1016/j.jclepro.2016.01.083.

[49] Ozer I, Soyer-Uzun S. Relations between the structural characteristics and compressive strength in metakaolin based geopolymers with different molar Si/Al ratios. Ceram Int 2015;41:10192–8. https://doi.org/10.1016/j.ceramint.2015.04.125.

[50] Redden R, Neithalath N. Microstructure, strength, and moisture stability of alkali activated glass powder-based binders. Cem Concr Compos 2014;45:46–56. https://doi.org/10.1016/j.cemconcomp.2013.09.011.

[51] Cristelo N, Fernández-Jiménez A, Vieira C, Miranda T, Palomo Á. Stabilisation of construction and demolition waste with a high fines content using alkali activated fly

ash. Constr Build Mater 2018;170:26–39. https://doi.org/10.1016/j.conbuildmat.2018.03.057.

[52] Fořt J, Vejmelková E, Koňáková D, Alblová N, Čáchová M, Keppert M, et al. Application of waste brick powder in alkali activated aluminosilicates: Functional and environmental aspects. J Clean Prod 2018;194:714–25. https://doi.org/10.1016/j.jclepro.2018.05.181.

[53] Lu JX, Poon CS. Use of waste glass in alkali activated cement mortar. Constr Build Mater 2018;160:399–407. https://doi.org/10.1016/j.conbuildmat.2017.11.080.

[54] Manjunath R, Narasimhan MC, Umesh KM, Shivam Kumar, Bala Bharathi UK. Studies on development of high performance, self-compacting alkali activated slag concrete mixes using industrial wastes. Constr Build Mater 2019;198:133–47. https://doi.org/10.1016/j.conbuildmat.2018.11.242.

[55] Tuyan M, Andiç-Çakir Ö, Ramyar K. Effect of alkali activator concentration and curing condition on strength and microstructure of waste clay brick powder-based geopolymer. Compos Part B Eng 2018;135:242–52. https://doi.org/10.1016/j.compositesb.2017.10.013.

[56] Rovnaník P, Rovnaníková P, Vyšvařil M, Grzeszczyk S, Janowska-Renkas E. Rheological properties and microstructure of binary waste red brick powder/metakaolin geopolymer. Constr Build Mater 2018;188:924–33. https://doi.org/10.1016/j.conbuildmat.2018.08.150.

[57] Abdollahnejad Z, Luukkonen T, Mastali M, Kinnunen P, Illikainen M. Development of one-part alkali-activated ceramic/slag binders containing recycled ceramic aggregates. J Mater Civ Eng 2019;31:1–13. https://doi.org/10.1061/(ASCE)MT.1943-5533.0002608.

[58] Robayo-Salazar R, Mejía-Arcila J, Mejía de Gutiérrez R, Martínez E. Life cycle assessment (LCA) of an alkali-activated binary concrete based on natural volcanic pozzolan: A comparative analysis to OPC concrete. Constr Build Mater 2018;176:103–11. https://doi.org/10.1016/j.conbuildmat.2018.05.017.

[59] Tho-In T, Sata V, Boonserm K, Chindaprasirt P. Compressive strength and microstructure analysis of geopolymer paste using waste glass powder and fly ash. J Clean Prod 2016;172:2892–8. https://doi.org/10.1016/j.jclepro.2017.11.125.

[60] Batista RP, Trindade ACC, Borges PHR, Silva F de A. Silica fume as precursor in the development of sustainable and high-performance MK-based alkali-activated materials reinforced with short PVA fibers. Front Mater 2019;6:1–15. https://doi.org/10.3389/fmats.2019.00077.

[61] de Vargas AS, Dal Molin DCC, Vilela ACF, Silva FJ da, Pavão B, Veit H. The effects of Na2O/SiO2molar ratio, curing temperature and age on compressive strength, morphology and microstructure of alkali-activated fly ash-based geopolymers. Cem Concr Compos 2011;33:653–60. https://doi.org/10.1016/j.cemconcomp.2011.03.006.

[62] Tänzer R, Jin Y, Stephan D. Alkali activated slag binder: effect of cations from silicate activators. Mater Struct 2017;50:91. https://doi.org/10.1617/s11527-016-0961-y.

[63] Yang K-H, Cho A-R, Song J-K, Nam S-H. Hydration products and strength development of calcium hydroxide-based alkali-activated slag mortars. Constr Build Mater 2012;29:410–9. https://doi.org/10.1016/j.conbuildmat.2011.10.063.

[64] Wang H, Li H, Yan F. Synthesis and mechanical properties of metakaolinite-based geopolymer. Colloids Surfaces A Physicochem Eng Asp 2005;268:1–6. https://doi.org/10.1016/j.colsurfa.2005.01.016.

[65] Phoo-ngernkham T, Maegawa A, Mishima N, Hatanaka S, Chindaprasirt P. Effects of sodium hydroxide and sodium silicate solutions on compressive and shear bond strengths of FA–GBFS geopolymer. Constr Build Mater 2015;91:1–8. https://doi.org/10.1016/j.conbuildmat.2015.05.001.

[66] Phoo-ngernkham T, Hanjitsuwan S, Damrongwiriyanupap N, Chindaprasirt P. Effect of sodium hydroxide and sodium silicate solutions on strengths of alkali activated high calcium fly ash containing Portland cement. KSCE J Civ Eng 2017;21:2202–10. https://doi.org/10.1007/s12205-016-0327-6.

[67] Zhang Z, Provis JL, Wang H, Bullen F, Reid A. Quantitative kinetic and structural analysis of geopolymers. Part 2. Thermodynamics of sodium silicate activation of metakaolin. Thermochim Acta 2013;565:163–71. https://doi.org/10.1016/j.tca.2013.01.040.

[68] Xu H, Van Deventer JSJ. The geopolymerisation of alumino-silicate minerals. Int J Miner Process 2000;59:247–66. https://doi.org/10.1016/S0301-7516(99)00074-5.

[69] Phair JW, Van Deventer JSJ. Effect of silicate activator pH on the leaching and material characteristics of waste-based inorganic polymers. Miner Eng 2001;14:289–304. https://doi.org/10.1016/S0892-6875(01)00002-4.

[70] Khale D, Chaudhary R. Mechanism of geopolymerization and factors influencing its development: A review. J Mater Sci 2007;42:729–46. https://doi.org/10.1007/s10853-006-0401-4.

[71] PQ Europe. Sodium and potassium silicates 2004:16.

[72] Tchakouté HK, Rüscher CH, Kong S, Kamseu E, Leonelli C. Geopolymer binders from metakaolin using sodium waterglass from waste glass and rice husk ash as alternative activators: A comparative study. Constr Build Mater 2016;114:276–89. https://doi.org/10.1016/j.conbuildmat.2016.03.184.

[73] Jeon D, Jun Y, Jeong Y, Oh JE. Microstructural and strength improvements through the use of Na 2 CO 3 in a cementless Ca(OH) 2 -activated Class F fly ash system. Cem Concr Res 2015;67:215–25. https://doi.org/10.1016/j.cemconres.2014.10.001.

[74] Akturk B, Kizilkanat AB, Kabay N. Effect of calcium hydroxide on fresh state behavior

of sodium carbonate activated blast furnace slag pastes. Constr Build Mater 2019;212:388–99. https://doi.org/10.1016/j.conbuildmat.2019.03.328.

[75] Yuan B, Yu QL, Brouwers HJH. Assessing the chemical involvement of limestone powder in sodium carbonate activated slag. Mater Struct 2017;50:136. https://doi.org/10.1617/s11527-017-1003-0.

[76] Barbosa VF., MacKenzie KJ., Thaumaturgo C. Synthesis and characterisation of materials based on inorganic polymers of alumina and silica: sodium polysialate polymers. Int J Inorg Mater 2000;2:309–17. https://doi.org/10.1016/S1466-6049(00)00041-6.

[77] Hanjitsuwan S, Injorhor B, Phoo-ngernkham T, Damrongwiriyanupap N, Li L-Y, Sukontasukkul P, et al. Drying shrinkage, strength and microstructure of alkali-activated high-calcium fly ash using FGD-gypsum and dolomite as expansive additive. Cem Concr Compos 2020;114:103760. https://doi.org/10.1016/j.cemconcomp.2020.103760.

[78] de Vargas AS, Dal Molin DCC, Masuero ÂB, Vilela ACF, Castro-Gomes J, de Gutierrez RM. Strength development of alkali-activated fly ash produced with combined NaOH and Ca(OH) 2 activators. Cem Concr Compos 2014;53:341–9. https://doi.org/10.1016/j.cemconcomp.2014.06.012.

[79] Bouzón N, Payá J, Borrachero MV, Soriano L, Tashima MM, Monzó J. Refluxed rice husk ash/NaOH suspension for preparing alkali activated binders. Mater Lett 2014;115:72–4. https://doi.org/10.1016/j.matlet.2013.10.001.

[80] Bernal SA, Rodríguez ED, Mejia de Gutiérrez R, Provis JL, Delvasto S. Activation of Metakaolin/Slag Blends Using Alkaline Solutions Based on Chemically Modified Silica Fume and Rice Husk Ash. Waste and Biomass Valorization 2012;3:99–108. https://doi.org/10.1007/s12649-011-9093-3.

[81] Mejía JM, Mejía de Gutiérrez R, Puertas F. Ceniza de cascarilla de arroz como fuente de sílice en sistemas cementicios de ceniza volante y escoria activados alcalinamente. Mater Constr 2013;63:361–75. https://doi.org/10.3989/mc.2013.04712.

[82] Tong KT, Vinai R, Soutsos MN. Use of Vietnamese rice husk ash for the production of sodium silicate as the activator for alkali-activated binders. J Clean Prod 2018;201:272–86. https://doi.org/10.1016/j.jclepro.2018.08.025.

[83] Geraldo RH, Fernandes LFR, Camarini G. Water treatment sludge and rice husk ash to sustainable geopolymer production. J Clean Prod 2017;149:146–55. https://doi.org/10.1016/j.jclepro.2017.02.076.

[84] Torres-Carrasco M, Puertas F. Waste glass in the geopolymer preparation. Mechanical and microstructural characterisation. J Clean Prod 2015;90:397–408. https://doi.org/10.1016/j.jclepro.2014.11.074.

[85] Vinai R, Soutsos M. Production of sodium silicate powder from waste glass cullet for alkali activation of alternative binders. Cem Concr Res 2019;116:45–56.

https://doi.org/10.1016/j.cemconres.2018.11.008.

[86] Živica V. Effectiveness of new silica fume alkali activator. Cem Concr Compos 2006;28:21–5. https://doi.org/10.1016/j.cemconcomp.2005.07.004.

[87] Villaquirán-Caicedo MA. Studying different silica sources for preparation of alternative waterglass used in preparation of binary geopolymer binders from metakaolin/boiler slag. Constr Build Mater 2019;227:1–13. https://doi.org/10.1016/j.conbuildmat.2019.08.002.

[88] Rodríguez ED, Bernal SA, Provis JL, Paya J, Monzo JM, Borrachero MV. Effect of nanosilica-based activators on the performance of an alkali-activated fly ash binder. Cem Concr Compos 2013;35:1–11. https://doi.org/10.1016/j.cemconcomp.2012.08.025.

[89] Moraes JCB, Tashima MM, Akasaki JL, Melges JLP, Monzó J, Borrachero MV, et al. Increasing the sustainability of alkali-activated binders: The use of sugar cane straw ash (SCSA). Constr Build Mater 2016;124:148–54. https://doi.org/10.1016/j.conbuildmat.2016.07.090.

[90] Alonso MM, Gascó C, Morales MM, Suárez-Navarro JA, Zamorano M, Puertas F. Olive biomass ash as an alternative activator in geopolymer formation: A study of strength, durability, radiology and leaching behaviour. Cem Concr Compos 2019;104:103384. https://doi.org/10.1016/j.cemconcomp.2019.103384.

[91] de Moraes Pinheiro SM, Font A, Soriano L, Tashima MM, Monzó J, Borrachero MV, et al. Olive-stone biomass ash (OBA): An alternative alkaline source for the blast furnace slag activation. Constr Build Mater 2018;178:327–38. https://doi.org/10.1016/j.conbuildmat.2018.05.157.

[92] Font A, Soriano L, Moraes JCB, Tashima MM, Monzó J, Borrachero MV, et al. A 100% waste-based alkali-activated material by using olive-stone biomass ash (OBA) and blast furnace slag (BFS). Mater Lett 2017;203:46–9. https://doi.org/10.1016/j.matlet.2017.05.129.

[93] Soriano L, Font A, Tashima MM, Monzó J, Borrachero MV, Payá J. One-part blast furnace slag mortars activated with almond-shell biomass ash: A new 100% waste-based material. Mater Lett 2020;272:127882. https://doi.org/10.1016/j.matlet.2020.127882.

[94] Ban CC, Ken PW, Ramli M. Mechanical and Durability Performance of Novel Self-activating Geopolymer Mortars. Procedia Eng 2017;171:564–71. https://doi.org/10.1016/j.proeng.2017.01.374.

[95] Peys A, Rahier H, Pontikes Y. Potassium-rich biomass ashes as activators in metakaolin-based inorganic polymers. Appl Clay Sci 2016;119:401–9. https://doi.org/10.1016/j.clay.2015.11.003.

[96] Pourabbas Bilondi M, Toufigh MM, Toufigh V. Using calcium carbide residue as an alkaline activator for glass powder–clay geopolymer. Constr Build Mater 2018;183:417–28. https://doi.org/10.1016/j.conbuildmat.2018.06.190.

[97] Phetchuay C, Horpibulsuk S, Suksiripattanapong C, Chinkulkijniwat A, Arulrajah A, Disfani MM. Calcium carbide residue: Alkaline activator for clay–fly ash geopolymer. Constr Build Mater 2014;69:285–94. https://doi.org/10.1016/j.conbuildmat.2014.07.018.

[98] Fernández-Jiménez A, Cristelo N, Miranda T, Palomo Á. Sustainable alkali activated materials: Precursor and activator derived from industrial wastes. J Clean Prod 2017;162:1200–9. https://doi.org/10.1016/j.jclepro.2017.06.151.

[99] van Riessen A, Jamieson E, Kealley CS, Hart RD, Williams RP. Bayer-geopolymers: An exploration of synergy between the alumina and geopolymer industries. Cem Concr Compos 2013;41:29–33. https://doi.org/10.1016/j.cemconcomp.2013.04.010.

[100] Choo H, Lim S, Lee W, Lee C. Compressive strength of one-part alkali activated fly ash using red mud as alkali supplier. Constr Build Mater 2016;125:21–8. https://doi.org/10.1016/j.conbuildmat.2016.08.015.

[101] Font A, Soriano L, Reig L, Tashima MM, Borrachero MV, Monzó J, et al. Use of residual diatomaceous earth as a silica source in geopolymer production. Mater Lett 2018;223:10–3. https://doi.org/10.1016/j.matlet.2018.04.010.

[102] He J, Jie Y, Zhang J, Yu Y, Zhang G. Synthesis and characterization of red mud and rice husk ash-based geopolymer composites. Cem Concr Compos 2013;37:108–18. https://doi.org/10.1016/j.cemconcomp.2012.11.010.

[103] Koteswara Rao D, Pranav PR., Anusha M. STABILIZATION OF EXPANSIVE SOIL WITH RICE HUSK ASH, LIME AND GYPSUM – AN EXPERIMENTAL STUDY. Int J Eng Sci Technol 2011;3:8076–85.

[104] Sturm P, Gluth GJG, Brouwers HJH, Kühne H-C. Synthesizing one-part geopolymers from rice husk ash. Constr Build Mater 2016;124:961–6. https://doi.org/10.1016/j.conbuildmat.2016.08.017.

[105] Singh B. Rice husk ash. Waste Suppl. Cem. Mater. Concr., Elsevier; 2018, p. 417–60. https://doi.org/10.1016/B978-0-08-102156-9.00013-4.

[106] Nimwinya E, Arjharn W, Horpibulsuk S, Phoo-ngernkham T, Poowancum A. A sustainable calcined water treatment sludge and rice husk ash geopolymer. J Clean Prod 2016;119:128–34. https://doi.org/10.1016/j.jclepro.2016.01.060.

[107] Hwang C-L, Huynh T-P. Effect of alkali-activator and rice husk ash content on strength development of fly ash and residual rice husk ash-based geopolymers. Constr Build Mater 2015;101:1–9. https://doi.org/10.1016/j.conbuildmat.2015.10.025.

[108] Rodríguez de Sensale G. Effect of rice-husk ash on durability of cementitious materials. Cem Concr Compos 2010;32:718–25. https://doi.org/10.1016/j.cemconcomp.2010.07.008.

[109] Songpiriyakij S, Kubprasit T, Jaturapitakkul C, Chindaprasirt P. Compressive strength

and degree of reaction of biomass- and fly ash-based geopolymer. Constr Build Mater 2010;24:236–40. https://doi.org/10.1016/j.conbuildmat.2009.09.002.

[110] Mellado A, Catalán C, Bouzón N, Borrachero M V., Monzó JM, Payá J. Carbon footprint of geopolymeric mortar: study of the contribution of the alkaline activating solution and assessment of an alternative route. RSC Adv 2014;4:23846–52. https://doi.org/10.1039/C4RA03375B.

[111] de Azevedo ARG, Alexandre J, Zanelato EB, Marvila MT. Influence of incorporation of glass waste on the rheological properties of adhesive mortar. Constr Build Mater 2017;148:359–68. https://doi.org/10.1016/j.conbuildmat.2017.04.208.

[112] Lu J, Duan Z, Poon CS. Fresh properties of cement pastes or mortars incorporating waste glass powder and cullet. Constr Build Mater 2017;131:793–9. https://doi.org/10.1016/j.conbuildmat.2016.11.011.

[113] Menchaca-Ballinas LE, Escalante-Garcia JI. Low CO2 emission cements of waste glass activated by CaO and NaOH. J Clean Prod 2019;239:117992. https://doi.org/10.1016/j.jclepro.2019.117992.

[114] Zhang Z, Zhang B, Yan P. Comparative study of effect of raw and densified silica fume in the paste, mortar and concrete. Constr Build Mater 2016;105:82–93. https://doi.org/10.1016/j.conbuildmat.2015.12.045.

[115] Nochaiya T, Wongkeo W, Chaipanich A. Utilization of fly ash with silica fume and properties of Portland cement-fly ash-silica fume concrete. Fuel 2010;89:768–74. https://doi.org/10.1016/j.fuel.2009.10.003.

[116] Siddique R. Utilization of silica fume in concrete: Review of hardened properties. Resour Conserv Recycl 2011;55:923–32. https://doi.org/10.1016/j.resconrec.2011.06.012.

[117] Sukontasukkul P, Chindaprasirt P, Pongsopha P, Phoo-Ngernkham T, Tangchirapat W, Banthia N. Effect of fly ash/silica fume ratio and curing condition on mechanical properties of fiber-reinforced geopolymer. J Sustain Cem Mater 2020;9:218–32. https://doi.org/10.1080/21650373.2019.1709999.

[118] Moraes JCB, Font A, Soriano L, Akasaki JL, Tashima MM, Monzó J, et al. New use of sugar cane straw ash in alkali-activated materials: A silica source for the preparation of the alkaline activator. Mag Concr Res 2018;171:1256–64. https://doi.org/10.1016/j.conbuildmat.2018.03.230.

[119] Phummiphan I, Horpibulsuk S, Phoo-ngernkham T, Arulrajah A, Shen S-L. Marginal Lateritic Soil Stabilized with Calcium Carbide Residue and Fly Ash Geopolymers as a Sustainable Pavement Base Material. J Mater Civ Eng 2017;29:04016195. https://doi.org/10.1061/(ASCE)MT.1943-5533.0001708.

[120] Hanjitsuwan S, Phoo-ngernkham T, Li L, Damrongwiriyanupap N, Chindaprasirt P. Strength development and durability of alkali-activated fly ash mortar with calcium carbide residue as additive. Constr Build Mater 2018;162:714–23.

https://doi.org/10.1016/j.conbuildmat.2017.12.034.

[121] Hanjitsuwan S, Phoo-ngernkham T, Damrongwiriyanupap N. Comparative study using Portland cement and calcium carbide residue as a promoter in bottom ash geopolymer mortar. Constr Build Mater 2017;133:128–34. https://doi.org/10.1016/j.conbuildmat.2016.12.046.

[122] Suksiripattanapong C, Horpibulsuk S, Phetchuay C, Suebsuk J, Phoo-ngernkham T, Arulrajah A. Water Treatment Sludge–Calcium Carbide Residue Geopolymers as Nonbearing Masonry Units. J Mater Civ Eng 2017;29:04017095. https://doi.org/10.1061/(ASCE)MT.1943-5533.0001944.

[123] Phoo-ngernkham T, Phiangphimai C, Intarabut D, Hanjitsuwan S, Damrongwiriyanupap N, Li L, et al. Low cost and sustainable repair material made from alkali-activated high-calcium fly ash with calcium carbide residue. Constr Build Mater 2020;247:118543. https://doi.org/10.1016/j.conbuildmat.2020.118543.

ARTICLE 2

EVALUATION OF ECO-EFFICIENT GEOPOLYMER USING CHAMOTTE AND WASTE GLASS-BASED ALKALINE SOLUTIONS [2]

Abstract:

Geopolymers are binder materials that can be an alternative to replace Portland cement. They are considered less aggressive to the environment because of the lower emission of CO_2 and use of energy in their production chain. This work aimed to manufacture a more eco-efficient product and recycle industrial waste, contributing to the solution of the disposal problem. Thus, this study evaluated the performance of alkali-activated pastes produced from industrial wastes in both phases, using chamotte as the precursor and waste glass (WG) as a component of the activating solution. The effects of molar concentration and WG content in the alkaline solutions were investigated. A factorial design of experiments was developed, considering three levels of molar concentration (8 mol/L, 10 mol/L and 12 mol/L) and four levels of WG content per 100 ml of solution (0, 5, 10 and 15 g). Physical and mechanical tests were performed, as well as the microstructural analyses using XRD and FT-IR techniques. The environmental impacts of replacing the traditional activator by the WG-based one were also assessed. The results showed that the WG content strongly affects the mechanical strength of geopolymers and the quality of the matrices, promoting a greater formation of geopolymerization products. Using an alternative activator can reduce 69.8 % of the embodied energy and 78.0 % of CO_2 footprint compared to the traditional waterglass activators. Therefore, this study proved the sustainability potential and technical viability of using WG as an activator in chamotte-based geopolymer.

Keywords: geopolymer; waste glass; chamotte; eco-efficiency; sustainability.

[2] Manuscript published by the journal "Case Studies in Construction Materials". Accepted in 16 December 2021. Available online in 17 December 2021. First author: Beatryz Cardoso Mendes. https://doi.org/10.1016/j.cscm.2021.e00847.

1 INTRODUCTION

Geopolymeric materials can be eco-friendly binders with a great range of potential applications [1]. They were developed as an alternative to conventional Portland cement, which is known for the environmental damages caused by its production. Geopolymer is an aluminosilicate material synthesized by the alkali-activation of a source of silica and alumina [2]. The alkali-activation can be described as the mixture of a liquid phase, rich in alkaline ions, and a solid phase with suitable proportions of reactive silica and alumina [3]. The final product consists of a hydrated alkaline aluminosilicate (N-A-S-H type gel) with a three-dimensional structure at the nanoscale [4]. Both Si and Al ions have tetrahedral coordination. The alkali compensates the electric charge produced by replacing the Al^{3+} by Si^{4+} and is placed in the voids of three-dimensional structure. Remain hydroxyls are also found on the gel surface, but they do not play a significant role in the geopolymer formation [5].

The sources of silica and alumina conventionally used for geopolymer production are calcined clays and class F fly ashes. The main criterion for applying some material in the solid phase is the content of reactive (or amorphous) silica and alumina [6]. The liquid phase consists of an alkaline solution with the presence of compounds named activators. The type and dosage of the activator play an important role in the rheology control and structural properties of geopolymer [7]. The activators commonly used are hydroxides and silicates, such as sodium hydroxide, potassium hydroxide and sodium silicate. These compounds can be applied separately or mixed. The soluble silicate provides additional SiO_2 to the system while the hydroxide ensures the high alkalinity of the solution [8].

Although geopolymers are recognized as more environmentally friendly than conventional Portland cement, some disadvantages about their use in civil construction need to be mentioned. They are difficult to handle due to the high alkalinity of the materials applied, that can cause safety and health risks. These materials also need a careful control of curing, which can be not assured for in situ applications. Besides, to assure higher levels of sustainability, it is necessary to improve the geopolymer chain production [9]. The use of conventional activators, such as commercial sodium and potassium hydroxides and silicates increases the embodied energy, CO_2 emissions and costs of geopolymers due to their manufacturing process [10,11]. Sourcing of commercial activactors can also be challenging in remote locations [9]. Thus, the development of alternative activators based on waste sources of silica and sodium is extremely required to make the product more sustainable, cost-competitive and accessible.

In recent years, many researches have been developed using alternative aluminosilicate materials, basically industrial wastes such as rice husk ash [12], red mud [13,14], copper mining tailings [15] and chamotte [16,17]. Chamotte is a ceramic industry waste obtained from the production of roof tiles and bricks. This material contains amorphous aluminosilicates, presenting pozzolanic activity and potential to be used as a geopolymer precursor. Although its reactivity is lower than metakaolin, its application can be optimized through formulations control and adjustment of preparing conditions. It is possible to achieve values of compressive strength above 20 MPa [18–20]. Alternative activators have also been studied, such as silica fume [21,22], waste glass [23,24] and agricultural ashes [24-26]. Waste glass presents high contents of SiO_2 (>70%), most being amorphous. That makes the waste a viable alternative for producing sodium silicate alkaline solutions, replacing the commercial products. Some studies have shown that the mechanical resistance and crystalline phases formed in geopolymerization are similar to those observed using conventional activators [24,28].

It is necessary to highlight the risks related to the use of industrial waste, especially waste glass. It is important to mention the toxicity that can occur in some types of glass, and also the risks of handling this waste when it is originated by culets, for example [29]. These risks are minimized when the waste glass is already originated or discarded as mud or powder. However, handling waste glass powder can be a health issue due to the possibility to cause diseases such as silicosis, which occurs after long-term exposure to silica dust [30]. These notes do not prevent the application of the waste in building materials, but it must be done with caution.

There are a substantial number of studies approaching the use of wastes as precursors in geopolymers. However, there are few researches about the application of industrial waste materials in both phases of geopolymer - solid phase and alkaline solution. The objective of this study is the mechanical and structural assessment of geopolymeric pastes produced from chamotte as the solid precursor and waste glass-based solutions as alternative activators. This combination is also innovative in the technical literature. The effect of two processing factors was investigated: molar concentration of the solutions and waste glass content. The factorial experimental design was applied to obtain the significant factors and optimal levels of each factor. The structural analyses were performed by X-ray diffraction (XRD) and Fourier-transform infrared spectroscopy (FTIR) techniques. The environmental analysis was also assessed, comparing the eco-efficiency performance between traditional waterglass-based activators and the proposed waste glass-based activator.

2 MATERIALS AND METHODS

2.1 Materials

The chamotte was provided by a ceramic industry located at Ouro Branco, MG, Brazil. The waste was obtained from broken pieces such as bricks and roof tiles. It was grounded using a Los Angeles abrasion machine for 90 minutes to reduce its particle size. The waste glass powder (WG) was obtained from the glass cutting process and supplied by NewTemper company, located at Rio das Ostras, RJ, Brazil. The material was crushed and passed through the ASTM 325 sieve. The alkaline solutions were produced with commercial sodium hydroxide pellets (NaOH P.A., 99%, CRQ) and distilled water.

2.1.1 Characterization of raw materials

The specific mass of chamotte and WG was determined using the volumetric flask of *Le Chatelier*, the same used in cementitious materials tests. The determination of particle size distribution was performed using a *Bettersize2000 laser* particle size analyzer in a range of 0.02 μm to 2,000 μm.

The chemical compositions of chamotte and WG were obtained by X-ray fluorescence by dispersive energy, using a *Shimadzu Micro-EDX-1300* spectrometer. The high voltage (50 keV and 50 μA) was applied, mapping 1200 points. The loss on ignition (LOI) was also determined at a temperature of 950 °C. The mineralogical compositions were assessed by X-ray diffraction through the *D8 Discover (Bruker)* diffractometer. The XRD was conducted with CuKα radiation (1.5418 Å), 2θ varying from 3° to 70°, 0.05° 2θ step-scan and 1.0 s/step.

Table 2.1 shows the results of specific mass and average particle size (d_{50}) of chamotte and waste glass. Chamotte has a higher specific mass (2.75 g/cm³) than waste glass (2.40 g/cm³). The chemical composition of the materials can explain it since chamotte has a higher iron and aluminum oxides content.

Table 2.1. Physical characterization of chamotte and waste glass.

Raw material	**Specific mass (g/cm³)**	**Mean particle size – D50 (μm)**
Chamotte	2.75	22.74
Waste glass	2.40	7.46

Figure 2.1 shows the particle size distribution of the materials. The technical literature reports that the particle size of the precursor affects the geopolymer formation since finer material tends to be more reactive [31]. Chamotte presented an average particle size of 22.74 μm, which is close to the values applied by other authors [32,33]. Waste glass is a finer material, with an average particle size of 7.46 μm. The lower particle size benefits the reaction kinetics of dissolution and geopolymerization [34].

Figure 2.1. Particle size distribution of chamotte and waste glass.

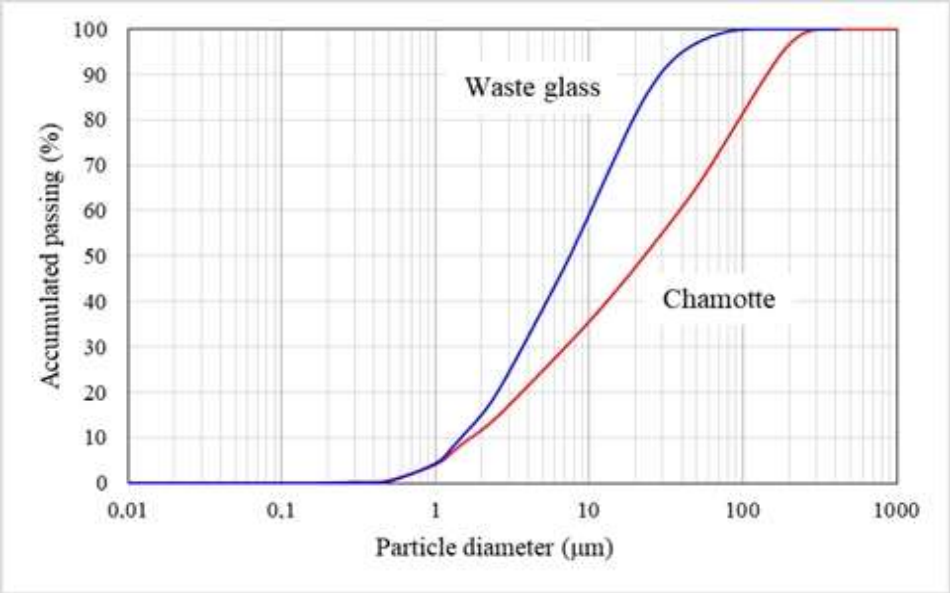

Table 2.2 shows the chemical composition and loss on ignition of chamotte and waste glass. Chamotte is basically composed by silica (49.74%) and alumina (30.55%). The SiO_2/Al_2O_3 molar ratio is 2.76. Fort et al. [35], Terrones-Saeta et al. [36] and Robayo et al. [37] also used chamotte to produce geopolymers. The ratios found by the authors were 1.78, 3.22 and 5.57, respectively, indicating that the chamotte used in this research is suitable for geopolymer production. Waste glass has a great presence of SiO_2 (60.21%) and smaller amounts of CaO (7.4%), Al_2O_3 (2.93%) and Na_2O (2.61%). The significant content of silica is an important factor in choosing an alternative activator [38]. Tchakouté et al. [9] and Torres-Carrasco et al. [22] applied waste glass with 68.70% and 70.71% of total silica to activate metakaolin and fly ash, respectively.

The XRD patterns of chamotte and waste glass are shown in Figure 2.2. The main crystalline phases in chamotte are quartz (d = 4.262, 3.344, 2.284 and 2.129 Å), kaolinite (d = 7.215 Å), epidote (d = 2.907 Å) and hematite (d = 2.699 Å). One can notice that only the major peak of kaolinite appears on the XRD pattern. It occurs because kaolinite was turned into

metakaolinite (amorphous phase) in the firing process of red ceramic production. A broad hump diffraction peak between 15° and 30° also suggests the presence of amorphous silica and alumina compounds. The waste glass is basically amorphous with weak peaks of quartz ad calcite. It is a desirable characteristic for application in geopolymer synthesis since the soluble and reactive silica is amorphous.

Table 2.2. Chemical composition of chamotte and waste glass.

Raw material	Chemical composition (%)								
	SiO_2	Al_2O_3	Fe_2O_3	CaO	K_2O	MgO	Ti_2O	Na_2O	Other
Chamotte	49.74	30.55	5.29	0.54	1.27	1.61	1.08	1.54	6.07
Waste glass	60.21	2.93	0.29	7.40	0.23	1.65	0.01	2.61	4.94

Figure 2.2. XRD patterns of chamotte and waste glass (K – kaolinite (ICDD: 00-029-1488); Q – quartz (COD: 96-900-9667); E – epidote (COD ID: 1529622); R – rutile (ICDD: 00-034-080); H – hematite (ICDD: 01-085-0987; C – calcite ICDD: 01-072-1937)).

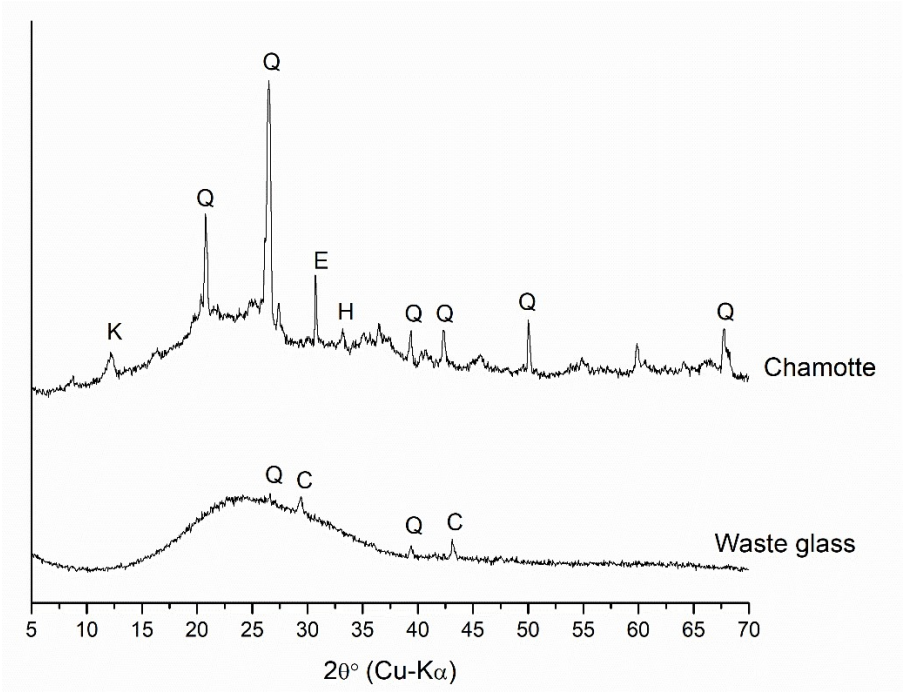

2.2 Mix design

The production of the waste-based pastes followed the two-part methodology. The chamotte was the precursor, and the WG was added to the alkaline solution, such as an additional source of soluble silica. Chamotte was chosen as precursor because it has similar behavior to calcined clays, i. e. metakaolin. However, the use of this waste does not require any thermal treatment to turn the raw material more reactive. This is an advantage from both

economy and sustainability points of view. Waste glass was used due to the high content of amorphous silica, the availability and the low particle size, not being necessary the application of mechanical treatment to reduce the particles size. The alkaline activator was manufactured with 8 M, 10 M and 12 M NaOH solutions and 0 g, 5 g, 10 g and 15 g of WG per 100mL of solution.

It was applied the factorial design of experiments, analyzing two quantitative factors – NaOH molar concentration of the solution and content of WG – with three and four levels, respectively. The experimental design was completely randomized. Table 2.3 shows the twelve mixtures produced, the liquid to solid ratio and the characteristics of the related alkaline solutions: the levels of molar concentration and WG content, and the SiO_2/Na_2O molar ratio. In the solutions without waste glass, there is no content of SiO_2.

Table 2.3. Characteristics of geopolymer mixtures (L/S: liquid/solid).

Mixture	Molar concentration	WG content (g/100mL)	L/S ratio	SiO_2/ Na_2O molar ratio
M1-8M-0	8M	0	0.4	-
M2-8M-5	8M	5	0.4	0.124
M3-8M-10	8M	10	0.4	0.248
M4-8M-15	8M	15	0.4	0.370
M5-10M-0	10M	0	0.4	-
M6-10M-5	10M	5	0.4	0.100
M7-10M-10	10M	10	0.4	0.199
M8-10M-15	10M	15	0.4	0.297
M9-12M-0	12M	0	0.4	-
M10-12M-5	12M	5	0.4	0.083
M11-12M-10	12M	10	0.4	0.166
M12-12M-15	12M	15	0.4	0.248

After obtaining the experimental results, statistical treatments applicable to the factorial experimental design were performed using the Minitab® software, such as ANOVA, analysis of variance, Tukey Test and optimal experiment selection. The aim was to observe the interference of the evaluated factors in the results, the correlation between them, and the optimal levels of each one. In order to better understand the ANOVA analyses, Pareto charts were made. This chart indicates the significance of the factors and the interaction between them, showing how they affect the responses. The chart presents a reference line which indicates the statistical significance of the terms. It is represented by a t-value associated to the null hypothesis for $\alpha = 0.05$ (significance level of 5%).

The Tukey test is widely used by researchers for multiple comparisons. The test is based on the distribution of studentized range and establishes the difference among means at a certain

significance level of probability [39,40]. In the results, the same letter is applied when the means are statistically equal. The significance level applied at this analyses was 5%.

The NaOH solutions were prepared with the addition of solid NaOH (pellets) in distilled water. The solid NaOH was dissolved using a magnetic stirrer until the solution homogenization. The procedure for preparing the WG-based solutions was based on the work of Torres-Carrasco and Puertas [23]. The determined content of WG was added to the solution and magnetically stirred at 80 ± 2 °C for three hours. Then, the solution was filtered, and the liquid part was used as an activator. After the preparation, the pH and density were measured. All the solutions were prepared at least 24 hours before the production of geopolymers.

The liquid/solid ratio was 0.40. This value was determined after previous analysis and ensured good conditions of mixing and molding. Firstly, the solution was poured into the chamotte powder and manually mixed for one minute. After, the mixing was carried out by a mechanical process with the following steps: (1) one minute at lower velocity (195 rpm); (2) one-minute interval; and (3) two minutes at higher velocity (205 rpm). The paste was transferred to prismatic acrylic molds measuring 2 cm x 2 cm x 8 cm. They were taken to the vibration table for one minute and covered with a plastic film. The samples were kept at room temperature for 24 hours. Afterward, they were allocated in plastic bags and immersed in a thermal chamber at 60 ± 1 °C for 24 hours. After this period, they were cured at room temperature until the mechanical tests were carried out.

2.3 Test methods

2.3.1 Physical and mechanical properties of geopolymers

The bulk density was determined as the relation between the weight and the volume. A caliper was used for measuring the height and diameter of the samples. The mechanical characterization consisted of determining the flexural and compressive strengths. The flexural strength was obtained through a three-point bending test in three samples of each mixture (by age), with a loading rate of 186.4 N/s. The prismatic sample was divided into two parts subjected to a conventional uniaxial compressive strength test (loading rate of 500 N/s). Thus, six pieces of each mixture were tested. The specimens were assessed at ages of 7, 28 and 56 days to evaluate the increase of mechanical strength over time.

2.3.2 Microstructural characterization of geopolymers

After performing the mechanical tests, the geopolymers were subjected to microstructural analysis to identify the compounds formed by the reactions and evaluate the morphology. The analyses were conducted in 28-days specimens. When it was no possible to perform the tests on this exact day, the geopolymerization reactions were stopped at this age using the methodology described by Reig et al. [20]. The samples were immersed in acetone solution (P.A.) and then dried at 60°C in an oven for 30 minutes, after crushing and passing the samples through a 125 μm sieve. X-ray diffraction technique was applied, using the same parameters listed in topic 2.3.1. The assessment of chemical bonds in the geopolymeric matrices was obtained through Fourier Transform Infrared (FTIR) spectroscopy (Varian 660-IR, equipped with GladiATR (attenuated total reflection, ATR)). The infrared spectrum range was 400-4000 cm^{-1} with a resolution of 4 cm^{-1} and 64 scans by spectrum.

Scanning electronic microscopy (SEM) and energy dispersive spectroscopy (EDS) were performed in fractured pieces of geopolymers, using a *JEOL – JSM6010LA* equipment, excitation voltage of 15 kV and working distance of 10 mm. The images approximations were 500x, 1000x, 2500x and 5000x. EDS analysis were obtained at 2500x approximation.

2.4. Environmental analysis

The assessment of environmental factors in alkali-activated materials is a complex process, which requires a deep study of the life cycle of each component. However, a preliminary and simplified analysis can be done in order to compare the performance of traditional raw materials and alternative sources. This analysis can provide initial data about the saves of consumed energy (or embodied energy) and CO_2 emission when an industrial waste can be used as a precursor or activator.

The environmental impact evaluation when sodium silicate-based solution is replaced by waste glass-based solution was carried out following the SUB-RAW Index method, proposed by Bontempi [41]. This method is based on the values of embodied energy and CO_2 footprint of the raw material and its potential "substitute". The index can be calculated using Equation 2.1:

$$SUB - RAW = \frac{\log(EE_{raw}) - \log(EE_{sub}) + \log(CF_{raw}) - \log(CF_{sub})}{2} \quad (2.1)$$

where EE_{raw} is the embodied energy of original material (MJ/kg); EE_{sub} represents the embodied energy of the substitute material (MJ/kg); CF_{raw} is the CO_2 footprint of the raw material (kg/kg); and CF_{sub} represents the CO_2 footprint of the substitute material (kg/kg). The result of the equation can vary from -9 to 9. When the index is positive, the substitute material has a better performance in terms of eco-efficiency than the traditional raw material.

The embodied energy (*EE*) and CO_2 footprint (*CF*) values were estimated for commercial waterglass and the waste glass-based alkaline solution produced in this research. The 8M-15 solution was selected for the evaluation since it presented better mechanical performance and a higher content of WG. It is highlighted that the adopted values are an indicative, which depends on the local conditions or further considerations.

3 RESULTS AND DISCUSSION

3.1 Characterization of solutions

The characteristics of pH and density of the 12 solutions are shown in Table 2.4. The pH values varied from 11.41 to 12.54. The pH decreased with the molar concentration of the solution. This could be due to the solution saturation, limiting the release of OH- ions and affecting the pH. Comparing the solutions without waste glass, 12M-0 presented the lowest pH. Due to the low pH, when WG was added, the level of network destruction after the Si-O-Si and Al-O-Al bonds were broken was lower than the other concentrations [42]. The addition of waste glass increased the pH for all the molar concentrations, but with low changes as the waste glass content increased.

Table 2.4. Characteristics of the alkaline solutions.

Alkaline solution	pH	Density (g/cm³)
8M-0	12.39	1.35
8M-5	12.54	1.36
8M-10	12.54	1.41
8M-15	12.44	1.45
10M-0	11.91	1.39
10M-5	12.14	1.41
10M-10	12.10	1.46
10M-15	12.06	1.43
12M-0	11.41	1.45
12M-5	11.42	1.49
12M-10	11.53	1.50
12M-15	11.54	1.55

For the same molar concentration, the density of the solution increased with higher additions of WG, which is related to the higher content of soluble material. The incorporation of 5 g promoted a small change in the density values. When 15 g of WG was added, the density increase was 7.4% for 8M, 2.9% for 10M and 6.9% for 12M. In general, the density values were higher to 12M solutions, which presented the lowest pH values. As mentioned before, the high density reflects the saturation of the solution and the limitation of ionic mobility.

3.2. Physical and mechanical characterization of pastes

Figure 2.3-a shows the results of bulk density. The bulk density values varied in a range of 1.83 to 1.95 g/cm³. Most mixtures presented a decrease in bulk density with age. Figure 2.3-b shows the relationship between the compressive strength and the bulk density of the samples by age. One can notice there is not a clear correlation between the properties considering the results in general. However, Figure 2.3-a shows that the 8M-15 and 8M-10 mixtures presented higher compressive strength and bulk density values. In this case, the higher bulk density values possibly indicate lower values of void volume [43]. The density of the alkaline solutions and content of waste glass can also affect this property, making its behavior more complex.

Figure 2.3. (a) Results of bulk density at 7, 28 and 56 days; (b) relationship between compressive strength and bulk density of geopolymers.

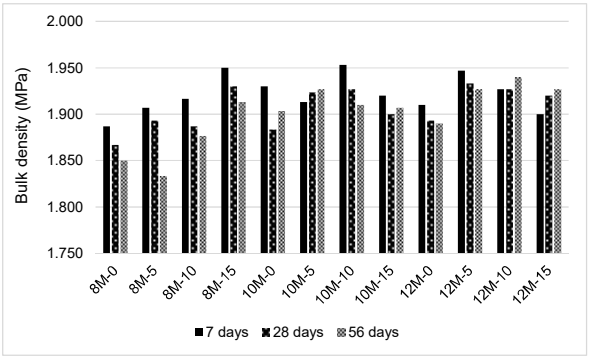

(a)

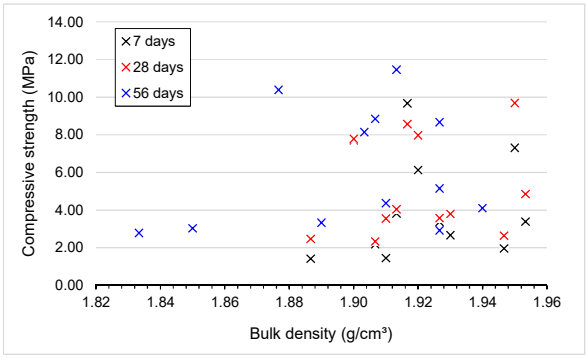

(b)

The flexural and compressive strengths of geopolymer pastes were evaluated in three different ages (7, 28 and 56 days), and the results are shown in Figure 2.4 and

Figure 2.5. In general, the mixtures with higher contents of waste glass (10 g and 15 g/100 mL) exceed the strength of geopolymers with NaOH only. For lower content of WG (5 g/100 mL), the effect was antagonic. It is important to mention that higher variability of results is observed in pastes with WG. One possible explanation can be the increase of brittleness

exhibited by these binders [44], although the reason is still unclear. The mechanical strength results are similar to those reported by Robayo et al. [37] and Rovnanik et al. [45] for chamotte-based geopolymers.

Figure 2.4. Results of flexural strength at 7, 28 and 56 days.

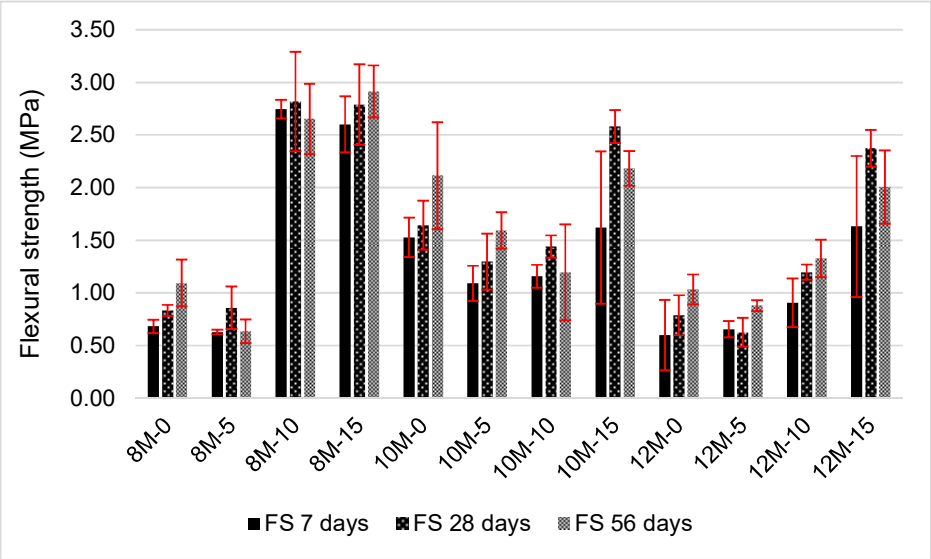

Figure 2.5. Results of compressive strength at 7, 28 and 56 days.

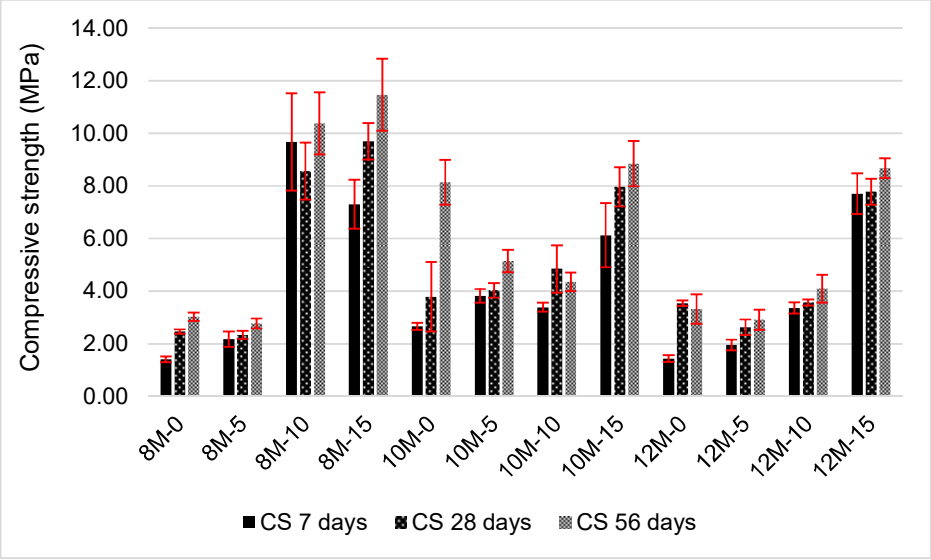

In general, both flexural and compressive strength increased over time. Considering the 10M-10 mixture, the mechanical strength at 56 days was lower than at 28 days, but the standard deviation bars indicate no statistically significant difference between the values. Except for the 10M-0 mixture, the increase of strength after 28 days is low. It probably occurred due to the influence of thermal curing time (60 °C for 24 h) at early ages and higher availability of reactive

silica at the beginning of the reaction process [21]. Over time, the rate of geopolymerization decreases, promoting no significant changes in the geopolymer matrix and its strength. Chamotte presents a slower reaction comparing with other precursors, such as metakaolin and fly ash. Metakaolin and fly ash-based geopolymers can achieve maximum strengths at the age of 7 days [45,46].

The results obtained at 28 days were statistically analyzed using Minitab® software. For flexural strength, Figure 2.6-a shows the Pareto chart. The dashed line is the reference line that indicates the statistical significance of the terms. The number 2.06 is the t-value associated to the null hypothesis for $\alpha = 0.05$. The chart indicates that both factors and the interaction are significant and affect the responses. The WG content has a stronger influence on flexural strength than the molar concentration of the solution. The higher the addition of WG, the higher the flexural strength. This confirms the availability of reactive silica in WG and the importance of providing additional soluble silica to the system. According to Zhang et al. [47], using activators with dissolved silicates is preferable over using only hydroxide because the resulting products tend to develop higher strength and denser microstructure.

It is important to mention the interaction between WG content and molar concentration, as seen in Figure 2.6-b. For small amounts of WG addition (0 and 5 g), the molar concentration of 10 mol/L presented better mechanical behavior, which was also confirmed by Torres-Carrasco et al. [23]. However, the authors did not assess the incorporation of WG in NaOH 8 M solution, only in NaOH 10 M solution. This research demonstrated that, for higher addition levels (10 e 15 g), the solution with a concentration of 8 mol/L led to better results. This could be due to the excess of alkalis in the 10 M and 12 M solutions. Besides the low availability of soluble silica to form sodium silicate, the excess of alkalis results in the limitation of ions mobility in the solution, promoting the decrease of mechanical strength [48].

Mix 8M-10 presented the highest flexural strength, reaching 2.82 MPa. Mix 8M-15 showed the second-highest value, 2.79 MPa. After performing the Tukey test (Table 2.5), it is concluded that the mean flexural strength of mixtures 8M-10, 8M-15, 10M-15 and 12M-15 are statistically equal at a significance level of 5%. It is noteworthy that the model adjusted in the analysis of variance presented R^2 equal to 94.39%, the errors presented random distribution around the mean equal to zero (homogeneity of variances) and the residues are normally distributed. Thus, the statistical analysis is valid, as well as the trends observed previously.

Figure 2.6. (a) Pareto chart of flexural strength at 28 days; (b) interaction plot for the property of flexural strength (FS).

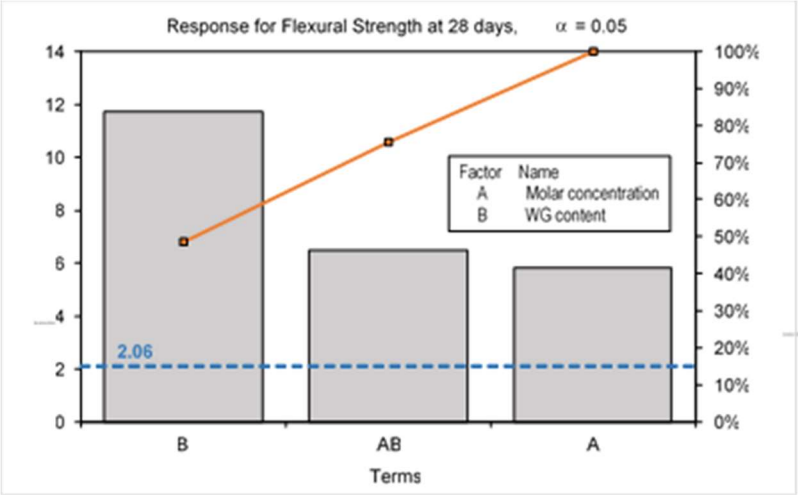

a)

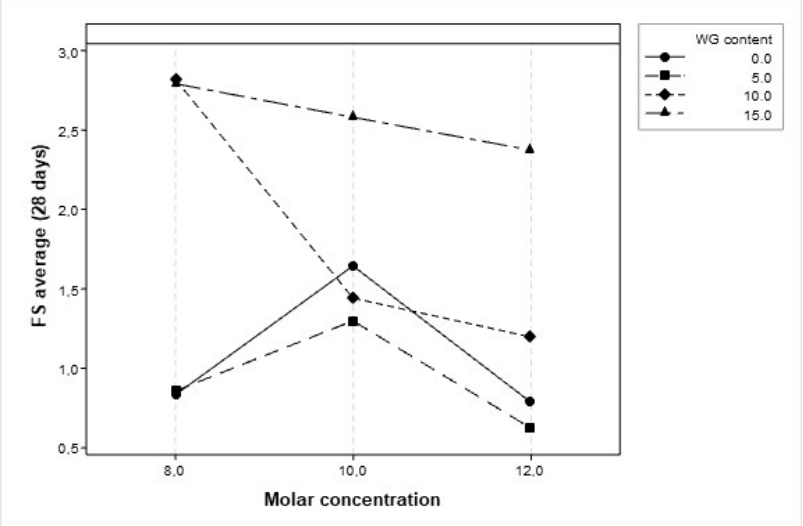

b)

Table 2.5. Tukey test results of flexural and compressive strength at 28 days.

Paste	Flexural strength (MPa)		Compressive strength (MPa)	
8M-10	2.82	A	8.56	A
8M-15	2.79	A	9.08	A
10M-15	2.58	A	7.96	A
12M-15	2.37	A	7.48	A
10M-0	1.64	B	3.78	B C D
10M-10	1.44	B C	4.84	B
10M-5	1.30	B C D	4.03	B C
12M-10	1.20	B C D	3.45	B C D
8M-5	0.86	C D	2.24	D
8M-0	0.83	C D	2.47	C D
12M-0	0.79	C D	3.43	B C D
12M-5	0.62	D	2.63	C D

Regarding the analysis of compressive strength at 28 days, Figure 2.7-a) shows the Pareto chart. The trends are similar to those pointed out for flexural strength. For this property, the interaction between the factors and the WG content are the most significant terms of the adjusted model. The influence of each factor is represented in Figure 2.7-b). The increase of molar concentration decreases compressive strength, which was also observed by other authors [49,50]. At higher NaOH concentrations, the accelerated dissolution of silica and alumina delayed the polycondensation. Besides, an excess hydroxide ion caused the precipitation of aluminosilicate gel at the early stage and reduced the quality and strength of geopolymer pastes [51].

Figure 2.7. (a) Pareto chart of compressive strength at 28 days; (b) Influence of each factor on the compressive strength at 28 days (CS).

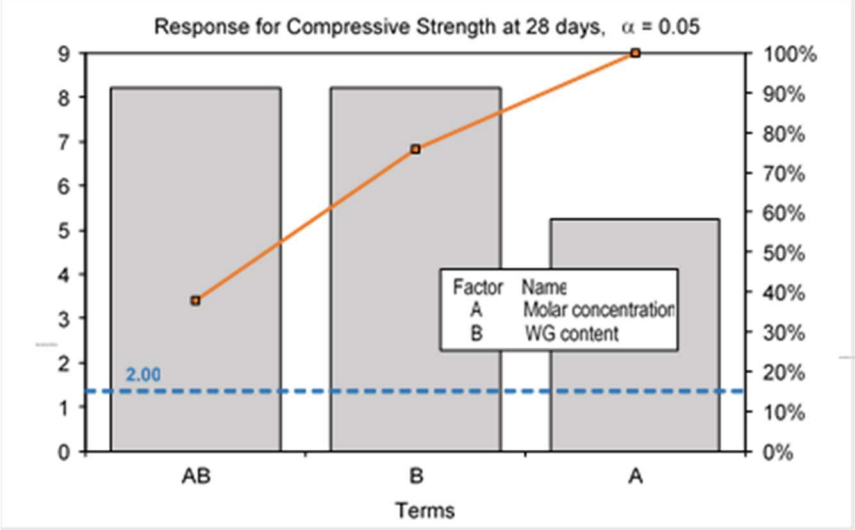

a)

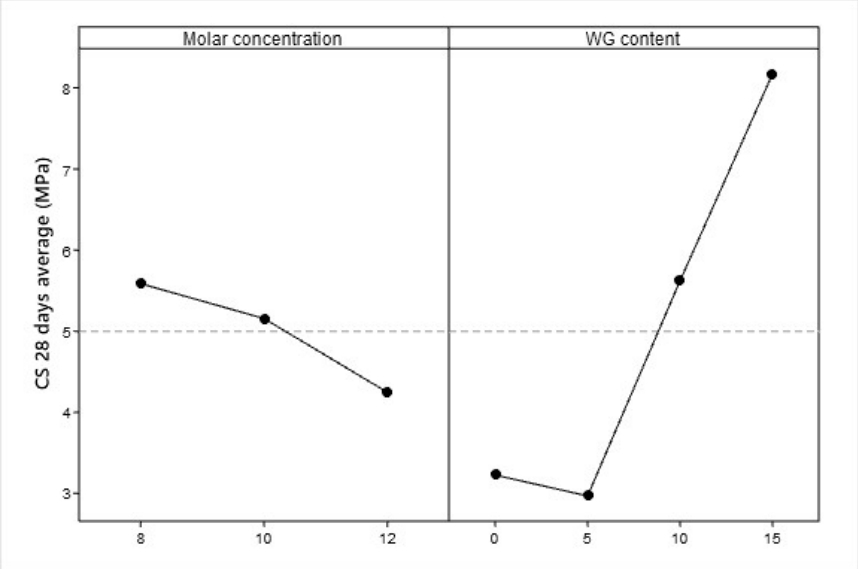

b)

The effect of NaOH concentration also depends on the precursor of geopolymer and curing temperature. Livi and Repette [52] noted that higher molar concentrations can be applied for higher curing temperatures (above 85 °C) with no decrease of mechanical strength. Xu and Van Deventer [53] explain that high amounts of OH^- require a longer time to eliminate the excess of water or a higher curing temperature due to the viscosity of the solution.

Concerning the NaOH concentration, the negative effect on the mechanical strength can also be explained in terms of the pH solution. As seen in Table 2.4, pH decreased with the increase of molar concentration. The pH of NaOH 12 M solutions were lower than the others, with values between 11.41 and 11.54, resulting in low values of compressive strength. The pH controls the alkalinity of the medium, promoting the solubility of silicates monomers. Therefore, the decrease of pH affects the availability of ionic species that form the geopolymeric products (N-A-S-H gel) [54].

The addition of 5 g (per 100 ml of solution) led to lower values than the use of NaOH only. Above 5 g, the increasing incorporation of WG promotes the enhancement of mechanical strength. The average compressive strength of 15 g WG (8.17 MPa) is 275.08% higher than the average of 5 g (2.97 MPa). The addition of WG in the solution changes its SiO_2/Na_2O molar ratio, which influences the mechanical strength of the geopolymer. According to Puertas and Torres-Carrasco [55], the increase of the modules SiO_2/Na_2O also increases the compressive strength. This trend can be observed in Figure 2.8, which shows the relationship between the compressive strength at 28 and 56 days and the modules SiO_2/Na_2O in the activators.

Figure 2.8. Relationship between compressive strength and the SiO_2/Na_2O molar ratio in the alkaline solutions.

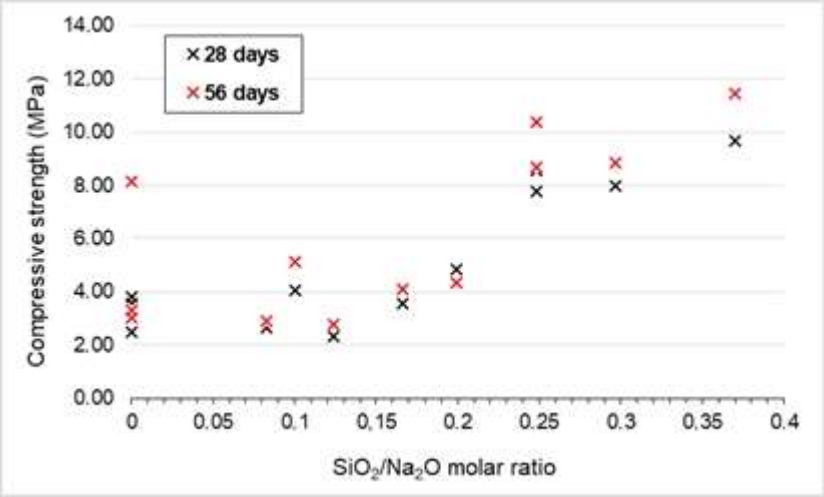

According to the Tukey test (Table 2.5), 8M-15, 8M-10, 10M-15, and 12M-15 samples presented averages statistically equal, being the best results for compressive strength. These results are consistent with the flexural strength analysis. The 8M-15 mix achieved the highest values at 28 and 56 days (9.70 MPa and 11.47 MPa, respectively). The squared-R obtained for adjusted ANOVA was 91.27%, indicating a good fitting of the experimental values.

3.3 Microstructural analyses

3.3.1 XRD analyses

Figure 2.9 shows the diffraction patterns of 8M-0, 10M-0 and 12M-0 pastes at 28 days. 10M-0 and 12M-0 samples presented a typical amorphous halo around 28°, corresponding to the N-A-S-H gel formed during hydration [56]. Zeolite X (chemical composition $Na_{88}(H_2O)_{220}[Si_{104}Al_{88}O_{384}]$) was also found at the XRD pattern of 10M-0 and 12M-0, which is expected considering the N-A-S-H gel composition. Davidovits [57] suggests that the application of hydrothermal curing promotes the formation of zeolitic species. In this study, hydrothermal curing at 60 ºC was applied, justifying the formation of zeolite X.

Figure 2.9. XRD patterns of 8M-0, 10M-0 and 12M-0 samples at 28 days.

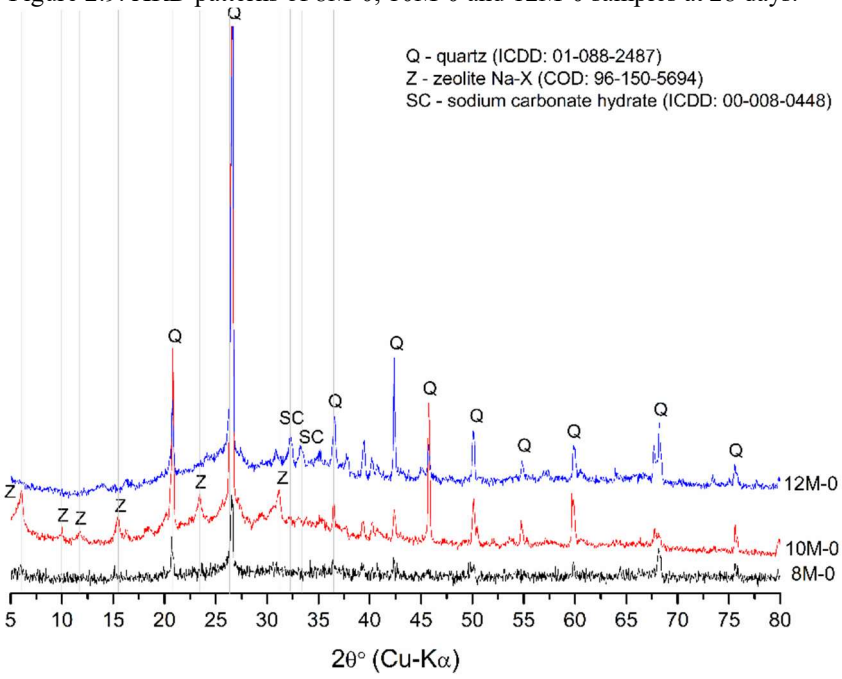

The diffractogram of 8M-0 presents peaks of quartz and small peaks of zeolite X, indicating the lower formation of crystalline structures. This is consistent with the mechanical strength results since the 8M-0 geopolymer had the worst performance. The 10M-0 geopolymer presented higher mechanical strength than the 8M-0 and 12M-0 and showed higher zeolite X peaks intensity. Peaks of sodium carbonate were also found in the 12M-0 pattern, confirming the results of FT-IR analysis.

Figure 2.10 shows the XRD patterns of the 8M series. The addition of WG (above 5 g) promoted the formation of another kind of zeolite – zeolite Y or faujasite (chemical composition $Na_{16}Ca_{16}(H_2O)_{42.7}[Si_{134.4}Al_{57.6}O_{384}]$). Both structures are composed of silicon-oxygen and aluminum-oxygen tetrahedrons that form a complex structural unit of cubooctahedron. The structural difference is the combination of these units and the number of member rings that interconnect them. The chemical difference is mainly defined by the Si/Al ratio. Faujasite structure is synthesized when the starting mixture has a higher Si/Al ratio [58]. Besides, faujasite crystal has Ca atoms in its composition, and the WG is the raw material that presents significant content of CaO (7.4%). It explains the formation of this zeolite type only in geopolymers with the addition of WG.

Figure 2.10. XRD patterns of 8M series (8M-0, 8M-5, 8M-10 and 8M-15) at 28 days.

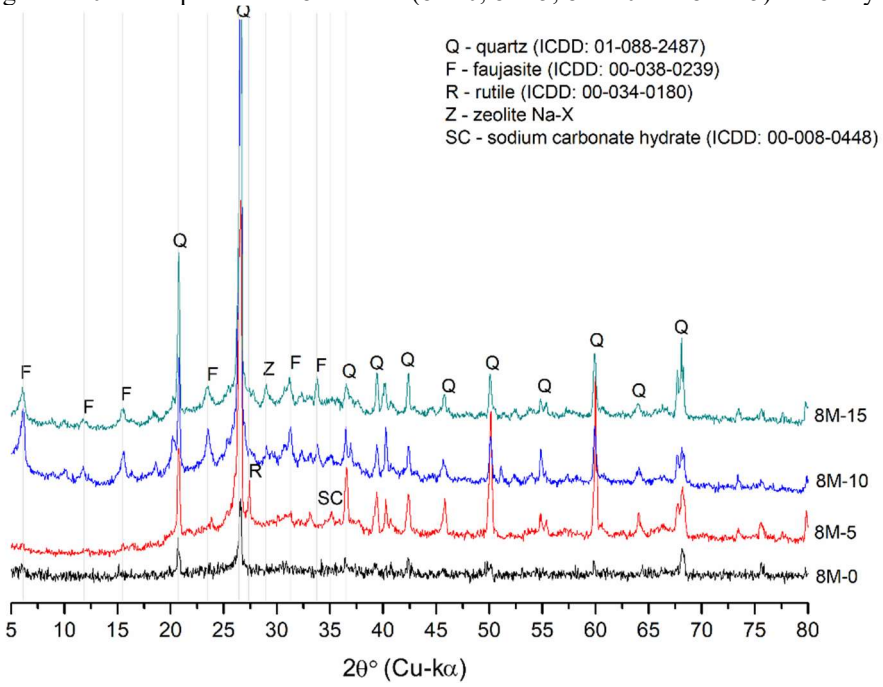

In all XRD patterns, there is the presence of quartz. The presence of faujasite was clearly observed only in geopolymers 8M-10 and 8M-15, suggesting that these matrices have higher

quality. This is in agreement with the mechanical strength results. The XRD patterns of 8M-10 and 8M-15 do not have significant differences, justifying the similar results of both flexural and compressive strengths. The XRD pattern of 8M-5 presents peaks of the remaining compounds of chamotte, such as rutile, and the presence of sodium carbonate hydrate.

Figure 2.11 shows the XRD patterns of mixtures with the same content of waste glass and different levels of molar concentration (8M-10, 10M-10 and 12M-10). With this content of WG, it is easier to note and analyze the effect of varying molar concentration on the microstructure. One can observe that 8M-10 patterns and 10M-10 present the same phases, but the peaks of faujasite are more intense in 8M-10.

Zeolites structures were not detected in the 12M-10 sample, even with the additional silica in the system. The XRD patterns of 12M-0 (Figure 9) and 12M-10 are similar, indicating that the addition of waste glass up to 10 g promoted few changes in the microstructure of the pastes. Indeed, the significantly improved compressive strength related to this molar concentration occurred only for WG content equal to 15 g.

Figure 2.11. XRD patterns of 10WG series (8M-10, 10M-10 and 12M-10) at 28 days.

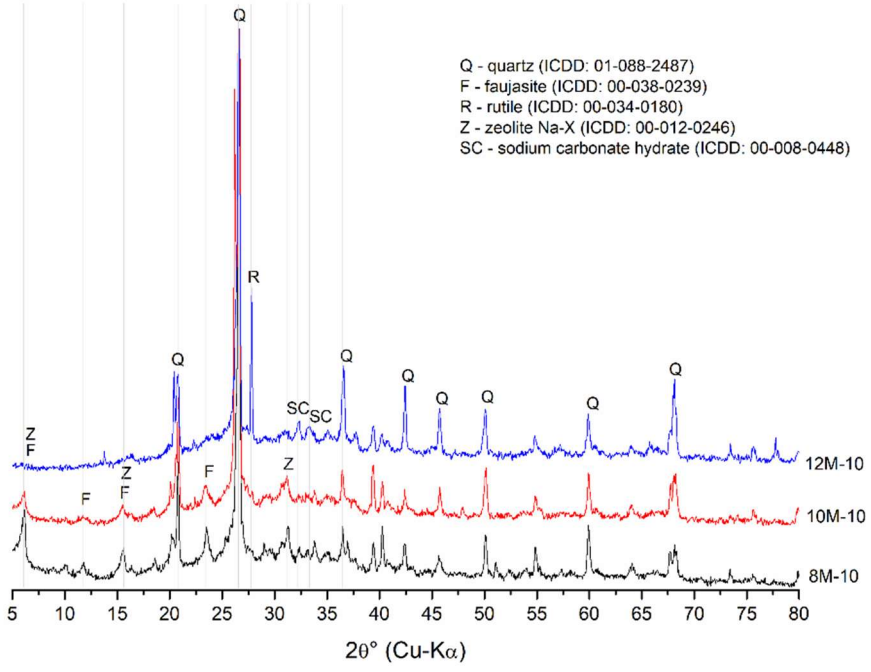

3.3.2 FTIR analyses

Figure 2.12 shows the FT-IR spectrum of chamotte and 8M-0, 10M-0 and 12M-0 mixtures, in order to evaluate the influence of NaOH molar concentration. Chamotte presents a

major band at 1036 cm^{-1} wavenumber, related to the asymmetrical stretching of Si-O-T, being T Si or Al tetrahedral. According to Chindaprasirt et al. [59], this band can be used to determine the degree of polymerization in geopolymer. The band at 447 cm^{-1} is associated with bending vibrations of O-Si-O [60]. The principal band occurred at the range of 1036 to 981 cm^{-1}.

The most intense set of bands in this interval (about 1000 cm^{-1}) is recognized as the indicator of polysialation extent and incorporation of aluminum [61]. With the addition of NaOH alkaline solution, the position of the principal band was found to shift to lower wavenumber due to the alkali-activation and formation of aluminosilicate gel [62]. This shift is related to the dissolution of precursors due to the alkaline hydrolysis and occurrence of polycondensation reactions. Therefore, amorphous structures are developed, and silicates species are partially replaced by aluminates species [21]. As NaOH concentration increases, the Si-O-T vibration band appears at a lower wavenumber (981 cm^{-1} for 12M-0 geopolymer). The tetrahedral framework becomes more depolymerized at higher NaOH concentrations as the bonding between the TO4 units is more ionic. Therefore, the T-O bonds show smaller vibration forces [62]. The shift of the major band also suggests the higher incorporation of Al into geopolymeric gel. This is a consequence of the smaller force of the Al-O bond compared to the Si-O bond [60].

Figure 2.12. FT-IR spectrum of 8M-0, 10M-0 and 12M-0 samples at 28 days.

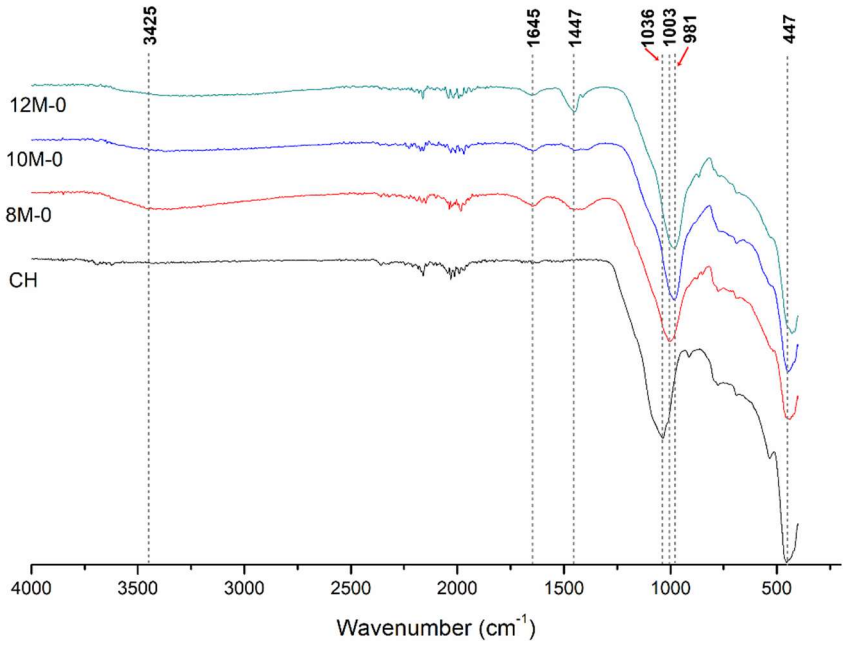

The band at 1447 cm^{-1} becomes narrower with the increase of NaOH molar concentration. This band suggests the presence of O-C-O bonds of CO_3^{-2} groups associated with

carbonate phases. Its formation is due to the carbonation reactions between the alkalis and atmospheric CO_2 [63,64]. One can notice that the carbonation level is higher in the case of 12M-0 geopolymer since there is more availability of alkalis. The 10M-0 mixture presented less intensity of this band, probably due to the higher extension of geopolymerization and inclusion of Na into the structure, reducing the content of unreacted Na in the sample. This corroborates the results of mechanical behavior since 10M-0 samples had higher strength than 8M-0 and 12M-0.

The band at 1645 cm^{-1} is associated with the bending mode of absorbed H_2O, i.e., the vibration of O-H of the hydrated reaction products. The broader band at 3425 cm^{-1} is related to the stretching mode of H-OH, and it can be representative of the water incorporated into the porous microstructure and possibly linked into the N-A-S-H gel [63].

The FT-IR spectrum of the 8M series, with the addition of WG, is shown in Figure 2.13. The satellite bands are similar to those seen in Figure 2.12. The major band occurred at 1003 cm^{-1} to 8M-0 and 990 cm^{-1} to 8M-15. The shift proves that the addition of WG increases the formation of geopolymeric structure, which agrees with the mechanical strength results. At this band, higher wavenumbers are related to the lower inclusion of Al into the geopolymer structure, indicating the greater amount of unreacted particles in the mixtures with less content of WG [21].

Figure 2.13. FT-IR spectrum of 8M series (8M-0, 8M-5, 8M-10 and 8M-15) at 28 days.

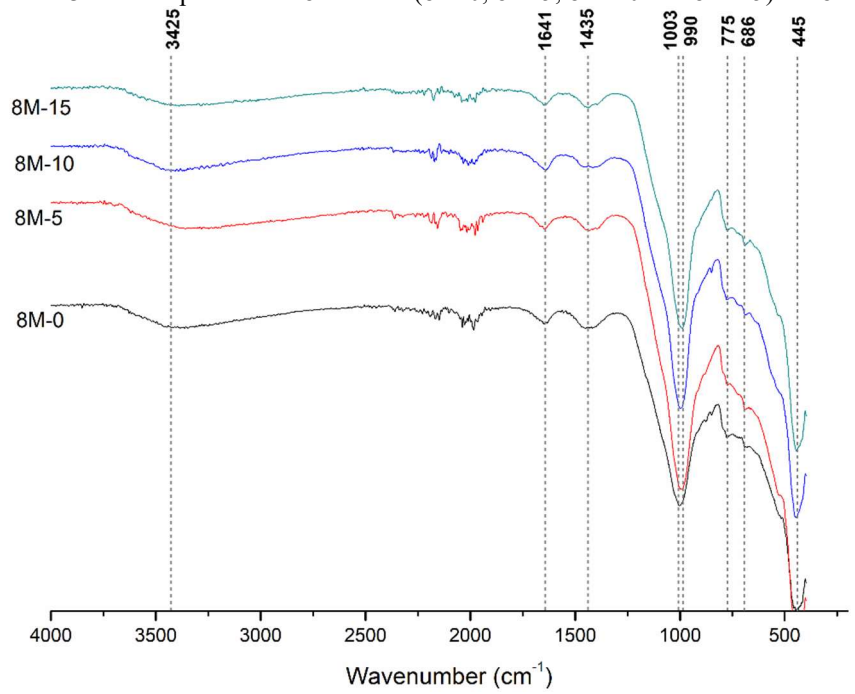

Weak bands around 775 cm^{-1} are related to O-Al-O bending vibrations and Si-O-Si symmetric stretching vibrations. The band at 686 cm^{-1} is probably associated with zeolitic structures [65], which were found in the XRD patterns of geopolymers. It can also be related to the symmetric stretching vibrations of Al-O bonds and the formation of new Al-O-Si cyclic structures after geopolymerization [66]. It indicates that the main geopolymer structure generated after the reactions was a Si-O-Al bending. Lecomte et al. [67] also highlighted that the formation of this band is related to the formation of a cross-linking geopolymer framework. Comparing the bands at 1435 cm^{-1}, the incorporation of WG tends to decrease the intensity of the CO_3^{-2} band, which means that the waste glass can limit the carbonation of the pastes. The bands related to bending and stretching mode of O-H (δO-H and νO-H) are positioned at 1641 cm^{-1} and 3425 cm^{-1}, respectively.

Figure 2.14 shows the FT-IR spectrum of the mixtures with different molar concentrations and the same content of WG (8M-10, 10M-10 and 12M-10). The major band is less intense for the 12M-10 mixture, which presented lower compressive strength than 8M-10 and 10M-10. As expected, the band at 1396 cm^{-1}, related to carbonation, increases the intensity with increased molar concentration. When no waste glass was added to the alkaline solution, 10M pastes presented lower intensity of this band than 8M pastes. Figure 2.14 shows that incorporating WG (10 g/100 mL) changed the chemical behavior of the geopolymers. Probably, the 8M-10 mixture has lower availability of alkalis due to the higher extension of geopolymeric reactions.

Figure 2.14. FT-IR spectrum of 10WG series (8M-10, 10M-10 and 12M-10) at 28 days.

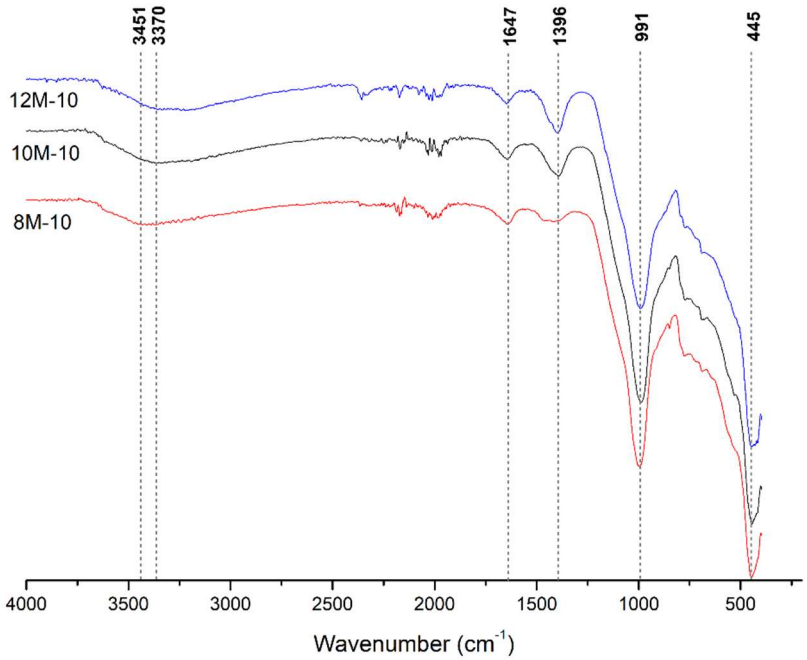

3.3.3 SEM/EDS analyses

Figure 2.15 shows the SEM images of 8M-0, 10M-0 and 12M-0 samples (2500x). One can notice that the 8M-0 paste presented a more homogeneous surface than 10M-0 and 12M-0. On the other hand, the presence of globular particles similar to the zeolitics crystals can be observed in 10M-0 paste surface, which does not occur in 8M-0 and 12M-0. This observation is in agreement with the XRD results, since the zeolite-X was found only in the 10M-0 mixture. The 12M-0 sample presented more angular and needle-shaped structures, different from the others samples. EDS analyses revealed high percentage of Na in this mixture compared to the percentages of Si and Al (Figure 2.16). Therefore, the newly formed platy and needle-like crystals can be associated to sodium carbonate on the surface [68], besides unreacted NaOH and particles from precursor.

Figure 2.15. SEM images of 0WG series (8M-0, 10M-0 and 12M-0) at 28 days.

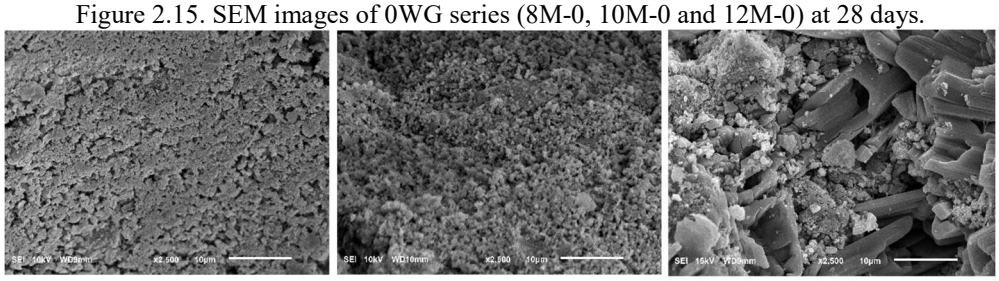

(a) 8M-0 (b) 10M-0 (c) 12M-0

Figure 2.17 shows the SEM images of 8M-5, 8M-10 and 8M-15 pastes (500x and 5000x). 8M-5 sample also presented sodium carbonate particles. Its surface was more heteregenous, with the presence of microcracks and voids and lower incidence of geopolymeric products. EDS results revealed that this paste had the lower Si/Al ratio, equal to 1.19. 8M-10 sample presented basically globular structures, associated to the nanocrystals formed in geopolymeric reactions (zeolites Na-X and faujasite). This paste had the higher Si/Al ratio (1.79). 8M-15 sample presented the lower porous surface, with lower incidence of microcracks. The surface was more homogeneous compared to the others and the presence of zeolitic structures was also found. The Si/Al ratio was 1.30. Considering all the three pastes, one can notice other phases associated to remaining compounds from the raw materials, such as quartz (volumetric structures with smooth surface) and non-reacted NaOH particles (needle-shaped structures).

Figure 2.16. EDS analyses of 0WG series (8M-0, 10M-0 and 12M-0) at 28 days.

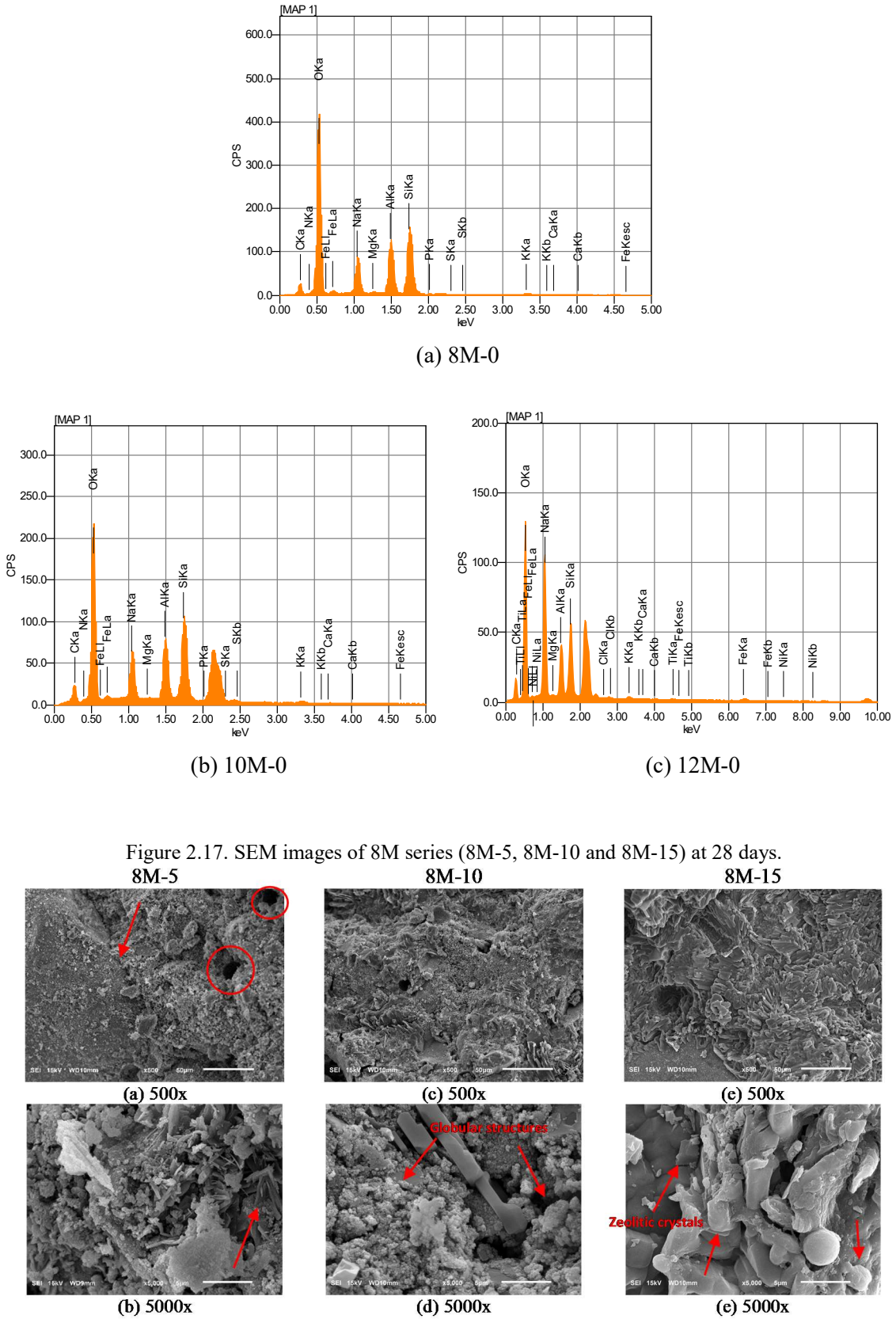

(a) 8M-0

(b) 10M-0

(c) 12M-0

Figure 2.17. SEM images of 8M series (8M-5, 8M-10 and 8M-15) at 28 days.

(a) 500x (c) 500x (e) 500x

(b) 5000x (d) 5000x (e) 5000x

3.4 Environmental analysis

EE and *CF* values related to commercial waterglass were obtained from the technical literature [11,34,35,69]. The adopted values were EE_{raw} = 5.40 MJ/kg and CF_{raw} = 1.5 kg/kg. For the production of geopolymer, the use of waterglass also requires the addition of NaOH in order to achieve a suitable pH. However, only the sodium silicate solution has been taken into account.

The WG powder applied in this study was obtained from the cutting process. The grinding operation was not necessary because of the small particle size in the "natural" state. Therefore, the *EE* and *CF* contribution of WG is negligible compared to the other components. Considering a critical scenario, values obtained from Hossain et al. [70] were applied. 150 g of WG powder and 222.92 g of NaOH are required to produce 1 kg of waste glass-based solution. The energy required for processing the waste was estimated to be 0.76 MJ/kg. Thus, considering that all the electricity is supplied by thermoelectric production, the CO_2 footprint related to the energy consumption is 0.05 kg/kg. Scaling down the values according to the amount of WG per 1 kg of solution, the final *EE* and *CF* are 0.11 MJ/kg and 0.01 kg/kg, respectively.

The *EE* and *CF* related to heating the solution were obtained from Tong et al. [34] since they applied the same duration and temperature (80°C for 3 hours). The values are 0.74 MJ/kg and 0.18 kg/kg, respectively. The *EE* and *CF* data for NaOH were also obtained from the literature [1,34,69,71], although the information was significantly variable. The values adopted were 3.50 MJ/kg and 0.63 kg/kg, respectively, obtained from a specific study about the life cycle assessment of sodium hydroxide [71]. For the production of 1 kg of solution, these values correspond to 0.78 MJ/kg and 0.14 kg/kg.

The selected values for the analysis and SUB-RAW Index were shown in Table 2.6. The calculated index was 0.589, which means that replacing conventional waterglass with waste glass-based solution has a positive effect on the environmental performance of the activator. The reduction of *EE* and *CF* levels were 69.8% and 78.0%, respectively. Even with the addition of NaOH, the alternative alkaline solution can be more eco-efficient when compared to the sodium silicate solution.

Although the use of chamotte as a precursor was not included in this analysis, it also contributes to raising the sustainability of the geopolymers. Besides being an industrial by-product that needs proper disposal, chamotte is also considered a ready-to-use material. Therefore, operations that demand high levels of energy consumption and CO_2 emissions (i.e.,

thermal treatments) are not required, further reducing the environmental impacts of the final product.

Table 2.6. Embodied energy and CO_2 footprint values of commercial waterglass and waste glass-based solution.

Constituent	Embodied energy (MJ/kg)	CO_2 footprint (kg/kg)
Commercial sodium silicate	5.40	1.50
WG-based solution	1.63	0.33
Waste glass	0.11	0.01
NaOH	0.78	0.14
Heating contribution	0.74	0.18
	SUB-RAW Index	**0.589**

4 CONCLUSIONS

The content of waste glass in the activator has a stronger influence on the mechanical strength and microstructure of geopolymers than the molar concentration factor. The addition of WG above 5 g per 100 mL of solution increases the flexural and compressive strength regardless of the molar concentration. When no WG content was added to the solution, the better mixture was 10M-0. After the inclusion of WG, the best mixtures were 8M-15 and 8M-10. It indicates that the interaction between the factors also affects the geopolymer performance. In addition, the increase of SiO_2/Na_2O molar concentration leads to better mechanical results.

The microstructural analyses showed that the WG promoted the formation of N-A-S-H gel and zeolitic species in the pastes and reduced the carbonation reactions between Na and CO_2. FT-IR results demonstrated that the increase of WG content also promoted a higher extent of geopolymerization and is related to the increase of mechanical strength. The occurrence of the principal bands in the range of 1003 to 981 cm^{-1} confirms the aluminosilicate character of the reaction products and corroborates the XRD and SEM analyses.

The environmental analysis proved that the alternative alkaline solution presents a better performance in terms of embodied energy and CO_2 emission. The reductions in embodied energy and CO_2 footprint were 69.8% and 78.0%, respectively. It demonstrates the high environmental impact caused by the replacement of commercial products by industrial wastes.

Finally, both chamotte and waste glass have the potential to be applied as raw materials in geopolymer products that do not demand high compressive strength, such as construction bricks and coating mortars. For future works, these products should be developed and characterized according to the type. In order to attest the technical feasibility of the products,

the behavior regarding to durability should be investigated by means of accelerated aging tests that simulate the environmental weathering.

5 ACKNOWLEDGMENTS

This study was financed in part by the Coordenação de Aperfeiçoamento Pessoal de Nível Superior – Brasil (CAPES) – Finance Code 001. The authors also want to thank the FAPEMIG agency for the financial support, and the Sustainable and Innovative Construction Research Group (SICon) for technical assistance.

REFERENCES

[1] Xiao R, Ma Y, Jiang X, Zhang M, Zhang Y, Wang Y, et al. Strength, microstructure, efflorescence behavior and environmental impacts of waste glass geopolymers cured at ambient temperature. J Clean Prod 2020;252:119610. https://doi.org/10.1016/j.jclepro.2019.119610.

[2] Davidovits J. Properties of Geopolymer Cements. First Int Conf Alkaline Cem Concr 1994:131–49.

[3] Weng L, Sagoe-Crentsil K, Brown T, Song S. Effects of aluminates on the formation of geopolymers. Mater Sci Eng B Solid-State Mater Adv Technol 2005;117:163–8. https://doi.org/10.1016/j.mseb.2004.11.008.

[4] Provis JL, Lukey GC, Van Deventer JSJ. Do geopolymers actually contain nanocrystalline zeolites? a reexamination of existing results. Chem Mater 2005;17:3075–85. https://doi.org/10.1021/cm050230i.

[5] Shi C, Jiménez AF, Palomo A. New cements for the 21st century: The pursuit of an alternative to Portland cement. Cem Concr Res 2011;41:750–63. https://doi.org/10.1016/j.cemconres.2011.03.016.

[6] Fernández-Jiménez A, Cristelo N, Miranda T, Palomo Á. Sustainable alkali activated materials: Precursor and activator derived from industrial wastes. J Clean Prod 2017;162:1200–9. https://doi.org/10.1016/j.jclepro.2017.06.151.

[7] Zhang ZH, Zhu HJ, Zhou CH, Wang H. Geopolymer from kaolin in China: An overview. Appl Clay Sci 2016;119:31–41. https://doi.org/10.1016/j.clay.2015.04.023.

[8] Rocha T da S, Dias DP, França FCC, Guerra RR de S, Marques LR da C de O. Metakaolin-based geopolymer mortars with different alkaline activators (Na+and K+). Constr Build Mater 2018;178:453–61. https://doi.org/10.1016/j.conbuildmat.2018.05.172.

[9] Provis JL. Alkali-activated materials. Cem Concr Res 2018;114:40–8. https://doi.org/10.1016/j.cemconres.2017.02.009.

[10] Tchakouté HK, Rüscher CH, Kong S, Kamseu E, Leonelli C. Geopolymer binders from metakaolin using sodium waterglass from waste glass and rice husk ash as alternative activators: A comparative study. Constr Build Mater 2016;114:276–89. https://doi.org/10.1016/j.conbuildmat.2016.03.184.

[11] Turner LK, Collins FG. Carbon dioxide equivalent (CO2-e) emissions: A comparison between geopolymer and OPC cement concrete. Constr Build Mater 2013;43:125–30. https://doi.org/10.1016/j.conbuildmat.2013.01.023.

[12] Sturm P, Gluth GJG, Brouwers HJH, Kühne H-C. Synthesizing one-part geopolymers from rice husk ash. Constr Build Mater 2016;124:961–6. https://doi.org/10.1016/j.conbuildmat.2016.08.017.

[13] He J, Jie Y, Zhang J, Yu Y, Zhang G. Synthesis and characterization of red mud and rice husk ash-based geopolymer composites. Cem Concr Compos 2013;37:108–18. https://doi.org/10.1016/j.cemconcomp.2012.11.010.

[14] Mendes B, Andrade IK, de Carvalho JM, Pedroti L, de Oliveira Júnior A. Assessment of mechanical and microstructural properties of geopolymers produced from metakaolin, silica fume, and red mud. Int J Appl Ceram Technol 2021;18:262–74. https://doi.org/10.1111/ijac.13635.

[15] Ahmari S, Zhang L. Production of eco-friendly bricks from copper mine tailings through geopolymerization. Constr Build Mater 2012;29:323–31. https://doi.org/10.1016/j.conbuildmat.2011.10.048.

[16] Azevedo ARG, Vieira CMF, Ferreira WM, Faria KCP, Pedroti LG, Mendes BC. Potential use of ceramic waste as precursor in the geopolymerization reaction for the production of ceramic roof tiles. J Build Eng 2020;29. https://doi.org/10.1016/j.jobe.2019.101156.

[17] Carrillo-Beltran R, Corpas-Iglesias FA, Terrones-Saeta JM, Bertoya-Sol M. New geopolymers from industrial by-products: Olive biomass fly ash and chamotte as raw materials. Constr Build Mater 2021;272:121924. https://doi.org/10.1016/j.conbuildmat.2020.121924.

[18] Bernal SA, Rodríguez ED, Kirchheim AP, Provis JL. Management and valorisation of wastes through use in producing alkali-activated cement materials. J Chem Technol Biotechnol 2016;91:2365–88. https://doi.org/10.1002/jctb.4927.

[19] Gado RA, Hebda M, Łach M, Mikuła J. Alkali Activation of Waste Clay Bricks: Influence of The Silica Modulus, SiO2/Na2O, H2O/Na2O Molar Ratio, and Liquid/Solid Ratio. Materials (Basel) 2020;13:383. https://doi.org/10.3390/ma13020383.

[20] Reig L, Tashima MM, Borrachero MV, Monzó J, Cheeseman CR, Payá J. Properties and microstructure of alkali-activated red clay brick waste. Constr Build Mater 2013;43:98–

106. https://doi.org/10.1016/j.conbuildmat.2013.01.031.

[21] Villaquirán-Caicedo MA. Studying different silica sources for preparation of alternative waterglass used in preparation of binary geopolymer binders from metakaolin/boiler slag. Constr Build Mater 2019;227:1–13. https://doi.org/10.1016/j.conbuildmat.2019.08.002.

[22] Živica V. Effectiveness of new silica fume alkali activator. Cem Concr Compos 2006;28:21–5. https://doi.org/10.1016/j.cemconcomp.2005.07.004.

[23] Torres-Carrasco M, Puertas F. Waste glass in the geopolymer preparation. Mechanical and microstructural characterisation. J Clean Prod 2015;90:397–408. https://doi.org/10.1016/j.jclepro.2014.11.074.

[24] Vinai R, Soutsos M. Production of sodium silicate powder from waste glass cullet for alkali activation of alternative binders. Cem Concr Res 2019;116:45–56. https://doi.org/10.1016/j.cemconres.2018.11.008.

[25] Moraes JCB, Font A, Soriano L, Akasaki JL, Tashima MM, Monzó J, et al. New use of sugar cane straw ash in alkali-activated materials: A silica source for the preparation of the alkaline activator. Mag Concr Res 2018;171:1256–64. https://doi.org/10.1016/j.conbuildmat.2018.03.230.

[26] Alonso MM, Gascó C, Morales MM, Suárez-Navarro JA, Zamorano M, Puertas F. Olive biomass ash as an alternative activator in geopolymer formation: A study of strength, durability, radiology and leaching behaviour. Cem Concr Compos 2019;104:103384. https://doi.org/10.1016/j.cemconcomp.2019.103384.

[27] de Moraes Pinheiro SM, Font A, Soriano L, Tashima MM, Monzó J, Borrachero MV, et al. Olive-stone biomass ash (OBA): An alternative alkaline source for the blast furnace slag activation. Constr Build Mater 2018;178:327–38. https://doi.org/10.1016/j.conbuildmat.2018.05.157.

[28] Puertas F, Torres-Carrasco M, Alonso MM. Reuse of urban and industrial waste glass as a novel activator for alkali-activated slag cement pastes: a case study. Handb. Alkali-Activated Cem. Mortars Concr., Elsevier; 2015, p. 75–109. https://doi.org/10.1533/9781782422884.1.75.

[29] Mariaková D, Mocová KA, Fořtová K, Pavlů T, Hájek P. Waste Glass Powder Reusability in High-Performance Concrete: Leaching Behavior and Ecotoxicity. Materials (Basel) 2021;14:4476. https://doi.org/10.3390/ma14164476.

[30] Chen W, Liu Y, Wang H, Hnizdo E, Sun Y, Su L, et al. Long-Term Exposure to Silica Dust and Risk of Total and Cause-Specific Mortality in Chinese Workers: A Cohort Study. PLoS Med 2012;9:e1001206. https://doi.org/10.1371/journal.pmed.1001206.

[31] Marjanovi N, Komljenovi M, Baš Z, Nikoli V. Comparison of two alkali-activated systems : mechanically activated fly ash and fly ash-blast furnace slag blends 2015;108:231–8. https://doi.org/10.1016/j.proeng.2015.06.142.

[32] Reig L, Soriano L, Borrachero M V., Monzó J, Payá J. Influence of calcium aluminate cement (CAC) on alkaline activation of red clay brick waste (RCBW). Cem Concr Compos 2016;65:177–85. https://doi.org/10.1016/j.cemconcomp.2015.10.021.

[33] Tuyan M, Andiç-Çakir Ö, Ramyar K. Effect of alkali activator concentration and curing condition on strength and microstructure of waste clay brick powder-based geopolymer. Compos Part B Eng 2018;135:242–52. https://doi.org/10.1016/j.compositesb.2017.10.013.

[34] Tong KT, Vinai R, Soutsos MN. Use of Vietnamese rice husk ash for the production of sodium silicate as the activator for alkali-activated binders. J Clean Prod 2018;201:272–86. https://doi.org/10.1016/j.jclepro.2018.08.025.

[35] Fořt J, Vejmelková E, Koňáková D, Alblová N, Čáchová M, Keppert M, et al. Application of waste brick powder in alkali activated aluminosilicates: Functional and environmental aspects. J Clean Prod 2018;194:714–25. https://doi.org/10.1016/j.jclepro.2018.05.181.

[36] Terrones-Saeta JM, Suárez-Macías J, Iglesias-Godino FJ, Corpas-Iglesias FA. Development of Geopolymers as Substitutes for Traditional Ceramics for Bricks with Chamotte and Biomass Bottom Ash. Materials (Basel) 2021;14:199. https://doi.org/10.3390/ma14010199.

[37] Robayo RA, Mulford A, Munera J, Mejía de Gutiérrez R. Alternative cements based on alkali-activated red clay brick waste. Constr Build Mater 2016;128:163–9. https://doi.org/10.1016/j.conbuildmat.2016.10.023.

[38] Zhang L. Production of bricks from waste materials – A review. Constr Build Mater 2013;47:643–55. https://doi.org/10.1016/j.conbuildmat.2013.05.043.

[39] Keselman HJ. A Power Investigation of the Tukey Multiple Comparison Statistic. Educ Psychol Meas 1976;36:97–104. https://doi.org/10.1177/001316447603600108.

[40] Batista BD de O, Ferreira DF. Alternative to Tukey test. Ciência e Agrotecnologia 2020;44. https://doi.org/10.1590/1413-7054202044008020.

[41] Bontempi E. A new approach for evaluating the sustainability of raw materials substitution based on embodied energy and the CO2 footprint. J Clean Prod 2017;162:162–9. https://doi.org/10.1016/j.jclepro.2017.06.028.

[42] Torres-Carrasco M, Palomo JG, Puertas F. Sodium silicate solutions from dissolution of glasswastes. Statistical analysis. Mater Construcción 2014;64:e014. https://doi.org/10.3989/mc.2014.05213.

[43] Aredes FGM, Campos TMB, Machado JPB, Sakane KK, Thim GP, Brunelli DD. Effect of cure temperature on the formation of metakaolinite-based geopolymer. Ceram Int 2015;41:7302–11. https://doi.org/10.1016/j.ceramint.2015.02.022.

[44] Bernal SA, Rodríguez ED, Mejia de Gutiérrez R, Provis JL, Delvasto S. Activation of

Metakaolin/Slag Blends Using Alkaline Solutions Based on Chemically Modified Silica Fume and Rice Husk Ash. Waste and Biomass Valorization 2012;3:99–108. https://doi.org/10.1007/s12649-011-9093-3.

[45] Rovnaník P, Rovnaníková P, Vyšvařil M, Grzeszczyk S, Janowska-Renkas E. Rheological properties and microstructure of binary waste red brick powder/metakaolin geopolymer. Constr Build Mater 2018;188:924–33. https://doi.org/10.1016/j.conbuildmat.2018.08.150.

[46] de Vargas AS, Dal Molin DCC, Masuero ÂB, Vilela ACF, Castro-Gomes J, de Gutierrez RM. Strength development of alkali-activated fly ash produced with combined NaOH and Ca(OH) 2 activators. Cem Concr Compos 2014;53:341–9. https://doi.org/10.1016/j.cemconcomp.2014.06.012.

[47] Zhang Z, Wang H, Provis JL, Bullen F, Reid A, Zhu Y. Quantitative kinetic and structural analysis of geopolymers. Part 1. the activation of metakaolin with sodium hydroxide. Thermochim Acta 2012;539:23–33. https://doi.org/10.1016/j.tca.2012.03.021.

[48] Heah CY, Kamarudin H, Mustafa Al Bakri AM, Bnhussain M, Luqman M, Khairul Nizar I, et al. Study on solids-to-liquid and alkaline activator ratios on kaolin-based geopolymers. Constr Build Mater 2012;35:912–22. https://doi.org/10.1016/j.conbuildmat.2012.04.102.

[49] Law DW, Adam AA, Molyneaux TK, Patnaikuni I, Wardhono A. Long term durability properties of class F fly ash geopolymer concrete. Mater Struct 2015;48:721–31. https://doi.org/10.1617/s11527-014-0268-9.

[50] Barbosa VF., MacKenzie KJ., Thaumaturgo C. Synthesis and characterisation of materials based on inorganic polymers of alumina and silica: sodium polysialate polymers. Int J Inorg Mater 2000;2:309–17. https://doi.org/10.1016/S1466-6049(00)00041-6.

[51] Huseien GF, Ismail M, Khalid NHA, Hussin MW, Mirza J. Compressive strength and microstructure of assorted wastes incorporated geopolymer mortars: Effect of solution molarity. Alexandria Eng J 2018;57:3375–86. https://doi.org/10.1016/j.aej.2018.07.011.

[52] LIVI CN, REPETTE WL. Effect of NaOH concentration and curing regime on geopolymer. Rev IBRACON Estruturas e Mater 2017;10:1174–81. https://doi.org/10.1590/s1983-41952017000600003.

[53] Xu H, Van Deventer JSJ. The geopolymerisation of alumino-silicate minerals. Int J Miner Process 2000;59:247–66. https://doi.org/10.1016/S0301-7516(99)00074-5.

[54] Fernández-Jiménez A, Palomo A, Criado M. Microstructure development of alkali-activated fly ash cement: A descriptive model. Cem Concr Res 2005;35:1204–9. https://doi.org/10.1016/j.cemconres.2004.08.021.

[55] Puertas F, Torres-Carrasco M. Use of glass waste as an activator in the preparation of

alkali-activated slag. Mechanical strength and paste characterisation. Cem Concr Res 2014;57:95–104. https://doi.org/10.1016/j.cemconres.2013.12.005.

[56] Król M, Rożek P, Mozgawa W. Synthesis of the Sodalite by Geopolymerization Process Using Coal Fly Ash. Polish J Environ Stud 2017;26:2611–7. https://doi.org/10.15244/pjoes/70231.

[57] Davidovits J. Geopolymers - Inorganic polymeric new materials. J Therm Anal 1991;37:1633–56. https://doi.org/10.1007/BF01912193.

[58] Masoudian SK, Sadighi S, Abbasi A. Synthesis and Characterization of High Aluminum Zeolite X from Technical Grade Materials. Bull Chem React Eng Catal 2013;8. https://doi.org/10.9767/bcrec.8.1.4321.54-60.

[59] Chindaprasirt P, Jaturapitakkul C, Chalee W, Rattanasak U. Comparative study on the characteristics of fly ash and bottom ash geopolymers. Waste Manag 2009;29:539–43. https://doi.org/10.1016/j.wasman.2008.06.023.

[60] Rożek P, Król M, Mozgawa W. Spectroscopic studies of fly ash-based geopolymers. Spectrochim Acta Part A Mol Biomol Spectrosc 2018;198:283–9. https://doi.org/10.1016/j.saa.2018.03.034.

[61] Zaharaki D, Komnitsas K, Perdikatsis V. Use of analytical techniques for identification of inorganic polymer gel composition. J Mater Sci 2010;45:2715–24. https://doi.org/10.1007/s10853-010-4257-2.

[62] Lee WKW, van Deventer JSJ. Use of Infrared Spectroscopy to Study Geopolymerization of Heterogeneous Amorphous Aluminosilicates. Langmuir 2003;19:8726–34. https://doi.org/10.1021/la026127e.

[63] Burciaga-Díaz O, Durón-Sifuentes M, Díaz-Guillén JA, Escalante-García JI. Effect of waste glass incorporation on the properties of geopolymers formulated with low purity metakaolin. Cem Concr Compos 2020;107:103492. https://doi.org/10.1016/j.cemconcomp.2019.103492.

[64] Rovnaník P, Rovnaníková P, Vyšvařil M, Grzeszczyk S, Janowska-Renkas E. Rheological properties and microstructure of binary waste red brick powder/metakaolin geopolymer. Constr Build Mater 2018;188:924–33. https://doi.org/10.1016/j.conbuildmat.2018.08.150.

[65] Mikuła A, Król M, Koleżyński A. Experimental and theoretical spectroscopic studies of Ag-, Cd- and Pb-sodalite. J Mol Struct 2016;1126:110–6. https://doi.org/10.1016/j.molstruc.2016.03.004.

[66] Zhang Z, Wang H, Provis JL. Quantitative study of the reactivity of fly ash in geopolymerization by FTIR. J Sustain Cem Mater 2012;1:154–66. https://doi.org/10.1080/21650373.2012.752620.

[67] Lecomte I, Henrist C, Liégeois M, Maseri F, Rulmont A, Cloots R. (Micro)-structural

comparison between geopolymers, alkali-activated slag cement and Portland cement. J Eur Ceram Soc 2006;26:3789–97. https://doi.org/10.1016/j.jeurceramsoc.2005.12.021.

[68] Nikolov A, Rostovsky I, Nugteren H. Geopolymer materials based on natural zeolite. Case Stud Constr Mater 2017;6:198–205. https://doi.org/10.1016/j.cscm.2017.03.001.

[69] Jyothi TK, Varsha BN, Raghunath S, Jagadish KS. Embodied Energy & Cost Issues of Tank-Bed-Lime Based Geopolymer Adobes. Open J Energy Effic 2017;06:128–39. https://doi.org/10.4236/ojee.2017.63010.

[70] Hossain MU, Poon CS, Lo IMC, Cheng JCP. Comparative LCA on using waste materials in the cement industry: A Hong Kong case study. Resour Conserv Recycl 2017;120:199–208. https://doi.org/10.1016/j.resconrec.2016.12.012.

[71] Thannimalay L, Yusoff S, Zawawi NZ. Life Cycle Assessment of Sodium Hydroxide. Aust J Basic Appl Sci 2013;7:421–31.

ARTICLE 3

PHYSICAL AND MECHANICAL CHARACTERIZATION OF MORTARS PRODUCED FROM CHAMOTTE AND WASTE GLASS GEOPOLYMER BINDER

Abstract:

Geopolymers have been widely studied as a binder in construction materials, such as mortars and concretes, replacing the conventional Portland cement. These materials must have adequate properties to be applied in constructions, related to physical and mechanical behavior in the fresh and hardened states. The aim of this article is to present the physical and mechanical characteristics of mortars produced with chamotte and waste glass-based alkaline solutions. For this, the best formulations of pastes were obtained from a previous study using a factorial design of experiments with two factors, being NaOH molar concentration and content of waste glass. Four selected pastes were submitted to mechanical strength tests, microstructural evaluation and isothermal calorimetry tests. Two mixtures of mortar were produced for each paste, the first being defined based on preliminary studies, and the second based on the modified Andreasen packing method. The microstructural analyses revealed that pastes with molar concentration of 8 mol/L and waste glass content of 10 g and 15 g demonstrated higher formation of zeolite structures and development of polycondensation reactions. Regarding to the characterization of mortars, it can be concluded that addition of sand and particle packing are key factors to determine the final properties in low-strength composites. At the fresh state, the nature of the alkaline solution, mainly the molar concentration, influenced the behavior of the two series of mortars.

Keywords: geopolymer; mortar; waste glass; chamotte.

1 INTRODUCTION

Alkali-activation of silico-aluminous materials, which gives rise to so-called geopolymers, can be described as the mixture of a liquid phase, with high alkali concentration, and a solid precursor, with adequate proportions of reactive silicates and aluminates [1]. The formed paste then initiates a process of setting and hardening in a similar way to Portland cement hydration.

The process of formation of geopolymers resembles the formation of some zeolites: initially, Al and Si ions dissolved in the medium react forming polyhydroxy-silicoaluminate complexes. The final product has a three-dimensional structure on an atomic to nanometer scale, similar to some zeolite structures in nanoscale [2]. Some authors have developed and studied models that describe the mechanisms that occur during the geopolymerization process [3–6]. In general, the first stage consists of the dissolution of amorphous aluminosilicates present in the precursor (solid phase), forming a series of ionic species. This dissolution happens immediately in a medium with high pH [7].

After, the agglutination of the smaller molecules occurs to form larger chains or molecules, which precipitate in the form of gel. At this stage, as the Al - O bonds are weaker; a metastable phase rich in Al is formed firstly. After some rearrangement and reorganization, a second gel is given rise, being a phase more stable and rich in Si, with three-dimensional structure. The next phase is that of growth, in which the nuclei reach critical sizes and the crystals begin to develop. This step occurs slower when compared to the previous stage. These structural reorganization processes determine the final composition of the N-A-S-H gel, as well as the microstructure and distribution of the pores of the material, which are critical in relation to some physical properties [6].

Alkali-activated binders can be used in traditionally cementitious composites, such as mortars and concretes. Some countries are already applying alkali-activated mortars and concretes in construction elements. In Australia, alkali-activated concretes have been commercialized under the name E-crete® [8]. It has been applied in infrastructure projects, such as pavements and bridges. In Spain, railway sleepers are being developed based on alkali-activated fly ash [9]. Nath and Sarker [10] produced geopolymeric mortars and concrete based on fly ash with 5 % of ordinary Portland cement (OCP). The compressive strength values at 28 days were higher than 50 MPa and 40 MPa for mortar and concrete, respectively. Reig et al. [11] studied chamotte-based geopolymer mortars under different curing conditions, and reached 35 MPa of compressive strength at 7 days (thermal curing of 65 °C).

Although geopolymeric mortars and concretes are promising, their application has some disadvantages. One of them is the fact that the activating solutions are usually highly viscous, which affects the workability and rheological properties of geopolymer. Consequently, it may be difficult to compact and vibrate satisfactorily, presenting higher permeability, absorption and porosity than Portland cement–based materials [12].

One way to improve the mechanical performance and durability of mortars or concretes is to control the dosage, in order to minimize the incidence of voids in the final matrix. Thus, adopting a proportion that promotes an increase in the packing of particles, a denser matrix with less porosity is obtained, which contributes to the gain of mechanical strength and hinders the access or action of aggressive environmental agents. Provis et al. [13] pointed out the importance of the study of particle packing methods on the development of Portland cement and geopolymer materials. In the technical literature, some methods for dosage of concrete and cementitious mortars are reported based on the packing conditions of the mixture, such as Andreasen, modified Andreasen (or Dinger-Funk equation) and Furnas methods. These methods consider the particle size distribution of the raw materials in order to establish the form of final particle size distribution that would promote densest packing [14].

In view of the above, the objective of this work is the physical and mechanical characterization of geopolymeric mortars produced with chamotte and waste glass-based alkaline solutions, from the best pastes obtained by Mendes *et al.* [15]. Two distinct proportions between chamotte and sand were evaluated: the first, obtained from preliminary tests, and the second, obtained by the modified Andreasen method. In addition, the chosen pastes were evaluated for mechanical strength, microstructural analyses and isothermal calorimetry.

2 MATERIALS AND METHODS

2.1 Materials

In this experimental phase, the same raw materials mentioned in the research of Mendes *et al.* [15] were used: chamotte, waste glass obtained from the polishing process, sodium hydroxide and distilled water. Chamotte and waste glass were characterized for:

- specific mass, using the volumetric flask of *Le Chatelier*; particle size distribution, using a *Bettersize2000 laser* particle size analyzer in a range of 0.02 μm to 2,000 μm;
- specific surface, by means of Blaine methodology;

- chemical composition, obtained by X-ray fluorescence by dispersive energy, using a *Shimadzu Micro-EDX-1300* spectrometer; and
- mineralogical composition, assessed by X-ray diffraction through the *D8 Discover (Bruker)* diffractometer. The XRD was conducted with CuKα radiation (1.5418 Å), 2θ varying from 3° to 70°, 0.05° 2θ step-scan and 1.0 s/step.

A summary containing the description and main characteristics of the raw materials used are shown in Table 3.1. The chemical compositions and XRD patterns are shown in Table 3.2 and Figure 3.1, respectively. For the production of mortars, washed river sand was also added, passing through the sieve ASTM 10 mesh (2.0 mm). The sand has a specific mass equal to 2.65 g/cm³ and particle size distribution shown in Figure 3.2.

Table 3.1. Characteristics of the raw materials.

Material	**Chamotte**	**Waste glass**	**Sodium hydroxide**
Origination	Red ceramic industry located in Ouro Branco – MG, Brazil	NewTemper company located in Rio das Ostras – RJ, Brazil	Commercial NaOH pellets, P.A., 99%, CRQ brand
Pre-treatment	Ground for 90 minutes using a Los Angeles abrasion machine	Crushed and passed through ASTM 325 sieve	-
Specific mass (g/cm³)	2.75	2.40	-
Specific surface (m²/kg)	652.98	1,073.09	-
D50 (μm)	22.74	7.46	-

Table 3.2. Chemical composition of chamotte and waste glass.

Raw material	**Chemical composition (%)**								
	SiO_2	**Al_2O_3**	**Fe_2O_3**	**CaO**	**K_2O**	**MgO**	**Ti_2O**	**Na_2O**	**Other**
Chamotte	49.74	30.55	5.29	0.54	1.27	1.61	1.08	1.54	6.07
Waste glass	60.21	2.93	0.29	7.40	0.23	1.65	0.01	2.61	4.94

Figure 3.1. XRD patterns of chamotte and waste glass (K – kaolinite (ICDD: 00-029-1488); Q – quartz (COD: 96-900-9667); E – epidote (COD ID: 1529622); R – rutile (ICDD: 00-034-080); H – hematite (ICDD: 01-085-0987; C – calcite ICDD: 01-072-1937)).

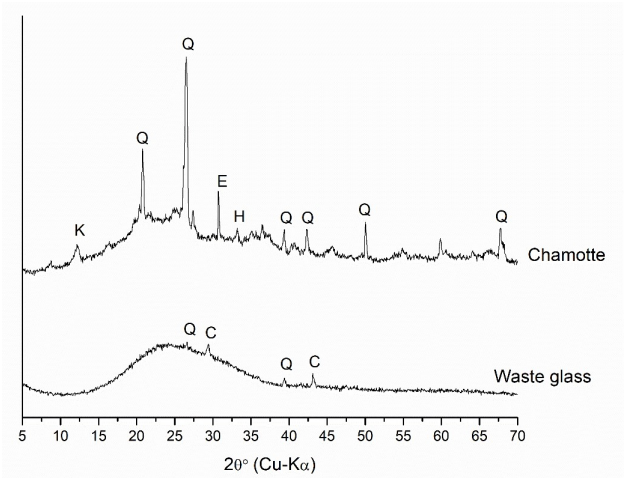

Figure 3.2. Particle size distribution curves of chamotte, waste glass and sand.

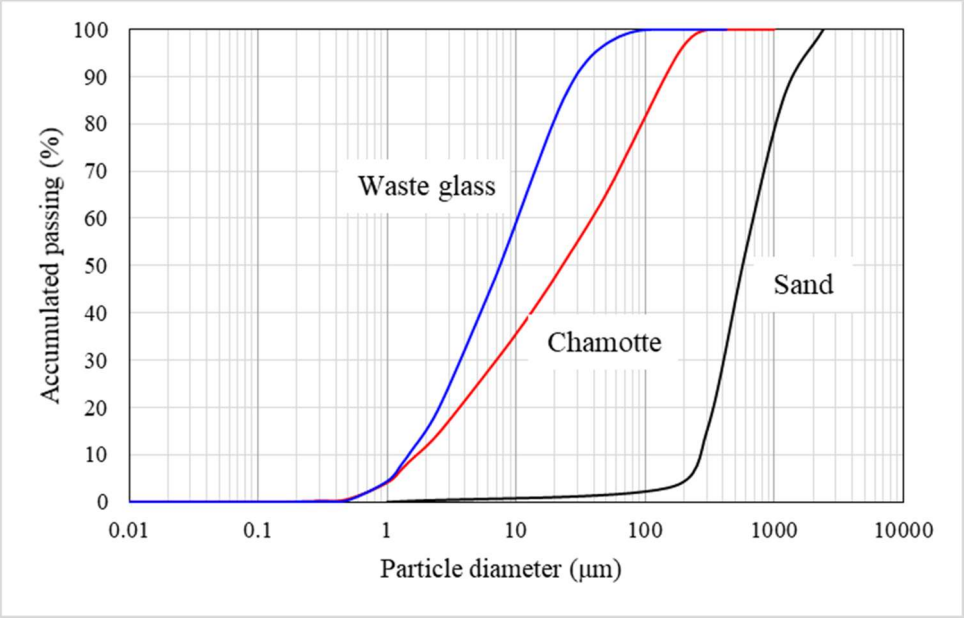

2.2 Selection and characterization of pastes

After a first experimental trial [15], four pastes were selected to produce mortars. The pastes were chosen based on the best mechanical results, being 8M-10, 8M-15, 10M-15 and 12M-15. The first number corresponds to the molar concentration of the NaOH-based alkaline solution, and the second number refers to the content of waste glass added into the solution, in grams per 100 mL of solution. According to Tukey test, these pastes presented averages statistically equal for both flexural and compressive strength.

These pastes were analyzed through mechanical tests, microstructural analysis – XRD and FTIR - and isothermal calorimetry tests, in order to investigate the initial reactions of geopolymerization and to observe the differences among them. The mechanical and microstructural tests followed the same setup described in Mendes *et al.* [15]. The calorimetry test was performed using a ICal 2000H (S/N A0068784) isothermal conduction calorimeter, at room temperature (23º) by an external mixing procedure. It was adopted the same liquid/solid ratio used to produce the pastes, equal to 0.40. The solutions were kept at the same temperature of the calorimeter before the test. The chamotte was weighted and placed in a plastic beaker, and then the solution was injected into the beaker. The materials were hand-mixed for three minutes, until all the chamotte was wetted. The beaker was placed in the calorimeter, where it was kept for 24 hours. The same preparation was applied to all the pastes. The heat flow was measured at 60 s interval. The room was maintained at the equipment temperature to avoid any heat disturbance caused by the environment.

2.3 Production and characterization of mortars

The first series of mortars (named as mortar A) was produced based on a mix proportion defined in a previous study, which used metakaolin as precursor. The proportion of precursor:sand was 1:2, and the liquid/precursor ratio equal to 0.67. The pastes were formulated for a solution/precursor ratio of 0.40. Therefore, distilled water was added to adjust the mortar consistency, resulting in the liquid/precursor ratio of 0.67.

The procedure of mixing consisted of the addition of solution to the precursor and both were manually mixed for one minute. Subsequently, the paste was mixed using a mechanical mixer, following the steps below:

- sixty seconds at lower velocity (velocity 1);
- pause of thirty seconds to remove the paste on the inner side of the bowl;
- ninety seconds at lower velocity (velocity 1), with gradual and slow addiction of sand;
- pause of thirty seconds to remove the mortar on the inner side of the bowl;
- sixty seconds at higher velocity (velocity 3).

After the mixing procedure, the mixture was poured into acrylic molds and then vibrated for one minute. The molds were covered with plastic film and cured for 24 hours at room temperature. Then, the specimens were placed into a hydrothermal curing chamber at 60 °C for 24 hours. After this time, the specimens were removed and cured again at room temperature, until the day of test.

In the fresh state, the mortars were characterized for consistency (flow table test) and content of incorporated air based on NBR 13278 [16]. The flow table test was performed using a reduced truncated cone, as shown in Table 3.3. In the hardened state, mechanical tests were performed to determine the flexural and compressive strength at 7 and 28 days. For each type of mortar and each age, three prismatic specimens with dimensions (2.0 x 2.0 x 8.0) cm were produced and tested, totalizing six results of compressive strength.

Table 3.3. Dimensions of reduced truncated cone used in flow table tests.

Dimension	Measurement
Diameter of larger base	69.0 mm
Diameter of minor base (top)	59.0 mm
Height	40.5 mm

Besides the mechanical strength tests, capillarity absorption tests were performed at 28 days, based on NBR 9778 [17]. For these tests, three prismatic specimens with dimensions (2.0 x 2.0 x 8.0) cm were used.

2.3.1 Modified Andreasen method (Dinger-Funk equation)

In order to improve the mechanical results obtained for mortars A, a new series of mortars was produced (mortar B), after the adjustment of the proportions and ratios previously established. For that, the modified Andreasen method was used as a tool to determine the suitable content of sand in the mortars.

Modified Andreasen's method is based on the hypothesis that particles have continuous distribution [12]. It was derived from Andreasen's equation (Equation 1). In this equation, the volumetric percentages of particles (*CPFT*) smaller than a *D* diameter are calculated using the diameter of the largest particle (D_L) and the coefficient of distribution (q).

$$CPFT(\%) = 100\left(\frac{D}{D_L}\right)^q \quad (1)$$

The main difference between modified Andreasen and Andreasen methods is that the second considers the minimum particle size as a finite factor. Thus, Equation 1 was adapted for that, including the parameter D_s that corresponds to the smallest particle size (Equation 2).

$$CPFT(\%) = 100\left(\frac{D^q - D_s^q}{D_L^q - D_s^q}\right) \quad (2)$$

To determine a satisfactory particle size composition, the particle size distribution of solid raw materials and the value of q are considered. According to Castro and Pandolfelli [18], for modified Andreasen method, q values equal to or less than 0.37 favor maximum packing. For values greater than 0.37, there is always a residual porosity. It is recommended to choose values between 0.30 and 0.25, for mixtures well-compacted by vibration and that present a good flowability, and less than 0.25 for self-compacting mixtures. The lower the q value, the greater the amount of fine particles in the composition.

To achieve good conditions of workability in mixtures compacted by vibration, the value of the coefficient of distribution equal to 0.28 and solution/precursor ratio equal to 0.57 were adopted, being obtained the modified Andreasen curve for the first parameter. For the

application of the method, the particle size distributions of chamotte and sand were considered, resulting in a particle size distribution with 46.0 % of chamotte and 54 % of sand by volume (Figure 3.3). The waste glass was not considered because it was dissolved in the alkaline solution. It is highlighted that these percentages were defined based on the curve that best fitted the reference. Figure 3.3 also shows the deviations between the modified Andreasen reference and the particle size distribution of the final proportion in the zones that it did not fit. The proportion, by weight, was 1:1.131 (chamotte: sand). In this second series of mortar, only mechanical tests of compressive and flexural strength at 7 days were performed.

Figure 3.3. Modified Andreasen curve for q = 0.28 and fitted mix proportion.

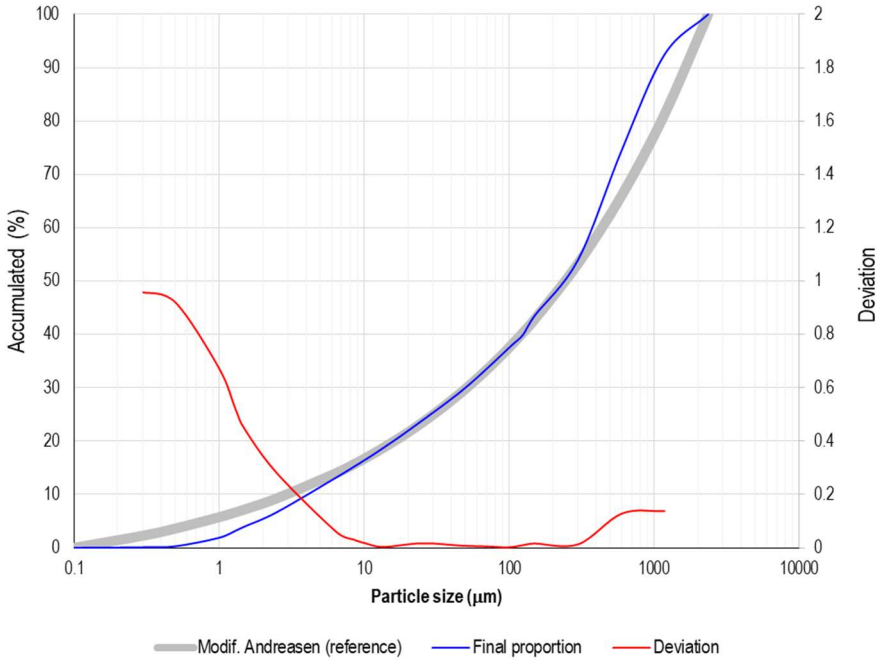

The final quantity of each material used to prepare the mortars A and B are shown in Table 3.4.

Table 3.4. Final composition of the mortars A and B.

Proportion	Chamotte (kg)	Sand (kg)	Solution (kg)	Water (kg)	Liquid/precursor ratio	Liquid/solids ratio
Mortar A (1:2)	0.30	0.60	0.12	0.08	0.67	0.22
Mortar B (1:1.131)	0.30	0.339	0.17	-	0.57	0.26

3 RESULTS AND DISCUSSION

3.1 Characterization of pastes

Figure 3.4 shows the results of flexural and compressive strength of the 8M-10, 8M-15, 10M-15 and 12M-15 pastes at 7, 28 and 56 days. Regarding to the flexural strength, 8M-10 and 8M-15 pastes reached values upper than 2.50 MPa at all ages considered. 10M-15 paste only exceeded this value at 28 days of curing. 10M-15 and 12M-15 presented a higher gain of strength between 7 and 28 days. It could be explained by the delayed polycondensation due to the high NaOH concentration [19].

Figure 3.4. Flexural and compressive strengths of 8M-10, 8M-15, 10M-15 and 12M-15 pastes.

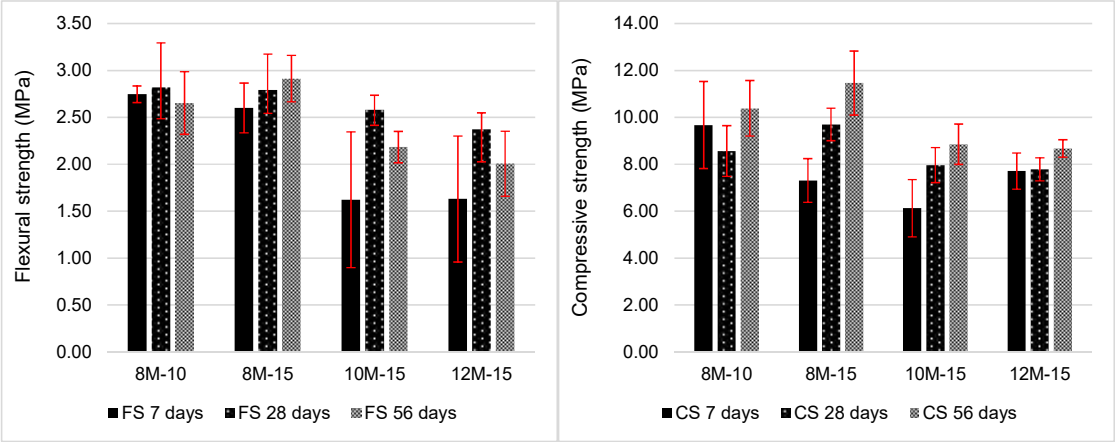

Considering the compressive strength results, all the pastes presented an increase of strength between 28 and 56 days. 8M-10 and 8M-15 pastes reached values upper to 10.00 MPa at 56 days. 8M-15 and 10M-15 showed the highest gain of compressive strength between 7 and 56 days, corresponding to 59.9 % and 44.4 %, respectively. 8M-10 paste showed the lowest gain in the same period, equal to 7.4 %. Probably, the total NaOH and soluble silica from the alkaline solution were almost consumed at the first days of geopolymerization, remaining few compounds available for the continuation of reactions.

The XRD patterns of the pastes are shown in Figure 3.5. The four pastes presented almost the same crystalline phases, being quartz, zeolite Na-X, zeolite Y (or faujasite) and sodium carbonate. However, 8M-10 and 8M-15 pastes presented more intense peaks of zeolite structures than 10M-15 and 12M-15. It agrees with the mechanical results, once these two pastes showed the lower mechanical strength values in general.

Figure 3.5. XRD patterns of 8M-10, 8M-15, 10M-15 and 12M-15 pastes.

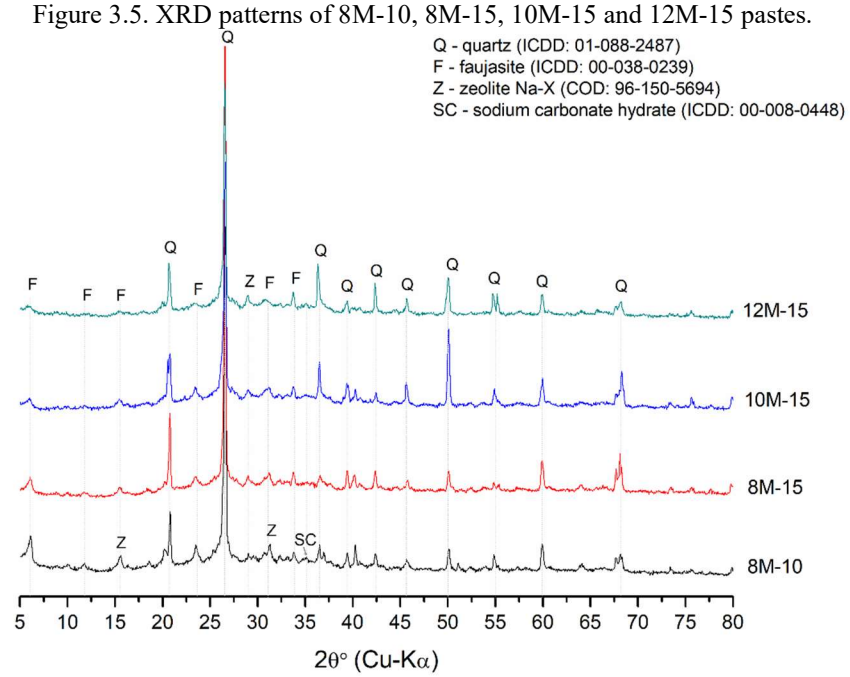

Figure 3.6 shows the FT-IR analysis of the pastes. 8M-15 presented the major band, related to the asymmetrical stretching of Si-O-T (where T stands for Si or Al tetrahedral), at 990 cm^{-1}. In relation to the position of this band in chamotte (1036 cm^{-1}), this mixture had the higher shift. The shift is associated to the formation of aluminosilicate gel and polycondensation reactions, which involves the inclusion of Al into geopolymeric gel. The higher wavenumber at this position was verified for 10M-15.

Figure 3.6. FTIR analysis of 8M-10, 8M-15, 10M-15 and 12M-15 pastes.

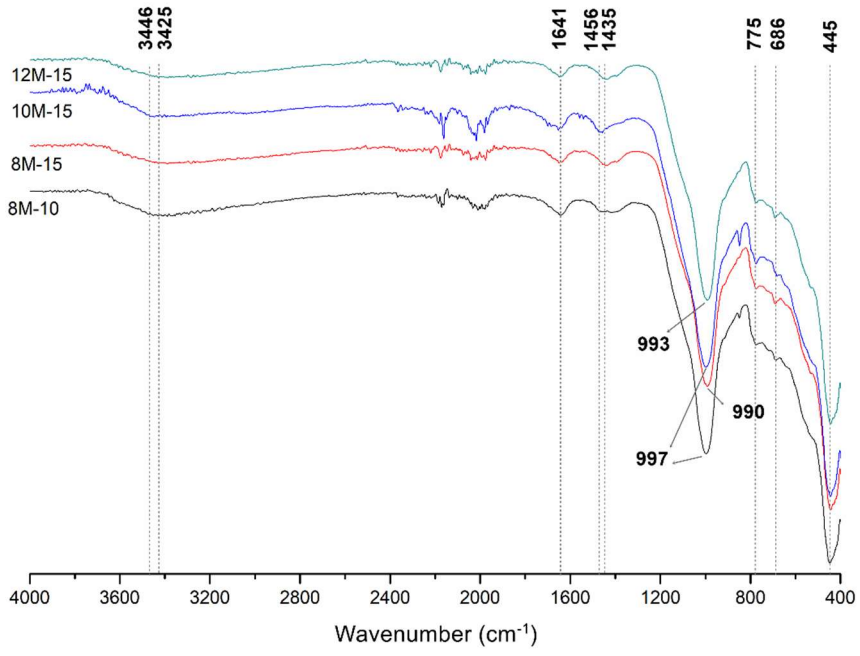

All the curves showed the band at around 686 cm^{-1}, related to the formation of zeolitic structures [20], which is in agreement with the XRD results. With high contents of WG, no significantly differences can be observed in the band at 1435 cm^{-1}, associated to the presence of O-C-O bonds of CO_3^{-2} groups or, in other words, carbonation reactions. It indicates that, at high levels of WG, the occurrence of carbonation is not significantly affected by the increase of molar concentration.

The geopolymerization is a complex and exothermic process that follows many steps, such as dissolution, precipitation, polycondensation and, in some cases, the reorganization of the amorphous aluminosilicates gel or crystallized structures into other more cross-linked and stable compounds [21]. These stages can be monitored by calorimetric tests. The isothermal calorimetry results are shown in Figure 3.7.

One can notice two distinct peaks in heat evolution: the first is sharp and begins immediately after the mixing of chamotte and the alkaline solution; the second is a broad peak that appears between 5 and 20 hours. The time required for peak I to reach the maximum value was 37 minutes for 8M-10, 29 minutes for 8M-15, 10 minutes for 10M-15 and 7 minutes for 12M-15. This peak is related to the instant sorption of alkaline solution on the surface of chamotte particles and the dissolution of the solid aluminosilicates precursor into silicate oligomers and aluminates monomers [22,23].

Comparing these results with studies which used metakaolin as precursor [23,24], it can be observed that the chamotte presents a slower reaction. Zhang et al. [23] investigated the heat evolution of metakaolin-based pastes activated with NaOH alkaline solutions and the maximum time required was 5 minutes. The higher the molar concentration of the solution, the higher the intensity of the peak I. It probably occurred because high concentration of Na^+ ions are beneficial to dissolve the aluminosilicates [24]. Besides, at the same molar concentration (8 M), heat evolution rate was higher for 8M-15, with higher content of WG.

Assessing the second broad peak, 8M-15 showed the highest heat evolution rate, followed by 8M-10 and 10M-15. For 12M-15, no peak was observed in this region. The second peak is related to the polymerization of the silicates and aluminates oligomers into small geopolymeric species and subsequently formation of aluminosilicate gel and crystalline phases [23,24]. Although high molar concentrations led to more intense peaks of dissolution, the same trend did not occur for polymerization stage. It means that high concentration of alkalis was undesirable to polymerization.

Figure 3.7. Isothermal calorimetry of 8M-10, 8M-15, 10M-15 and 12M-15 pastes.

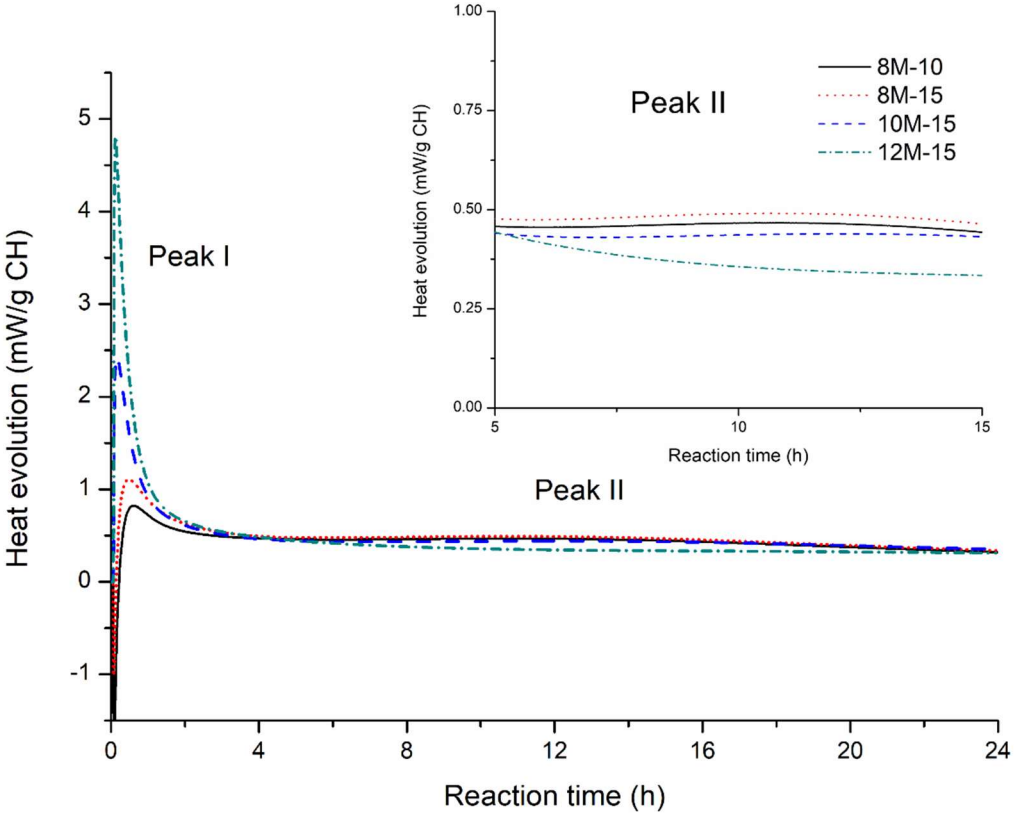

Pommer et al. [25] studied the alkali activation of ceramic waste using NaOH and commercial sodium silicate and they could not detect the second peak. Some authors point out that this peak only appears at elevated temperatures or depends on the activator composition [25,26]. Fort et al. [26] verified the heat power of pastes cured at 40 °C and 80 °C, and they also observed that the second peak was only found at 80 °C. This indicates that the addition of waste glass into the alkaline solution promoted significantly changes on the geopolymerization reactions.

Figure 3.8 shows the heat of hydration for each paste. 12M-15 presented higher heat of hydration until 16 hours. At the final time, 10M-15 and 8M-15 showed higher values of total heat evolved. It confirms the enhanced precipitation and polycondensation reactions with the use of alkaline solution with lower molar concentration and higher content of waste glass.

Figure 3.8. Heat of hydration of 8M-10, 8M-15, 10M-15 and 12M-15 pastes.

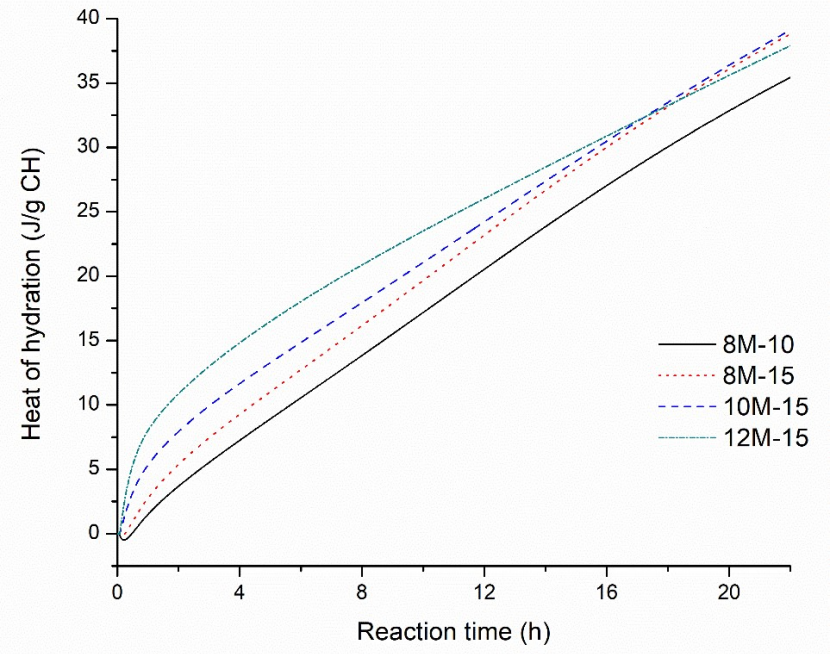

3.2 Characterization of mortars

The consistency of the mortars is shown in Figure 3.9. The flow values indicate that the consistency of the mortars varied in a broad range of 95 ± 20 mm. The results of mortars A are in agreement with the calorimetry analysis. The 8M-10 and 8M-15 pastes presented the slower rate of heat evolution in the earlier minutes. Therefore, the mixing water is used in the initial dissolution reactions at slower rates, improving the workability of the mortars [27]. For 12M-15, the higher alkali concentration enhances the consumption of water for the dissolution process, reducing the consistency index of the mortars. Phair and Van Deventer [28] also say that high alkali concentration increases the viscosity of the mixtures.

For mortars B, 8M-15 presented the higher workability, followed by 10M-15, 8M-10 and 12M-15. It should be highlighted the reduction of consistency index between 8M-15 and 12M-15, equal to 26.02 %. Considering mortars A, this percentage difference was 4.52 %. In general, the workability of mortars B was lower than mortars A, even with a higher total liquid/solid (precursor + sand) ratio. With higher content of sand, the reactions are delayed. Besides, the increase of sand increased the content of coarser and spherical particles in the mixture, which reduces the surface friction and enhances the workability [29].

Figure 3.9. Flow table results of mortars A and B.

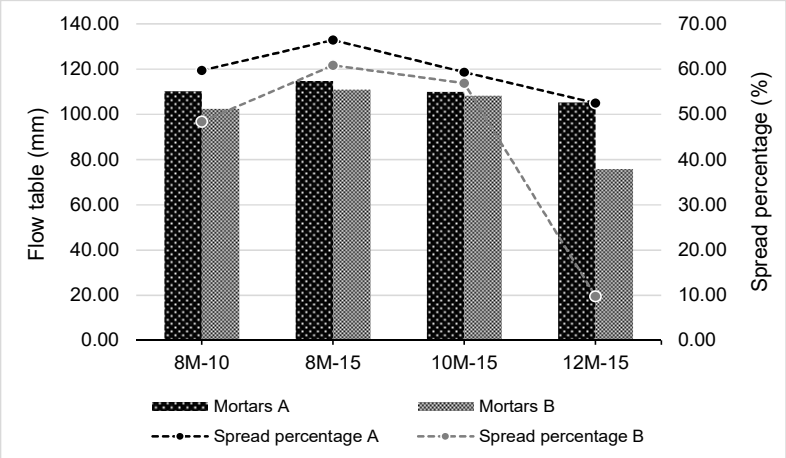

The results of incorporated air are shown in Figure 3.10. For mortars A, the mixture with higher content of incorporated air was 8M-15, and with the lower content was 10M-15. Regarding to mortars B, the incorporated air decreased with the increase of molar concentration. 12M-15 mixture presented the lowest value, equal to 3.37 %. 8M-10 presented the highest value, equal to 6.26 % and it was the mixture with lower compressive strength of this series of mortars.

Figure 3.10. Incorporated air of mortars A and B.

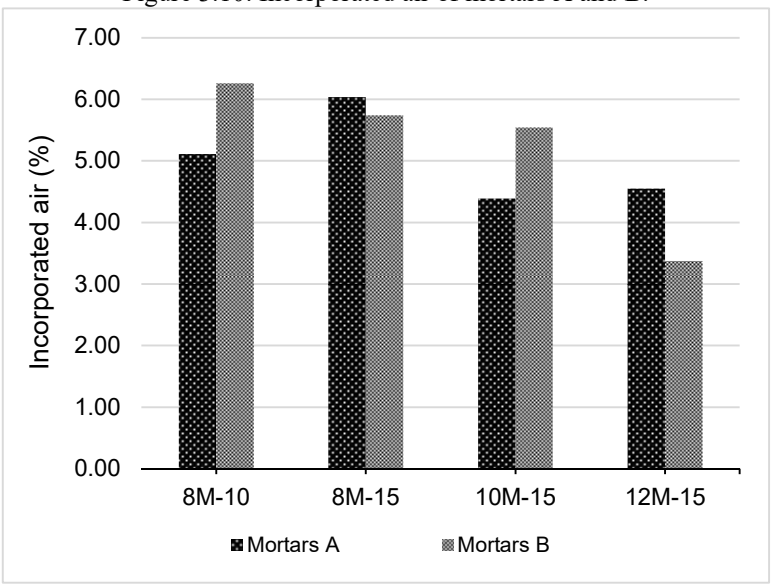

The flexural and compressive strength results of mortars A and B at 7 days are plotted on Figure 3.11. The behavior of the mortars changed with the increase of sand. For mortars B (1:1.131), 8M-15 and 10M-15 showed the highest values of both flexural and compressive strength, although lower than the mechanical strength results obtained for the pastes.

Figure 3.11. Flexural and compressive strength of mortars A and B at 7 days.

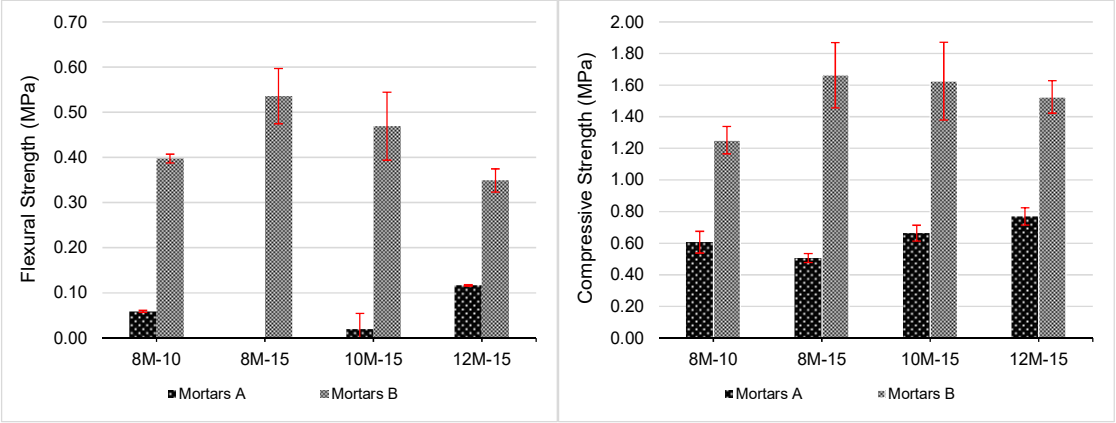

For mortars A (1:2), 8M-10 and 12M-15 showed higher values than the others. As discussed previously, the nature of the paste was not significant when high contents of sand are included. Besides, the values of mortars A were too low, probably indicating that the geopolymeric matrix was not sufficient to agglomerate the aggregate and form a strong material. Another point that should be highlighted is the addition of distilled water into mortars A, which might also affected the quality of geopolymer binder. However, in order to better investigate the cause of this behavior, some microstructural analysis need to be conducted in mortar samples.

It should be highlighted that the decrease of sand content promoted the raise of mechanical strength for all mixtures. In relation to compressive strength results, the increase was 106.32 %, 228.29 %, 144.97 % and 98.05 % for 8M-10, 8M-15, 10M-15 and 12M-15, respectively. About the flexural strength, for all mixtures the increase was higher than 199 %.

Figure 3.12 shows the capillarity coefficient and compressive strength at 28 days for mortars A. For this mix proportion (1:2), 10M-15 and 12M-15 showed the highest compressive strength. These results do not agree with the compressive strength of the pastes, since these mixtures presented the lower mechanical strength results. It suggests that the inclusion of sand affects the particle packing and this effect can play a major role compared with the chemical features of each alkaline solution. Indeed, these mortars presented the lower values of incorporated air. Although 8M-15 presented the lower compressive strength, it had the lower capillarity coefficient.

Evaluating the flexural and compressive strength at 28 days and capillarity coefficient, all mortars of series A can be classified as a P1, R1, C1 type (Table 3.5), according to the classification for coating and laying mortars proposed by NBR 13281 [30].

Figure 3.12. Compressive strength and capillarity coefficient of mortars A at 28 days.

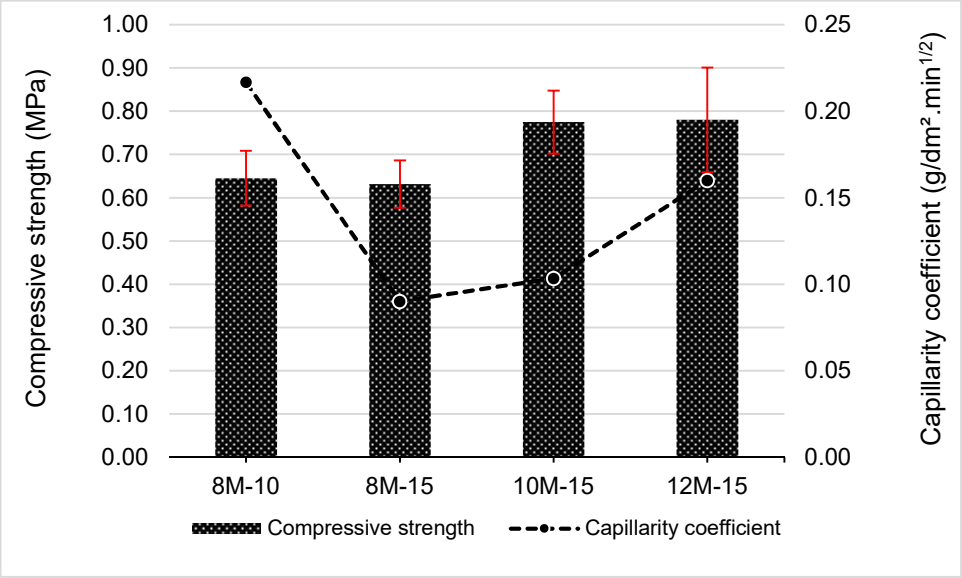

Table 3.5. Classification of mortars A according to NBR 13281 [28].

Group	Criterion
P1	Compressive strength less than 2.0 MPa
R1	Flexural strength less than 1.5 MPa
C1	Capillarity coefficient less than 1.5 g/dm².min$^{1/2}$

4 CONCLUSIONS

This article focused on the mechanical strength and microstructural analyses of selected pastes and the evaluation of mortars produced from them. The following conclusions can be inferred:

- Considering absolute values, 8M-10 and 8M-15 pastes presented the highest flexural and compressive strengths at 28 and 56 days. The XRD analysis showed the presence of more intense peaks of zeolite structures.
- XRD and FTIR results demonstrated that, at high incorporations of waste glass (15 g/100 mL of solution), the increase of molar concentration in the alkaline solution did not significantly affect the occurrence of carbonation.
- Isothermal calorimetry analysis revealed the presence of two peaks, related to the dissolution of the precursor aluminosilicates and the reactions of polycondensation, respectively. The increase of molar concentration enhanced the initial dissolution, but it is undesirable to polymerization. The total heat evolved confirms the enhanced

precipitation and polycondensation reactions with the use of alkaline solution with lower molar concentration and higher content of waste glass.

- High alkalis concentration reduced the consistency index and incorporated air of the mortars. Capillarity coefficient results did not demonstrated a clear relationship with the molar concentration of the solutions.
- The difference between the mechanical strength behavior of the pastes and the mortars indicates that, in composites with low resistance, the addition of sand and particle packing played a major role compared with the chemical interactions of the precursor and the alkaline solution.

5 ACKNOWLEDGMENTS

This study was financed in part by the Coordenação de Aperfeiçoamento Pessoal de Nível Superior – Brasil (CAPES) – Finance Code 001. The authors also want to thank the FAPEMIG agency for the financial support, and the Sustainable and Innovative Construction Research Group (SICon) for technical assistance.

REFERENCES

[1] Weng L, Sagoe-Crentsil K, Brown T, Song S. Effects of aluminates on the formation of geopolymers. Mater Sci Eng B Solid-State Mater Adv Technol 2005;117:163–8. https://doi.org/10.1016/j.mseb.2004.11.008.

[2] Provis JL, Lukey GC, Van Deventer JSJ. Do geopolymers actually contain nanocrystalline zeolites? a reexamination of existing results. Chem Mater 2005;17:3075–85. https://doi.org/10.1021/cm050230i.

[3] Shi C, Jiménez AF, Palomo A. New cements for the 21st century: The pursuit of an alternative to Portland cement. Cem Concr Res 2011;41:750–63. https://doi.org/10.1016/j.cemconres.2011.03.016.

[4] Fernández-Jiménez A, Palomo A, Criado M. Microstructure development of alkali-activated fly ash cement: A descriptive model. Cem Concr Res 2005;35:1204–9. https://doi.org/10.1016/j.cemconres.2004.08.021.

[5] Glukhovsky VD. Soil Silicate Articles and Structures. Kiev: 1967.

[6] Duxson P, Fernández-Jiménez A, Provis JL, Lukey GC, Palomo A, Van Deventer JSJ. Geopolymer technology: The current state of the art. J Mater Sci 2007;42:2917–33. https://doi.org/10.1007/s10853-006-0637-z.

[7] Fernández-Jiménez A, Palomo A. Composition and microstructure of alkali activated fly ash binder: Effect of the activator. Cem Concr Res 2005;35:1984–92. https://doi.org/10.1016/j.cemconres.2005.03.003.

[8] van Deventer JSJ, Provis JL, Duxson P, Brice DG. Chemical Research and Climate Change as Drivers in the Commercial Adoption of Alkali Activated Materials. Waste and Biomass Valorization 2010;1:145–55. https://doi.org/10.1007/s12649-010-9015-9.

[9] Palomo Á, Fernández Jiménez A, López Hombrados C, Lleyda JL. Railway sleepers made of alkali activated fly ash concrete. Rev Ing Construcción 2007;22. https://doi.org/10.4067/S0718-50732007000200001.

[10] Nath P, Sarker PK. Effect of GGBFS on setting, workability and early strength properties of fly ash geopolymer concrete cured in ambient condition. Constr Build Mater 2014;66:163–71. https://doi.org/10.1016/j.conbuildmat.2014.05.080.

[11] Reig L, Soriano L, Borrachero M V., Monzó J, Payá J. Influence of calcium aluminate cement (CAC) on alkaline activation of red clay brick waste (RCBW). Cem Concr Compos 2016;65:177–85. https://doi.org/10.1016/j.cemconcomp.2015.10.021.

[12] Borges PHR, Fonseca LF, Nunes VA, Panzera TH, Martuscelli CC. Andreasen Particle Packing Method on the Development of Geopolymer Concrete for Civil Engineering. J Mater Civ Eng 2014;26:692–7. https://doi.org/10.1061/(ASCE)MT.1943-5533.0000838.

[13] Provis JL, Duxson P, van Deventer JSJ. The role of particle technology in developing sustainable construction materials. Adv Powder Technol 2010;21:2–7. https://doi.org/10.1016/j.apt.2009.10.006.

[14] Funk JE, Dinger DR. Derivation of the Dinger-Funk Particle Size Distribution Equation. Predict. Process Control Crowded Part. Suspens., Boston, MA: Springer US; 1994, p. 75–83. https://doi.org/10.1007/978-1-4615-3118-0_6.

[15] Mendes BC, Pedroti LG, Vieira CMF, Carvalho JMF, Ribeiro JCL, Albuini-Oliveira NM, et al. Evaluation of eco-efficient geopolymer using chamotte and waste glass-based alkaline solutions. Case Stud Constr Mater 2022;16:e00847. https://doi.org/10.1016/j.cscm.2021.e00847.

[16] Brazilian Association of Technical Standars. NBR 13278: Mortars applied on walls and ceilings - Determination of the specific gravity and the air entrained content in the fresh stage 2005:4.

[17] Brazilian Association of Technical Standars. NBR 9778: Hardened mortar and concrete - Determination of absorption, voids and specific gravity 2009:4.

[18] Castro AL de, Pandolfelli VC. Revisão: conceitos de dispersão e empacotamento de partículas para a produção de concretos especiais aplicados na construção civil. Cerâmica 2009;55:18–32. https://doi.org/10.1590/S0366-69132009000100003.

[19] Huseien GF, Ismail M, Khalid NHA, Hussin MW, Mirza J. Compressive strength and microstructure of assorted wastes incorporated geopolymer mortars: Effect of solution molarity. Alexandria Eng J 2018;57:3375–86. https://doi.org/10.1016/j.aej.2018.07.011.

[20] Mikuła A, Król M, Koleżyński A. Experimental and theoretical spectroscopic studies of Ag-, Cd- and Pb-sodalite. J Mol Struct 2016;1126:110–6. https://doi.org/10.1016/j.molstruc.2016.03.004.

[21] Kumar S, Kumar R, Mehrotra SP. Influence of granulated blast furnace slag on the reaction, structure and properties of fly ash based geopolymer. J Mater Sci 2010;45:607–15. https://doi.org/10.1007/s10853-009-3934-5.

[22] Najafi Kani E, Allahverdi A, Provis JL. Calorimetric study of geopolymer binders based on natural pozzolan. J Therm Anal Calorim 2017;127:2181–90. https://doi.org/10.1007/s10973-016-5850-7.

[23] Zhang Z, Wang H, Provis JL, Bullen F, Reid A, Zhu Y. Quantitative kinetic and structural analysis of geopolymers. Part 1. The activation of metakaolin with sodium hydroxide. Thermochim Acta 2012;539:23–33. https://doi.org/10.1016/j.tca.2012.03.021.

[24] Yao X, Zhang Z, Zhu H, Chen Y. Geopolymerization process of alkali–metakaolinite characterized by isothermal calorimetry. Thermochim Acta 2009;493:49–54. https://doi.org/10.1016/j.tca.2009.04.002.

[25] Pommer V, Vejmelková E, Černý R, Keppert M. Alkali-activated waste ceramics: Importance of precursor particle size distribution. Ceram Int 2021;47:31574–82. https://doi.org/10.1016/j.ceramint.2021.08.037.

[26] Fořt J, Novotný R, Vejmelková E, Trník A, Rovnaníková P, Keppert M, et al. Characterization of geopolymers prepared using powdered brick. J Mater Res Technol 2019;8:6253–61. https://doi.org/10.1016/j.jmrt.2019.10.019.

[27] Hwang C-L, Damtie Yehualaw M, Vo D-H, Huynh T-P. Development of high-strength alkali-activated pastes containing high volumes of waste brick and ceramic powders. Constr Build Mater 2019;218:519–29. https://doi.org/10.1016/j.conbuildmat.2019.05.143.

[28] Phair JW, Van Deventer JSJ. Effect of silicate activator pH on the leaching and material characteristics of waste-based inorganic polymers. Miner Eng 2001;14:289–304. https://doi.org/10.1016/S0892-6875(01)00002-4.

[29] Barbhuiya SA, Gbagbo JK, Russell MI, Basheer PAM. Properties of fly ash concrete modified with hydrated lime and silica fume. Constr Build Mater 2009;23:3233–9. https://doi.org/10.1016/j.conbuildmat.2009.06.001.

[30] Brazilian Association of Technical Standars. NBR 13281: Argamassa para assentamento e revestimento de paredes e tetos - Requisitos 2005:7.

GENERAL CONCLUSIONS

1 FINAL CONSIDERATIONS

The state of the art on geopolymer shows that the current trend is the development of research on the use of sustainable raw materials (precursors or activators), in order to reduce the environmental impacts caused by the construction industry. Besides, researchers have sought to better understand the nature and occurrence of alkali-activation reactions, their kinetics and what are the factors that are relevant to their development, among other questions.

As seen in Article 1, products with good mechanical strength have been produced using alternative activators. The compressive strength values obtained are comparable to those of concretes, mortars and cementitious pastes, based on Portland cement. This makes the use of alkali-activated materials attractive for also structural functions.

In Article 2, it was investigated the effect of alternative alkaline solutions on the physical, mechanical and microstructural properties of geopolymeric pastes. The alkaline solutions were produced with waste glass powder and NaOH. The content of waste glass in the activator had a stronger influence on the mechanical strength and microstructure of geopolymers than the molar concentration factor. The SiO_2/Na_2O molar concentration of the alkaline solution was directly related to the compressive strength, suggesting that the increase of this module leads to better mechanical results.

The microstructural analyses showed that increasing WG enhanced the formation of geopolymerization products, including N-A-S-H gel and zeolitic species in the pastes. This was pointed out by both XRD and FT-IR results. The main zeolitic phase was the zeolite X in the geopolymers with 0 g and 5 g of WG (per 100 mL of solution). For additions above 5 g of WG, the zeolite Y (or faujasite) took place in the geopolymer composition. FT-IR results demonstrated that the increase of WG content also promoted a higher extent of geopolymerization and is related to the increase of mechanical strength.

The environmental analysis proved that the alternative alkaline solution presented a better performance in terms of embodied energy in its production and CO_2 emission. The reductions in embodied energy and CO_2 footprint were 69.8% and 78.0%, respectively. It demonstrates the high and positive environmental impact caused by the replacement of commercial products by industrial wastes.

The best pastes obtained based on mechanical strength results were 8M-10, 8M-15, 10M-15 and 12M-15. Although Tukey test classified the mechanical strength averages as

statistically equal, 8M-10 and 8M-15 presented a better performance at 28 and 56 days and higher incidence of zeolitic structures. Isothermal calorimetry curves demonstrated the presence of two peaks or two distinct phases of reactions, related to the dissolution of the aluminosilicates existent in the precursor and the reactions of polycondensation, respectively. The increase of molar concentration enhanced the initial dissolution, but it was undesirable to polycondensation. The polymerization reactions were enhanced by higher additions of waste glass.

The mortars produced from these mixtures presented lower mechanical performance compared with the pastes. The production and characterization of the two series of mortars, which were studied in Article 3, demonstrated that the inclusion of sand changed the behavior of the geopolymer, requiring the adjustment of some parameters, such as liquid/precursor ratio and appropriate proportion between chamotte and sand.

For the production of mortars, further investigation must be carried out in order to establish a geopolymeric matrix with higher quality and capable of properly agglomerate the fine aggregate.

As a final point, both chamotte and waste glass have the potential to be applied as raw materials in geopolymer products that require low compressive strength. It is possible to produce geopolymers with industrial wastes in both parts (precursor and alkaline solution), which makes it more sustainable and at a lower cost.

2 SUGGESTIONS FOR FUTURE WORKS

Some suggestions for future works are listed below:

i. The evaluation of durability “in service” of geopolymers based on chamotte and waste glass, applying aging accelerated tests that simulate UV radiation, rain (water spray) and condensation. It is interesting to establish a correlation between the natural weathering and accelerating aging, in order to predict the service life of the material.
ii. The investigation of the behavior of chamotte and waste glass-based geopolymers under fire condition, with the evaluation of changes caused in the physical and mechanical behavior of the material.
iii. Development of geopolymers with the inclusion of other industrial wastes as activator, including the production of one-part materials.

iv. The study of other ways of conformation of geopolymers, such as pressing, based on the increase in the degree of particle packing and this effect on pastes, mortars and geopolymeric concrete based on industrial wastes.

v. The environmental characterization of mortar and alkali-activated concrete produced from industrial or agricultural wastes. Few studies have investigated the potential for leaching and solubilization of elements that can be dangerous to the environment or to the building user.